TECHNICAL UNIVERSITY OF LIBEREC
Faculty of Mechanical Engineering

Modern Transmission Mechanism of Production Machines

Dissertation

Study programme:	P2302 – Machines and Equipment
Study branch:	2302V010 – Machine and Equipment Design
Author:	**Ha Nguyen Van, M.Sc.**
Supervisor:	prof. Ing. Ladislav Ševčík, CSc.

Liberec 2019

Declaration

I hereby certify I have been informed that my dissertation is fully governed by Act No. 121/2000 Coll., the Copyright Act, in particular Article 60 – School Work.

I acknowledge that the Technical University of Liberec (TUL) does not infringe my copyrights by using my dissertation for the TUL's internal purposes.

I am aware of my obligation to inform the TUL on having used or granted license to use the results of my dissertation; in such a case the TUL may require reimbursement of the costs incurred for creating the result up to their actual amount.

I have written my dissertation myself using the literature listed below and consulting it with my thesis supervisor and my tutor.

At the same time, I honestly declare that the texts of the printed version of my dissertation and of the electronic version uploaded into the IS STAG are identical.

11. 3. 2019 Ha Nguyen Van, M.Sc.

Acknowledgments

First and foremost, I would like to deeply thank my supervising Prof. Ing. Ladislav Ševčík, CSc., for all his guidance, great support, and encouragement throughout the past four years. He had been spending much time on me throughout the Ph.D. research studies, from choosing the theme of the research till correcting carefully the dissertation. Without his guidance and persistent support, this dissertation would not have been possible.

I would like to thank all members of my graduate committee for their helpful advice and encouragement.

I would like to acknowledge the general support provided by all members of the Department of Design of Machine Elements and Mechanisms, Faculty of Mechanical Engineering, Technical University of Liberec.

I would like to respect Mr. Josef Stuchlík for his help in completed the manufacturing work.

I am grateful to Ing. Petr KULHAVY, Ing. Pavel SRB, for many support, during not only finish my dissertation but also for all the time I study here.

In addition, I would like to express appreciation to all of my friends, especially to M.Sc. Tran Xuan Tien, who have helped me to overcome the difficulties in research and life for last four years.

Last but definitely not least, I would like to thank my family for their unconditional support, encouragement, and love. Especially my wife and my little daughters always gave strength to me and kept me laughing during the times of adversity while trying to fulfill my goal.

I am greatly indebted to you all for your kindness, support and helps. You will be in my heart, my soul forever.

Abstract

Cam design is constantly evolving. In recent years, with the rapid development and popularization of mechanical products in modern society, it has been such an important question on designing and producing mechanisms precisely. Also, together with the assistance of the numerically controlled manufacture system being widely applied in this time, which are useful tools for the designer to develop a new type of cam profile.

Therefore, this dissertation mainly focuses on designing a novel cam mechanism for converting the rotation cam to a desired rotary motion of the output shaft. The design based on the idea of altering the roller follower by the ball for a groove cam mechanism. Where the ball plays a roller of the follower in a conventional cam follower. Due to the balls connect the grooving cam and the grooves of the output shaft, they perform pure rolling motion without sliding. Hence, the main function of the balls transfers the moments and velocities from the camshaft into the output shaft. With the input, the body is the groove cam and the output shaft is driven one.

Due to the contact between the balls with their grooves on each part of the cam mechanism is very important can directly affect the lifespan and the ability working of the structure of the groove cam. Therefore, the thesis also determines the contact stress between the ball and the grooves on output camshaft, middle part as well as a circular groove on the input camshaft by using both theory and fine element analysis methods. Through contact analysis, the changes could be shown in contact pressure, strain, penetration, friction stress on the groove cam mechanism. Based on the results simulation by ANSYS Workbench can aid the designer to redesign model to obtain the optimal design. Finally, from the simulation results revealed that the computational values were consistent with theoretical values. It can be concluded that the proposed design has been successfully designing.

Finally, the groove cam mechanism was manufactured successfully at the Laboratory of Department of the Design of Machine Elements and Mechanism of Technical University of Liberec, Czech Republic.

Keywords: Groove cam, cam groove optimization, ball transition, contact analysis, novel cam, groove ball transmission.

CONTENT

LIST OF SYMBOLS, ABBREVIATIONS

A	Apparent area of contact	m^2
D	The center of the ball	
a_h	the half-width of the contact patch major axis	mm
B	Geometry factor	1/m
B_i	i^{th} constraint considered in the cam design	
b	The distance between the cam center and the point I_{23}	mm
C_i	The contact point between the ball ith and the groove cam	
D	Distance from the center of cam rotation to the point of force	mm
e	Auxiliary geometric	
E	Intersection point	
$f(u)$	Nodal force	N
F	Force acting on the steel ball	N
F_{A1}	Normal force	N
F_{A2}	Sliding force	N
h	Stroke of the follower	mm
I_{23}	Instantaneous center of velocity at the point I_{23}	

k	Distance between two center balls	mm
$K(u)$	Global stiffness matrix of the system	
L	Length of cylinder	mm
l	Distance between the center of the cam and the center of the ball	mm
lb	Lower bound	mm
M	Moment acting on the input cam shaft	Nm
m	Components mass	
m_1, m_2	Material constants of the ball and the groove	m^2/N
n	number of the grooves on the output shaft	
O	Center of the input camshaft	
O_1	Center of the circular groove of the input cam shaft	
O_2	Center of the output shaft	
O_b	Center of the ball	
P	Pressure in contact patch	Pa
P_{aveg}	Average pressure in contact patch	Pa
P_{max}	Max pressure in contact patch	Pa
R_i	Radius of the ith body in contact	mm

R_b	Base circle radius of the groove cam	mm
R_p	Prime circle radius of the groove cam	mm
R_r	Radius of the ball	mm
R_f	Radius of the plane	mm
$S(X, Y)$	2D global coordinate system	
$S_m(X_m, Y_m)$	2D mobile coordinate system of the groove cam	
s	Displacement of the ball follower	mm
$\dot{s}$	Velocity of the ball follower	mm/s
s'	First derivative of the ball follower displacement with respect to the cam angle	mm/rad
s''	Second derivative of the ball follower displacement with respect to the cam angle	mm/rad^2
s'''	Third derivative of the ball follower displacement with respect to the cam angle	mm/rad^3
t	Time	s
ub	Upper bound	mm
u	Nodal displacement	mm
V_f	The tangent volocity of I_{23}	mm/rad
v_c^t	Velocity of the contact point between the groove cam	mm/s

	surface and the ball tangent to the surface	
α	Angle between the direction of the force F_A and the force F_{A1}	degree
β	Angle of cam rotation to reach the stroke	rad
ω_b	Angular velocity of the ball about its center	rad/s
ψ	Pressure angle	rad
θ	Angular of the cam rotation	rad
φ_2	Rotary angle between the FCS and OCS	rad
η	Initial angle of the ball in the COS	rad
μ	Poisson's ratios of the steel material m_i	
α_b	Angular acceleration of the ball about its center	rad/s^2
φ_b	Angular jerk of the ball about its center	rad/s^3
ψ'	The first derivative of the pressure angle	
ψ''	The second derivative of the pressure angle	
ρ_p	Radius of curvature of the pitch curve	mm
ρ_{min}	Minimum radius of curvature	mm
ρ_c	Radius of the groove cam profile	mm

ε	Eccentricity axceleration	mm
ω	Angular velocity of the cam	rad/s
$\sigma_{xmax}\,\sigma_{ymax}\,\sigma_{z}$	maximum normal stress	Pa
τ	Shear stress	Pa
τ_{xymax} , τ_{yzmax}, τ_{zxmax}	Maximum shear stress	Pa
$Z_{@\ \tau maxsma}$	Distance below the surface	mm

LIST OF FIGURES

LIST OF TABLES

LIST OF ABBREVIATIONS

3D	Three-dimensional
CAD	Computer-aided design
CCW	Counter clockwise
CW	Clockwise
CEP	Critical extreme position
CPM	Critical path motion
FEM	Finite element method
FEA	Finite element analysis
CCS	Cam coordinate system
FOS	Frame coordinate system
OCS	Output coordinate system
DOF	Degree of freedom

Chapter 1

INTRODUCTION

1 Research review

1.2 Transmission mechanism

A mechanism is a device which transforms motion to some desirable pattern and typically develops very low forces and transmits little power. A machine typically contains mechanisms which are designed to provide significant forces and transmit significant power [1]. The mechanism is used in different types of industry in order to increase the effectiveness of the design machinery. Therefore, there are a lot of mechanisms have been invented, used and developed. Some common mechanisms are shown in figure 1.1 respectively as a four bar, a cam, belt and chain, and a planetary gear mechanism. Which are widely applied in many various machines, from cars, drilling machines, textile machines, wind wheel…

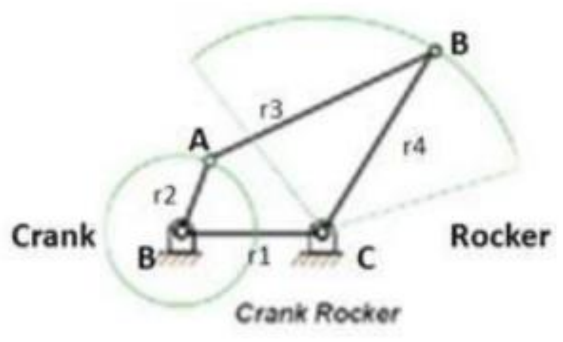

a) Four bar

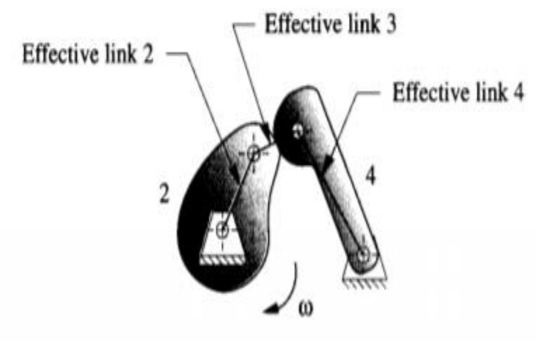

b) Cam

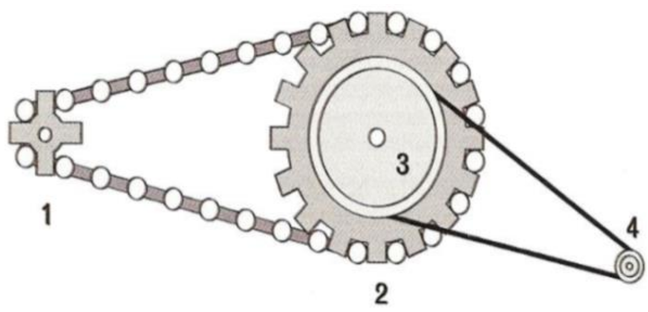

c) Belt and chain

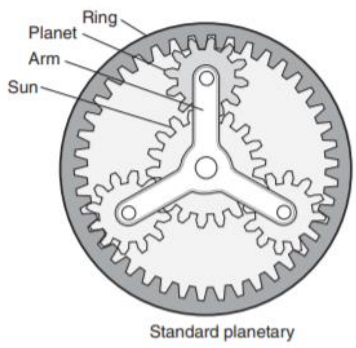

d) Planetary gear

Figure 1.1: Common mechanisms in mechanical engineering [1]

1.2 Cam mechanism

Among of those mechanisms foregoing. Cam mechanism is an extremely important and ubiquitous component in all kinds of machinery. It is difficult to find examples of machinery that do not use one or more cam in their designs. Cams are the first choice of many designers for motion control where high precision, repeatability, and long life are required. Therefore, cam mechanisms are widely used in many types of modern machines. The most common application for cams is valve actuation in internal combustion engines. Many sewing machines use cams to obtain patterned stitching. Also, mostly automated production machinery uses cam extensively.

Sometimes cams and cam mechanisms are coupled with linkages, thus giving a broader variety of output motions and applications. From the historical point of view, it is possible to derive cam mechanisms from some of the mechanical abilities in the antiquity.

The historical contribution starts with Leonardo da Vinci (1452-1519), one of the most famous artist-engineers of the Renaissance [2]. The idea of applying cam mechanisms in machines had kept and substantially developed. Till the 19 century, in the course of the invention of the steam engine by James Watt, then the developing of the automobile engines, cam mechanisms could be calculated, designed, manufactured and applied in the mechanical engineer of today. Therefore, it became more and more important in the industrial world to develop compact machines with the high performance-to-weight ratio, for automobiles as well as for manufacturing machines and machine tools.

Nowadays, with the development of the computer techniques, hardware, and softwares, technical manufacturing, which can aid to calculate, simulate, optimize and manufacture cams and cam mechanisms to achieve optimal performance and running quality for a given mechanical task. But it puts the cam designer has faced more challenging including the designing. Of course, we would like to design a cam model with as simple as possible but regarding that can work at high-speed motion with high efficiency, high contact factor, fully eliminated back-lash, reliability, lifetime and so on. Which are not easy tasks for designing causes vibrations in mass-elastic systems and must be encountered by properly chosen motion laws and most important by cams manufactured with the highest quality and precision [3-4].

Generally, cam follower are only one of the larger number of the cam and follower combinations and can be classified in several ways [5]: by type of follower motion, by type of joint closure, by type of motion constraints, by type of follower, by type of cam,or type of motion program.

According to the type of follower motion: The follower motion may be translating or oscillating. The translating follower is simple Figure 1.2 a, common to use and easy to design, the latter figure 1.2 b is known to be complicated and quite difficult to design but have less friction and higher efficiency and work more smoothly.

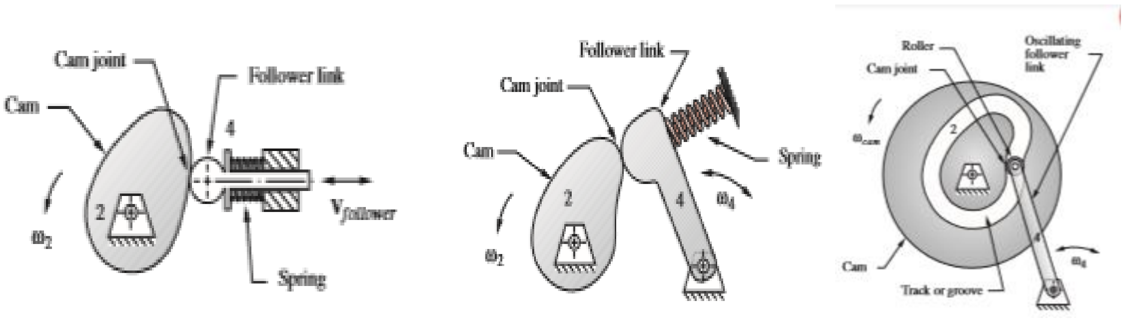

a) b) c)

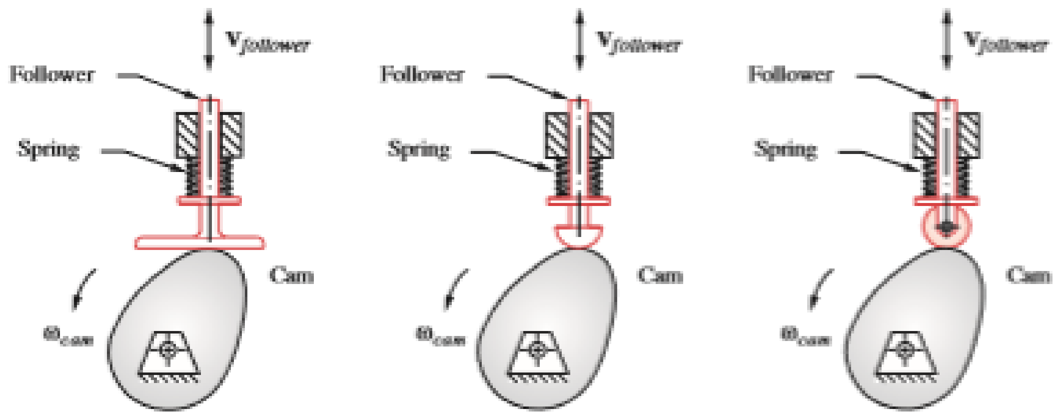

d) e) f)

Figure 1.2: Classified cam mechanism [1,5]

Moreover, depending on how the cam and follower contact is maintained, cam mechanisms can be divided into force-closed and form-closed (track or groove) cam mechanisms. For kind of force-closed cam mechanism figure 1.2 (a,b, d, e, f) in order to ensure constant contact between the cam and follower, an external force is required to be applied. This force is usually provided by a spring of sufficient stiffness or sometimes by an air cylinder. As a result, of the force effect, the driving torque and contact stress between the cam and follower in the rise are increased, it makes the wear on the cam and follower. Whereas, in the form-closed cam mechanism as shown in figure 1.2 c, the contact between cam and it's roller follower is obtained by letting the roller follower run in a cam groove or by using a conjugate condition. So no force is required to maintain the contact between its cam and the follower, therefore, the contact stress between the cam and follower will consequently be smaller and the driving torque in the rise can be reduced [5-6, 9]. However, a form-closed cam is more expensive to make than a force-closed (open) cam simply because there are two surfaces to be machined and ground. Also, heat-treating will often distort the track of a form-closed cam, narrowing or widening it such that the roller follower will not fit properly. This virtually requires post-heat-treat grinding for track cams in order to resize the groove. A force-closed cam will also distort on heat-treating but may still be usable without grinding.

By type of follower: Figure 1.2 (d, e, f) illustrates this type of cam with three different type followers: an in-line translating flat-faced follower, a mushroom (curved) and a roller follower, respectively. The roller follower has the advantage of lower (rolling) friction than the sliding contact of the other two but can be more expensive. Roller followers are commonly used in production machinery where their ease of replacement and availability from bearing manufacturers' stock in any quantities are advantages. Flat-faced followers can package smaller than roller followers for some cam designs; they are often favored for that reason as well as a cost for some automotive valve trains.

In terms of their shape of the cam: such as a wedge, radial, cylindrical, or three-dimensional are shown in figure 1.3

Follow type of motion constraints: There are two general categories of motion constraint, critical extreme position (CEP) and critical path motion (CPM). The first one refers to the case in which the design specifications define only the start and finish positions of the follower but do not specify any constraints of the path motion between this extreme position this case is the easier on to design. The last case is a more constrained problem than CEP because the path motion and/or one or more of its derivatives are defined overall match the given constraints.

Type of motion program: One of the special features of cam follower systems is that specific dwell action maybe designed for the follower motion. A dwell is defined as a lack of follower movement while the cam maintains its input driving action. In production machinery, dwell occurs when the follower does not move while a secondary task is performed. Figure 1.4 shows the four basic types of cams for the follower action:

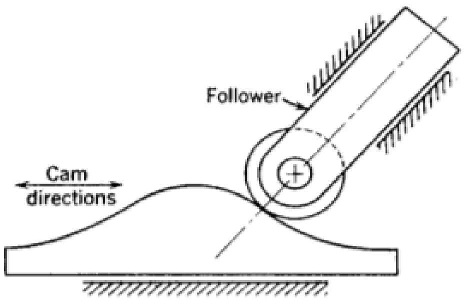

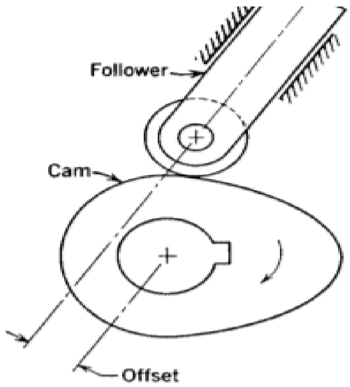

a) b)

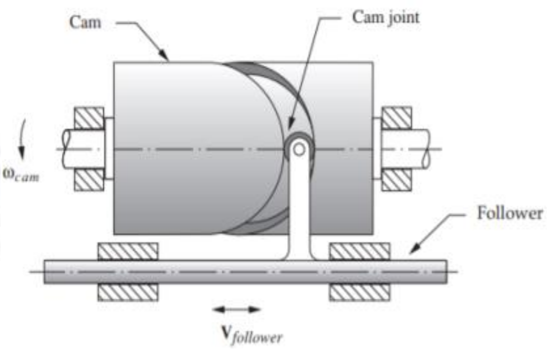

c) d)

Figure1.3: Cams of various types [5]

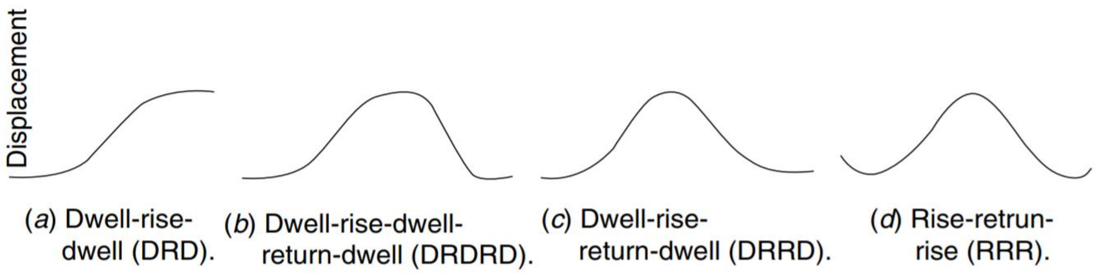

Figure 1.4: Types of cams in terms of follower motion [5]

1.3 Applications of the steel ball

As above stated, form-closed provides a geometric constraint at the joint such as the cam groove or conjugate cam. The no spring is needed to keep the follower in contact with these cams. The follower will run against one side or the other of the groove as necessary to provide both positive and negative forces. The design allows higher operation speed than a comparable force-closed system, it is not free of all vibration problems.

Moreover, as we know the ball has commonly applied in the bearing and ball screw field. Especially, in recent years, the idea uses the ball for gearing design has been developing by Sincroll Company [7]. By the technology, the roller or balls connect the wheels or bodies, while the performing pure rolling motion without sliding. Thus, the power efficiency is higher, the sliding friction is approximately eliminated and so on.

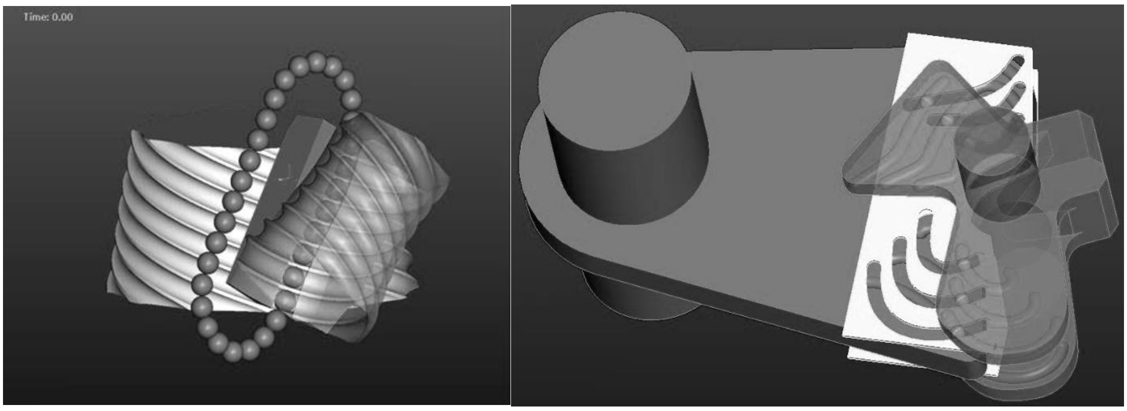

Figure 1.5: The ball gearing mechanism [7, 8]

By developing the idea’s Sincroll company, in this thesis, the idea of altering the roller follower by the balls is designed for a groove cam mechanism. The main function of the ball transfers the moments and velocities from the input camshaft into the output shaft. The input body is the groove cam and the output shaft is driven one.

The novel cam mechanism was proposed to design for converting a rotary cam into a rotary motion of the output shaft. By this design the cam mechanism which takes some characteristics of a form-closed and a breath cam, so the groove cam mechanism gets some advantages to other cam mechanisms because of following considerations [5, 9]: compared with a force-closed cam mechanism, the mechanism withstands lower contact stress because it is a form-closed cam mechanism and no force is required to maintain the contact between its cam and follower; compared with conjugate cam mechanism in which a set of two cams must be used, the cam mechanism is simpler in construction because only one cam is needed. So, it occupies small space and has lower cost; compared with a constant-breadth cam mechanism of which the cam profile should be convex everywhere, the cam mechanism possesses wider adaptability to the output motion because its groove cam profile could be concave. Another point in its favor of this model is the cam mechanism used the ball for the follower, where the ball is commonly used in production machinery and where their ease of replacement and availability from bearing manufacturers stock in any quantities are advantages.

The major drawback of the groove cam is the phenomenon of crossover shock. Every time the acceleration of the balls changes sign, the inertial force also does so. This causes the balls to abruptly shift from one side of the groove cam to the other. Due to the clearance between the balls and their circular grooves, even if the clearance is very small, there will still be an opportunity for the balls to develop some velocity in its short trip across the groove, and it will impact the other side. This causes significant made the balls slip and high wear compared to a force-closed cam. Therefore, the crossover shock phenomenon can be reduced or eliminated by improving the cam surface to get high precision to control the clearance, but it makes the cam tends to be more expensive.

Until now there are very few publications can be found in the literature that addresses the issue of designing of the groove cam using the ball for transmission. Therefore, the design of this mechanism remains to be a challenging task. Thus, this kind of cam mechanism has received some attention from any industrial machine parts and mechanisms as well as automated machine production and so on.

1.4 Objective of the dissertation and research methodology

The main objectives of the dissertation are:

1. Design a novel groove cam mechanism for converting a rotary cam to a desired rotary motion of the output shaft by applying the steel balls.
2. Due to the contact between the balls with their grooves on each part of the cam mechanism is very important can directly affect the lifespan and be ability working of the structure of the groove cam. Therefore, the research focus on determination of the contact stress between the balls and their

grooves on the output camshaft, the middle part as well as the circular groove of the input camshaft by using both theory and fine element analysis methods.

3. Based on the results of calculating simulations we suggested the ways to change the shape of the groove of the output shaft and the middle part to obtain the minimum contact pressure in contact between the balls and their grooves. Therefore, three groove design models were introduced to study in the thesis.
4. Finally, the shapes of the groove on each part for optimization of the groove cam are selected. The calculated result is matched nearly perfectly and the calculation can be used for the general design of the groove cam. So we can strongly confirm that the optimal design of the groove cam mechanism with respect to the Hertz pressure is obtained the goal of studying.
5. A groove design model was fabricated successfully at the laboratory of the Department of Design of Machine Elements and mechanism, Technical University of Liberec.

In order to achieve these objectives, many tasks related to mathematical calculations and CAD, ANSYS should be implemented. The followings are some main tasks in this research.

a) Brainstorming ideas to create a novel cam model by applying steel balls for transmitting motion.
b) Kinematic analysis of the groove cam and a methodology to deal with the cam size optimization of the groove cam are proposed.
c) Evaluating the contact analysis of the balls and their grooves of the groove cam mechanism by using Hertz theory and finite element methods.
d) Suggest the ways for optimal design for the groove cam mechanism.
e) Perform machining of the fabrication.

In this research some powerful tools were used such as CATIA, DYNACAM, ANSYS. The CATIA is a drawing programme with many additional features including mechanical design, structural analysis, digital mockup, which are really sufficient for CAD tasks.

Norton provided a computer program DYNACAM running on any MS-DOS computer with his book. Since it is designed for students to be learning tools to aid in the understanding of the relevant subject matter. It can be suitable for designing cam mechanisms.

While ANSYS is used for evaluating the contact analysis of the cam mechanism. The whole of manufacturing of the design was machined on the milling machine and lathe machine at the laboratory of the Department of Design of Machine Elements and mechanism, Technical University of Liberec.

1.5 Organization of the Dissertation

The dissertation is divided into seven Chapters follows: An introduction is presented in this chapter 1. In Chapter 2, the fundamental of the cam design model is presented. Also, the kinematics analysis of the groove cam design and deal with the cam size optimization of the groove cam are proposed in this Chapter. The Herzt theory and application of Herzt to solve the contact problems of the cam design are presented in Chapter 3. A Finite element method by using Ansys workbench is applied to investigate the contact problems between the balls and their grooves of the groove cam are conducted in Chapter 4. In Chapter 5, the ways for the optimal design for the groove cam mechanism to obtain the recommended value of contact pressure for steel material is presented. The performance of the machining of the design is shown in Chapter 6. Lastly, some conclusions are given in Chapter 7.

Chapter 2

FUNDAMENTAL THEORIES OF THE CAM MODEL DESIGN

According to author Norton [5-6], the fundamental law of cam design process can be stated as the cam-follower function must be continuous through the first and second derivatives of the displacement (i.e velocity and acceleration) across entire intervals. Besides, the jerk must be finite across entire as well. In short, the displacement, velocity, acceleration characteristics of the follower motion must be continuous functions.

In general case, a cam mechanism is required to be displaced through a specific rise and fall. Hence, the shape of the displacement curve plays a key role in the synthesis of a cam mechanism. So these functions are expressed in terms of the lift, the angle of the lift and as a function, the angle of rotation of the cam characterizing some specific cam laws. The most general form of the follower displacement for a translating roller follower can be written as,

$$s = hf\left(\frac{\theta}{\beta}\right), \tag{2.1}$$

where h and β are the lift and angle of the lift of the follower, respectively, θ represents the angle of rotation of the cam.

Now we can get the velocity and acceleration, jerk of the follower by successive derivatives of the displacement function with respect to the angle of cam rotation yields, respectively

$$\mu = s' = \frac{h}{\beta} f'\left(\frac{\theta}{\beta}\right), \tag{2.2}$$

$$a = s'' = \frac{h}{\beta^2} f''\left(\frac{\theta}{\beta}\right), \tag{2.3}$$

$$s''' = \frac{h}{\beta^3} f'''\left(\frac{\theta}{\beta}\right). \tag{2.4}$$

The displacement function serves only to define the cam contour for manufacturing purposes. It has little influence on the follower's dynamic behavior. The acceleration function has a large effect on the dynamic force especially if the follower mass is large causes by Newton's second law, $F=ma$. The follower velocity v affects the kinetic energy stored in the follower since equation $E=0.5\ mv^2$. The jerk function has an effect on vibrations in the follower system.

Therefore, the important task of the cam designer is necessary to select the motion properly, with which the follower will move in accordance with the system requirements before the cam contour can be determined. Depend on applications in machinery require a single-dwell or multiple-dwell cam program, as well as operation speed of the cam design. If operation is at a slow speed, the motion may be any one of several common motions like as parabolic, harmonic, fifth-order polynomial, or cycloidal so on.

For cams operating at higher speeds, the selection of the motion of the cam follower must be based not only on the displacement but also on the forces acting on the system as a result of the motion selected. With the trend toward higher machine speeds, it is necessary to consider the dynamic characteristics of the system and to select a cam contour that will minimize the dynamic loading and prevent cam and follower separation.

2.1 Model of the groove cam mechanism

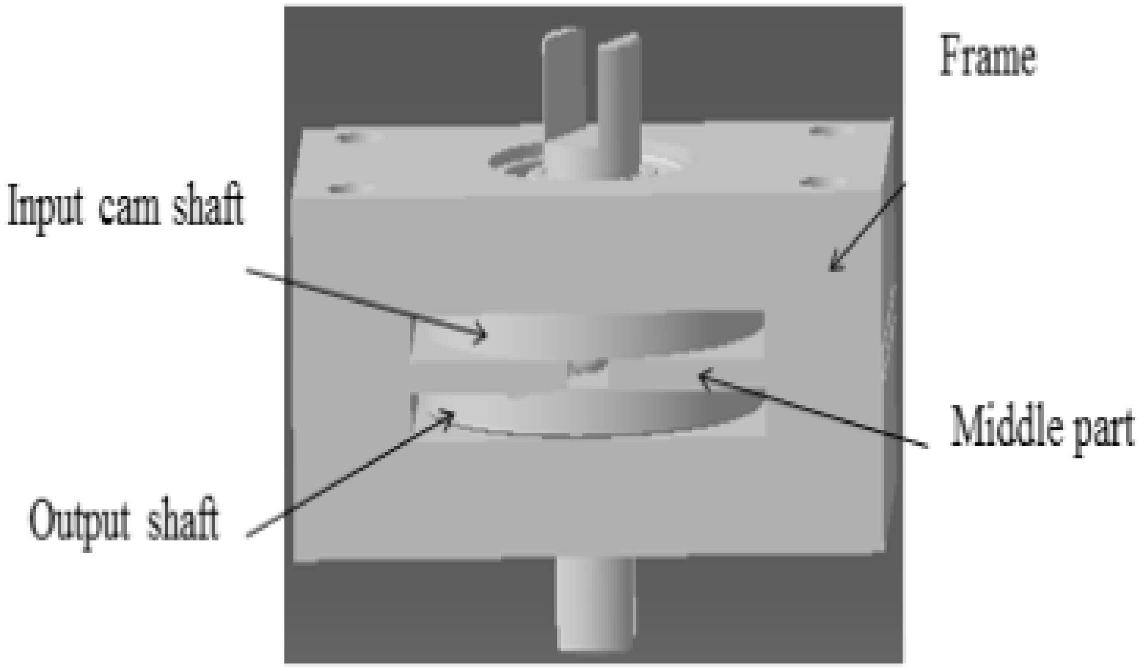

Figure 2.1: Layout of the groove cam

A novel transmission, called the groove cam mechanism is depicted in figure 2.1 is designed to transform a rotational motion to a rotational one. The groove cam consists of a circular groove on the input camshaft and two balls, a middle part and a frame to mount all these parts.

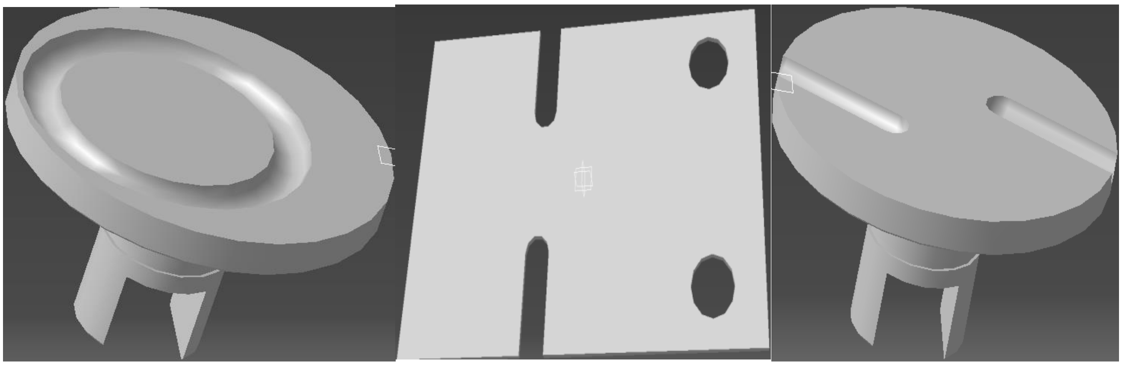

a) Input camshaft b) middle part c) output shaft

Figure 2.2: Groove cam geometry

As can be seen from figure 2.2 (a) shows the shape of the input camshaft is designed. According to this required design on one of the top of this part has an eccentric circular groove is designed with groove radius is *3* mm, the eccentric is 6 mm (the distance length between the center of the camshaft axis and the center of rotation of the circular groove), the radius of the circular groove from the its center is 20 mm.

Figure 2.2 (b) shows the middle part which is designed with two straight grooves. The width of the straight grooves is the same of the radius of the groove on the input camshaft and output shaft.

Figure 2.2 (c) depicts the shape of the output shaft. Like as the input camshaft, on one of the tops of the output shaft, which is designed with two straight grooves. Each of the straight groove in this designed must have the same groove radius with the circular groove on the input camshaft. In addition, to satisfy the requirements angle of rotation of the output shaft, two straight grooves on the output shaft must be symmetric across the central plane. Actually, the number of the straight grooves on the output shaft can be designed more or less than depends on the requirements of the design.

Figure 2.3 shows the assembly of the balls on the grooves of the input camshaft and the middle part. The thin middle part was designed with two straight grooves, which has the same radius as the groove on the camshafts and the output shaft. The main function of straight grooves on the middle part is to guide straight motion direction of the steels ball in their grooves. Figure 2.3 presented two steel balls in the straight and circular grooves. In case, the diameter of the steel ball is 6 mm.

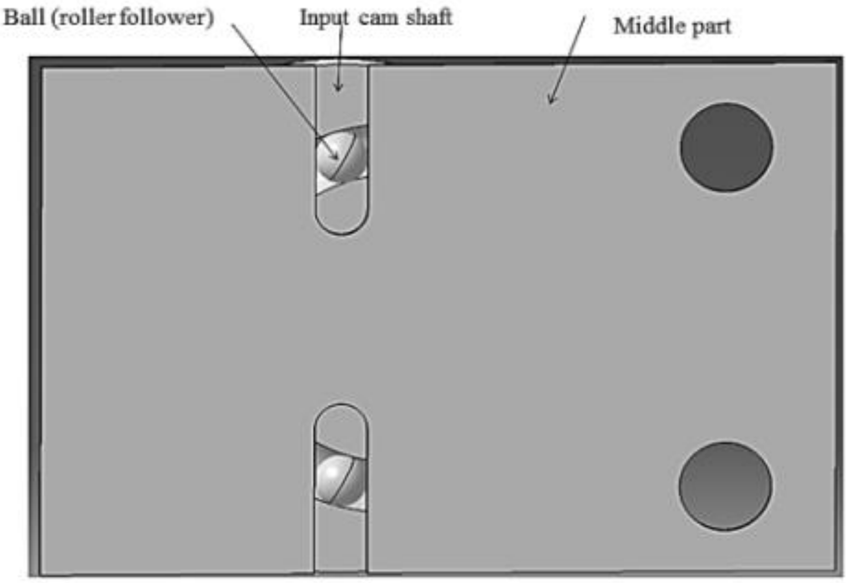

Figure 2.3: The assembly of two balls in the groove of the input camshaft and the middle part

With this cam model by using two steel balls to transmit rotary motion between two concentric shafts, the main function of the balls transfer the moments and velocities from the camshaft into the output shaft. So when the cam works each ball can be easy to roll up and down with respect to their straight groove on the middle part and output shaft correspondingly. Moreover, these balls must roll along in the circular groove on the input cam shaft.

Due to each steel ball only moves up and down in each straight groove of the middle part. Therefore, which play a role of a roller follower of a cam mechanism. Which means that the cam mechanism model is designed with a pair of followers for one cam but it is not a type of conjugate cam system. In addition, two balls always turn around in the circular groove of the input camshaft, which creates a constant-diameter between two of the centers of the balls (rollers). In this case, a constant distance is equal to the diameter of the circular groove on the input camshaft. Hence, the cam mechanism is designed taking some characteristics of a breadth cam.

As mentioned above, the cam mechanism is designed which takes some characteristics of a form-closed and a breadth cam, so the cam mechanism gets some advantages to other cam mechanisms because of following considerations: compared with a force-closed cam mechanism, the mechanism withstands lower contact stress because it is a form-closed cam mechanism and no force is required to maintain the contact between its cam and follower; compared with conjugate cam mechanism in which a set of two cams must be used, the cam mechanism is simpler in construction because only one cam is needed. So, it occupies small space and has lower cost; compared with a constant-breadth cam mechanism of which the cam profile should be convex everywhere, the cam mechanism possesses wider adaptability to the output motion because its groove cam profile could be concave. Another point in its favor of this cam model is the cam mechanism used ball followers, where the ball is commonly used in production machinery where their ease of replacement and availability from bearing manufacturers stock in any quantities are advantages.

Although, the mechanism also meets the major drawback of the groove cam is the phenomenon of crossover shock. Every time the acceleration of the follower changes sign, the inertial force also does so. This causes the follower to abruptly shift from one side of the groove cam to the other. Due to the clearance between the ball follower and the circular groove, even if the clearance is very small, there will still be an opportunity for the follower to develop some velocity in its short trip across the groove, and it will impact the other side. This causes significant follower slip and high wear on the roller followers compared to an open.

Therefore, the crossover shock can be reduced or eliminated by improving the cam surface to get high precision to control the clearance, but it makes the cam tends to be more expensive.

2.2 Synthesis of the groove cam mechanism

Let the X-Y frame be attached to the cam as depicted in figure 2.4 shows the geometry of a circular groove cam and translating ball follower in an arbitrary position. O is the origin of the cam, while O_b is the center of the ball, and C_1 is the contact point between the groove cam and the ball. The geometric parameters defining the cam mechanism are illustrated in the same figure. The notations of this figure are defined, namely, ε the eccentricity, which is the perpendicular distance between the follower's axis of motion and the center of the cam. Often this eccentricity ε will be zero, making it aligned follower; R_r the radius of the ball; ψ pressure angle; θ angle of rotation of the input camshaft; s position of the center of the ball, the displacement of the follower; R_p

the radius of the prime circle, which is defined as the smallest circle which can be drawn tangent to the locus of the centerline of the follower. The parameters above as well as the surface contact on the groove cam, are determined by the geometric relations.

2.2.1 The model with one ball

The cam rotates in counter-clockwise (*CCW*) with a constant angular velocity and drives the ball to translate up and down in reciprocating motion. When the cam makes a complete turn ($\theta = 2\pi$), the displacement of the ball is equal to *h*. Figure 2.4 shows a general case in that the axis of the motion of the follower does not intersect the center of the cam.

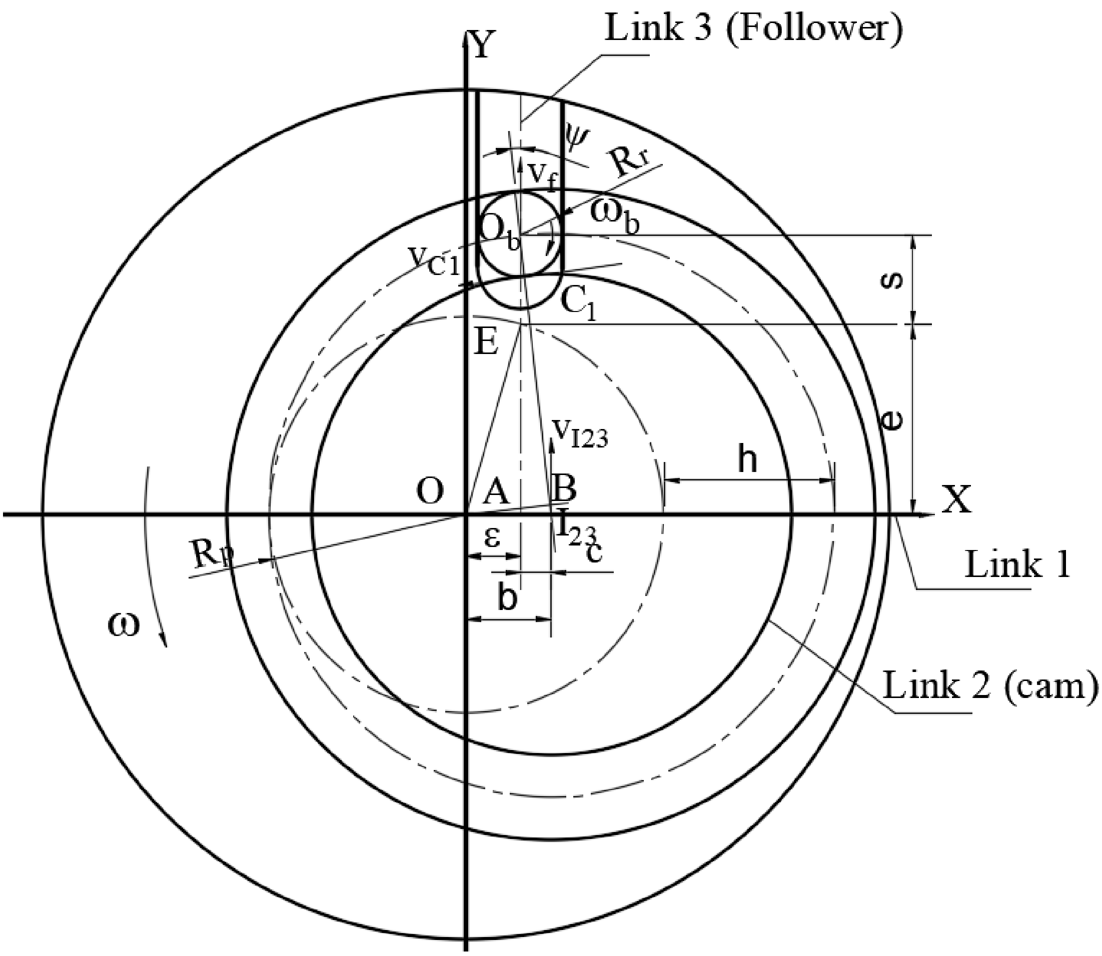

Figure 2.4: Parameterization of the groove cam mechanism

As can be seen figure 2.4, the axis of transmission is extended to intersect effective link 1, which is a frame (the ground link). This intersection is instant center I_{23}

(labeled I_{23}), which is defined as a point, common to two rigid bodies (links) in plane motion that has the same instantaneous velocity in each body. In other words, there is no relative velocity between these two points at that instant. Thus, one body can be considered to be in pure rotation with respect to the other about their common instant center. By definition above the velocity in link 2 (the cam) and link 3 (the ball follower) have the same value. All points on the follower have identical velocities V_f, which are equal to the velocity of I_{23} in link 2. We can write an expression for the tangent velocity at I_{23} by cam rotation:

$$V_{I23} = b\omega = \dot{s}\ , \tag{2.5}$$

where ω is the constant cam angular velocity and the radius b from cam center to I_{23}, s is the instantaneous displacement of the ball from the s diagram and $\dot{s}$ is its time derivative in units of length/sec. Now applying the chain rule with ω constant:

$$V_{I23} = b\omega = \dot{s} = \frac{ds}{dt}, \tag{2.6}$$

In other words, the equation 2.6 can express by

$$V_{I23} = \frac{ds}{dt}\frac{d\theta}{d\theta} = \frac{ds}{d\theta}\frac{d\theta}{dt} = \omega\mu. \tag{2.7}$$

From equations 2.5 and 2.7 can be formed as,

$$b\omega = \mu\omega. \tag{2.8}$$

To the final form of equation 2.8

$$b = \mu. \tag{2.9}$$

From equation 2.9 we conclude that the distance b to the instant center I_{23} is numerically equal to the velocity of the follower μ in units of length per radian, which is a strictly geometric relation.

2.2.1.1 Pressure angle

The pressure angle, ψ is defined the angle formed between the translating line of the follower's motion and the common normal direction at the contact point between the cam and roller, as shown in figure 2.4. The pressure angle is a measure of the efficiency of the force transmission between the cam and follower. It is known that the force can only be transmitted from the cam to the follower, or vice versa, along with the common normal direction. However, only the component of the force along the direction of the follower motion is useful, and, therefore, the perpendicular component must be kept as low as possible in order to reduce the sliding friction follower and its guideway. In practice, as a rule of thumb, we would like the pressure angle has value as small as to avoid undesirable levels like as jam, follower sliding or pivot friction. Therefore, cam pressure angles of 30^0 are about the largest that can be used without causing serious mechanical problems [5, 9-11]. So determining the pressure angle must be done in cam design. From figure 2.4 the pressure angle can be expressed in terms of displacement s, velocity v, eccentricity ε and the prime circle radius R_p.

By the construction is shown in figure 2.4, the point E is the intersection of the arc of radial R_p and the axis of motion of the follower at point E, where the length e is defined by the distance from link 1 to this intersection. For any chosen prime circle radius it is a constant value.

From triangle AO_bI_{23}:

$$c=(s+e)\tan\psi, \tag{2.10}$$

and

$$b=(s+e)\tan\psi+\varepsilon. \tag{2.11}$$

Substituting equation 2.9 into equation 2.11 we obtained

$$\mu=(s+e)\tan\psi+\varepsilon. \tag{2.12}$$

As clear from triangle AEO

$$e=\sqrt{R_p^2-\varepsilon^2}\ , \tag{2.13}$$

substituting equation 2.13 into equation 2.12 we get

$$\psi=\arctan\frac{\mu-\varepsilon}{s+\sqrt{R_p^2-\varepsilon^2}}. \tag{2.14}$$

According to equation 2.14, it can be concluded that for a given follower motion, that is, by knowing s and v, the three geometric parameters R_b, R_r, ε, $(R_p=R_b+R_r)$ can be adjusted to obtain a suitable pressure angle. As the pressure angle varies during the cam rotation what is important to evaluate is its maximum value during the system functioning. Therefore when determining cam we need to choose R_p

and ε to get an acceptable maximum pressure angle. If R_p is increased, ψ will be reduced but it makes the size of the cam is bigger, also increase cost. In general practice, we assume a trial value for R_p and an initial eccentricity of zero to calculate the values of ψ for the entire cam. Then adjust R_p and repeats the calculation until an acceptable is found.

2.2.1.2 Pitch-curve determination

The pitch curve is the trajectory of O_b, the center of the ball, distinct from the trajectory of the contact point C, which produces the cam profile. Hence, the Cartesian coordinates of the pitch-curve in the X-Y frame are

$$X(\theta) = \varepsilon cos\theta + s(\theta) sin\theta \tag{2.15}$$

$$Y(\theta) = -\varepsilon sin\theta + s(\theta) cos\theta$$

2.2.1.3 Curvature of the groove cam

Moreover, the radius of curvature of the groove cam surface, ρ_p is another important factor that affects the cam size and performance of the mechanism. When the groove cam surface is concave, the radius of curvature determines the minimum radius of the cutter tool which can be used to machine cam surface. Therefore, the radius of curvature of the groove cam cannot be smaller than the cutter radius when groove cam is concave. For the convex groove cam surface, the radius of curvature determines also the minimum radius of the roller (ball) that can be used with the cam [5]. Which can be stated as,

$$|\rho_{min}| \gg R_r. \tag{2.16}$$

As the rule of thumb is to keep the absolute value of the minimum radius of curvature ρ_p of the cam pitch curve preferably at least 1.5 to 3 times as large as the radius of the ball follower R_r.

A derivation for the radius of curvature can be found in any calculus text. For our case of a ball follower, we can write the equation for the radius of curvature of the pitch curve of the groove cam as [12-13]:

$$\rho_p = \frac{\left[(R_p+s)^2+\mu^2\right]^{3/2}}{(R_p+s)^2+2\mu^2-a(R_p+s)}, \tag{2.17}$$

where a positive value refers to a convex surface of the pitch curve and a negative value refers to a concave surface.

Let ρ_c and ρ_p be the radius of curvature of both the groove cam profile and the pitch curve, respectively, due to the definition of the pitch curve, it is apparent that

$$\rho_p = \rho_c + R_r \tag{2.18}$$

2.2.1.4 Analysis of the ball motion

From a kinematic point of view, the mathematical condition that represents the nonslip condition between the ball and groove cam surfaces states that the velocity of the contact point between the cam profile and the circumference of the ball tangent to this profile must be equal, as can be seen in figure 2.4, the tangential velocity of the contact point, when evaluated from the ball motion point of view, is given the following,

$$v_{c_1} = \omega_b R_r, \tag{2.19}$$

where ω_b is the angular velocity of the ball about its center. On the other hand, this tangential velocity can be expressed via the associated with the cam motion following,

$$v_{c_1} = \omega \overline{C_1 B}, \tag{2.20}$$

where $\overline{C_1 B}$ is defined as the distance between the contact point and the pole B, which varies continuously during the cam rotation.

The distance $\overline{C_1 B}$ can be determined from figure 2.4 by,

$$\overline{C_1 B} = \frac{e+s}{\cos\psi} - [\varepsilon + (e+s)\tan\psi]\sin\psi - R_r. \tag{2.21}$$

Assuming that there is no slip between ball and groove of the cam surface. The velocities in equation 2.19 and 2.20 are equal. Hence the angular velocity of the ball can be expressed following:

$$\omega_b = \frac{\omega}{R_r}\left(\frac{e+s}{\cos\psi} - [\varepsilon + (e+s)\tan\psi]\sin\psi - R_r\right). \tag{2.22}$$

In a special case, when there is no eccentricity between the direction of the follower motion and the axis of the cam rotation, it means $\varepsilon = 0$. Hence the angular velocity of the ball follows

$$\omega_b = \frac{\omega}{R_r}\left(\frac{e+s}{\cos\psi} - [(e+s)\tan\psi]\sin\psi - R_r\right). \tag{2.23}$$

From equation 2.22 and 2.23 obviously, show that the angular velocity of the ball varies with the cam rotation angle. Therefore, by differentiating equation 2.22 with respect to time to obtain the angular acceleration of the ball about its center as,

$$\alpha_b = \frac{\omega}{R_r}\left[\frac{s'\cos\psi + (e+s)\sin\psi\psi'}{\cos\psi} - \varepsilon\cos\psi\psi' - s'\tan\psi\sin\psi - (e+s)\frac{\psi'}{\cos^2\psi}\sin\psi - (e+s)\tan\psi\cos\psi\psi'\right]\frac{d\theta}{dt}, \tag{2.24}$$

thus,

$$\alpha_b = \frac{\omega^2}{R_r}\left[\frac{s'\cos\psi}{\cos^2\psi} - \varepsilon\cos\psi\psi' - s'\tan\psi\sin\psi - (e+s)\tan\psi\cos\psi\psi'\right], \tag{2.25}$$

then

$$\alpha_b = \frac{\omega^2}{R_r}\left[\frac{s'}{\cos^2\psi}(1-\sin^2\psi) - \cos\psi\psi'(\varepsilon + (e+s)\tan\psi\right]. \tag{2.26}$$

Substituting equation 2.14 into equation 2.26 we obtained

$$\alpha_b = \frac{\omega^2\cos\psi}{R_r}(s' - s'\psi'), \tag{2.27}$$

the dimensionless parameter ψ' represents the first derivative of the pressure angle with respect to cam angle θ. By differentiating equation 2.14 with respect to cam angle, we obtain ψ'.

From equation 2.14 with

$$\psi = arctan\frac{s'' - \varepsilon}{s+e}. \tag{2.28}$$

Hence,

$$\psi' = \frac{\frac{s''(e+s) - (s'-\varepsilon)s'}{(e+s)^2}}{1 + (\frac{s'-\varepsilon}{e+s})^2}, \tag{2.29}$$

to the final form

$$\psi' = \frac{s''(e+s) - (s'-\varepsilon)s'}{(e+s)^2 + (s'-\varepsilon)^2}. \tag{2.30}$$

Also, from equation 2.28 the relation can be expressed like as

$$(e+s)tan\psi = s' - \varepsilon. \tag{2.31}$$

Now, substituting equation 2.31 into equation 2.30 yields

$$\psi' = \frac{s''(e+s)-(s'-\varepsilon)s'}{(e+s)^2+(e+s)^2 tan^2\psi'}, \ . \tag{2.32}$$

Equation 2.32 is transformed by the same way into the form

$$\psi' = \frac{s''(e+s)-(s'-\varepsilon)s'}{(e+s)^2(1+tan^2\psi)}. \tag{2.33}$$

Finally, obtained

$$\psi' = \left(\frac{\cos\psi}{e+s}\right)^2 [s''(e+s)-(s'-\varepsilon)s'] \tag{2.34}$$

Similarly way, the second derivative of the angular velocity of the ball represents the angular jerk of the ball about its center and can be expressed by differentiating equation 2.27 with respect to time,

$$\varphi_b = \frac{\omega^2}{R_r}[-s'sin\psi\psi' + cos\psi s'' + \psi' s' sin\psi\psi' - cos\psi\psi'' s' - cos\psi\psi' s'']\frac{d\theta}{dt} \tag{2.35}$$

Equation 2.35 can be converted step by step

$$\varphi_b = \frac{\omega^3}{R_r}\left[-s'sin\psi\psi' + s''cos\psi + s'sin\psi\psi'^2 - s'cos\psi\psi'' - s''cos\psi\psi'\right], \tag{2.36}$$

$$\varphi_b = \frac{\omega^3 cos\psi}{R_r}\left[-s'tan\psi\psi' + s'' + s'tan\psi\psi'^2 - s'\psi'' - s''\psi'\right]. \tag{2.37}$$

Finally, obtained the form

$$\varphi_b = \frac{\omega^3 \cos\psi}{R_r}\left[s'' + s'\tan\psi\psi'^2 - s'(\tan\psi\psi' + \psi'') - \psi' s''\right]. \tag{2.38}$$

With ψ'' represents the second derivative of the pressure angle with respect to the cam angle. Which is obtained by differentiating equation 2.34 with respect to cam angle θ, yielding,

$$\psi'' = -2\frac{\cos\psi}{e+s}\left[\frac{sin\psi\psi'(e+s)+cos\psi s'}{(e+s)^2}\right][s''(e+s)-(s'-\varepsilon)s'] + \left(\frac{\cos\psi}{e+s}\right)^2 [s'''(e+s) + s''s' - s''s' + (s'-\varepsilon)s''], \tag{2.39}$$

then

$$\psi'' = -2\left(\frac{\cos\psi}{e+s}\right)^2 \left[tan\psi\psi' + \frac{s'}{e+s}\right][s''(e+s) - (s'-\varepsilon)s'] + \left(\frac{\cos\psi}{e+s}\right)^2 [s'''(e+s) + (s'-\varepsilon)s'']. \tag{2.40}$$

Substituting equation 2.31 into equation 2.40 obtains,

$$\psi'' = -2\left(\frac{\cos\psi}{e+s}\right)^2 \left[tan\psi\psi' + \frac{s'}{e+s}tan\psi\right][s''(e+s) - (s'-\varepsilon)s'] + \left(\frac{\cos\psi}{e+s}\right)^2 [s'''(e+s) + (s'-\varepsilon)s'']. \tag{2.41}$$

Also, can be expressed following

$$\psi'' = -2\psi' tan\psi\left[\psi' + \frac{s'}{s'-\varepsilon}\right] + \left(\frac{\cos\psi}{e+s}\right)^2 [s'''(e+s) + (s'-\varepsilon)s'']. \tag{2.42}$$

By substituting equation 2.34 into into equation 2.42, the ψ'' can be obtained as,

$$\psi'' = \left(\frac{\cos\psi}{e+s}\right)^2 [s'''(e+s) + (s'-\varepsilon)s''] - 2\psi'\left(\psi' + \frac{s'}{s'-\varepsilon}\right)\tan\psi. \tag{2.43}$$

2.2.2 The model of groove cam with two balls

As shown in figure 2.5, a groove cam mechanism is suggested to design [14-17]. Which has a pair of balls as followers. The cam rotates in counterclockwise at a constant angular velocity and drives the pair of the followers to translate up and down in reciprocating motion. The locus of the center of the followers is called the pitch curve of the cam. In this case, both centers must overlap over one rotation of the cam.

Hence, the groove cam mechanism must satisfy the kinematic conditions: ball followers on upper and lower sides have the same displacement, velocity, and acceleration. In order to design the groove cam profile to satisfy the kinematic conditions [18-20], instant velocity center for I_{23} by two followers must be met at the same point. This means that the normal lines at the contact points by the upper ball and lower ball must pass through the same point. Also, when the cam rotates one revolution, the position of the ball 1 and ball 2 with respect to the cam is opposite to the position. Therefore, the eccentricities ε_1 and ε_2 of the ball 1 and ball 2 have the same magnitude ε and must be located on both sides of the Y axis as seen in figure 2.5.

$$\begin{cases} |\varepsilon_1| = |\varepsilon_2| = \varepsilon \\ \varepsilon_1 = -\varepsilon_2 \end{cases}. \tag{2.44}$$

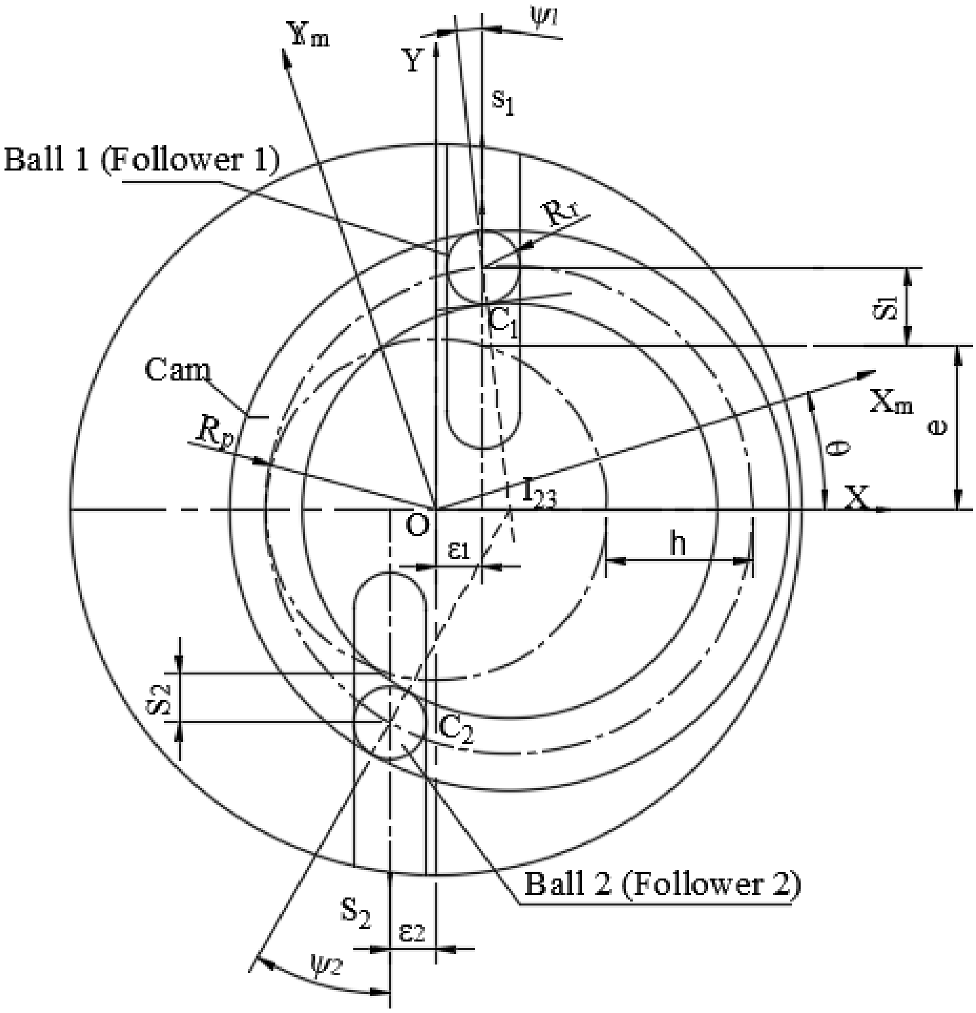

Figure 2.5: The geometry of groove cam with two ball followers

For deriving the profile equation of the groove cam, two coordinates systems are defined, as shown in figure 2.5, where ψ_1 and ψ_2 represent contact angle at the contact points C_1 and C_2, respectively. $S(X, Y)$ represents a stationary reference system and $S_m(X_m, Y_m)$ represents a mobile reference system. The reference system S_m is defined by the input cam shaft rotation angle θ.

Substituting equation 2.9 into equation 2.14, we get the contact point pressure angle for the upper and lower followers are represented by the following expressions, respectively

$$\psi_1 = actan\frac{\mu-\varepsilon}{s_1+\sqrt{R_p^2-\varepsilon^2}}, \tag{2.45}$$

$$\psi_2 = actan\frac{\mu-\varepsilon}{s_2+\sqrt{R_p^2-\varepsilon^2}}. \tag{2.45}$$

The coordinates $S(X_{c1}, Y_{c1})$ and $S(X_{c2}, Y_{c2})$ of the contact points between the ball 1, ball 2 and groove cam respectively are represented by the following expressions:

$$\begin{cases} X_{c1} = \varepsilon + R_r sin\,\psi_1 \\ Y_{c1} = e + s_1 - R_r cos\,\psi_1 \end{cases}, \tag{2.47}$$

$$\begin{cases} X_{c2} = -\varepsilon - R_r sin\psi_2 \\ Y_{c2} = -e - s_2 + R_r cos\psi_2 \end{cases}, \tag{2.48}$$

where $h=s(\theta)$, is the function of the follower.

Therefore, the coordinate of contact points C_1 and C_2 of the upper and lower followers in the fixed coordinate systems S are converted into the S_m coordinate system can be expressed in terms of the displacement S_1 and S_2 of the followers

$$\begin{aligned} \begin{bmatrix} {}^m x_{c1} \\ {}^m y_{c1} \end{bmatrix} &= \begin{bmatrix} \cos\theta & \sin\theta \\ -\sin\theta & \cos\theta \end{bmatrix} \begin{bmatrix} \varepsilon + R_r \sin\psi_1 \\ e + s_1 - R_r \cos\psi_1 \end{bmatrix} \\ \begin{bmatrix} {}^m x_{c2} \\ {}^m y_{c2} \end{bmatrix} &= \begin{bmatrix} \cos\theta & \sin\theta \\ -\sin\theta & \cos\theta \end{bmatrix} \begin{bmatrix} -\varepsilon - R_r \sin\psi_2 \\ -e - s_2 + R_r \cos\psi_2 \end{bmatrix} \end{aligned}. \tag{2.49}$$

From equation 2.49 the whole cam contours are obtained.

In order to lead to a feasible mechanism, the radius R_r of the ball must satisfy the condition, as shown in figure 2.6 two balls on the upper and lower side must not interfere with each other. Since k is defined the distance between the center of two consecutive balls, we have constraint $2R_r < k$. Hence, we obtained the condition on $2R_r$:

$$\frac{R_r}{k} < \frac{1}{2} \tag{2.50}$$

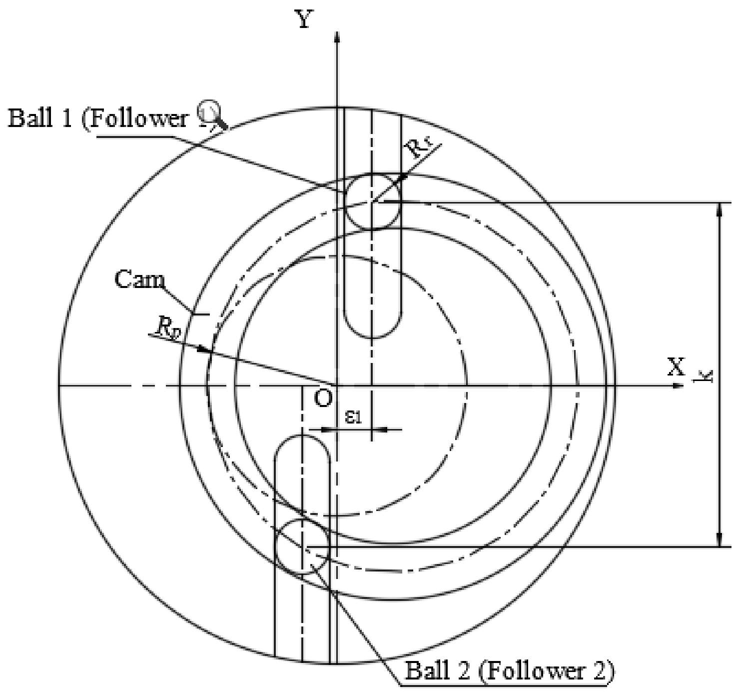

Figure 2.6: Home configuration of the groove cam mechanism

2.3 Objective function to obtain the minimum cam size and the maximum absolute pressure angle.

It is clear that, for a prescribed follower motion, the definition of the values for the base circle radius of the cam, the eccentricity and the radius of the ball (roller follower) is generally done before the determination of the cam profile. Then the values of the pressure angle and the radius of curvature are evaluated in order to check if the system will be operating in a good condition or not. In other words, it could be stated that the pressure angle is limited to values that avoid jamming between the ball and its guideway, while the radius of curvature of the groove cam surface is constrained to minimum values that prevent the undercutting phenomenon. In a general way, the pressure angle decreases and the radius of the curvature increase when the base circle radius of the cam increases. Moreover, the values of the eccentricity and the radius of the ball affect the pressure angle and the radius of curvature. So it can be concluded that these two parameters, the pressure angle and the radius of curvature vary inversely. Therefore, in what follows some of the most fundamental constraints and an objective function are presented in order to define a general procedure that can help in the definition of the optimum cam size for a prescribed follower motion.

The two first constraints associated with the cam synthesis procedure are the maximum allowed values of the pressure angle for the rise and the fall follower motions [5, 9] which can be expressed by,

$$B_1: \psi_{rise-max} = max\left|\psi\left(h, \beta_1, R_b, R_{r,}\varepsilon, s, s'\right)\right| \leq 30°; \tag{2.51}$$

$$B_2: \psi_{fall-max} = max\left|\psi\left(h, \beta_2, R_b, R_{r,}\varepsilon, s, s'\right)\right| \leq 30°; \tag{2.52}$$

where $\beta_1$and β_2 are the amplitudes of the cam angle rotation for the rise and the fall follower motion, respectively. The maximum value of the pressure angle can be obtained by equation 2.14 if the ball follower motion is prescribed, which is commonly known as cam law.

From equation 2.14 a constraint related to the pressure angle directly results from the domain analysis of the function obtained by,

$${R_p}^2 + \varepsilon^2 \geq 0$$

Also, we have constraint related by as

$$R_p = R_b + R_r.$$

Hence,

$$B_3: R_b + R_r \geq \varepsilon; \tag{2.53}$$

the value of the radius of curvature can be obtained from equation 2.16 when the ball motion is known. Thus, the conditions to the radius of curvature of the pitch curve $\rho_p$for the convex and concave cam surfaces of a groove cam, respectively,

$$B_4: \rho_p(R_b, R_r, s, s', s'') > R_r; \tag{2.54}$$

$$B_5: \rho_p(R_b, R_r, s, s', s'') < 0; \tag{2.55}$$

Obviously, concluded that unacceptable cam profiles are within the interval

$$0 \leq \rho_p \leq R_r.$$

In practical engineering to guarantee that the system can easily be assembled, two conditions should be satisfied following:

B_6: $R_r \leq \varepsilon$; (2.56)

B_7: $\varepsilon \leq R_b$; (2.57)

Finally, in order to ensure that the results obtained, in the cam synthesis procedure, are reasonable, some simple bounds are imposed to variable R_b, ε and R_r as follows,

B_8: $R_b^{lb} \leq R_b \leq R_b^{ub}$; (2.58)

B_9: $\varepsilon^{\mathrm{lb}} \leq \varepsilon \leq \varepsilon^{ub}$; (2.59)

B_{10}: $R_r^{lb} \leq R_r \leq R_r^{ub}$; (2.60)

with the superscripts *lb* and *ub* denote the lower and the upper bounds, respectively.

From the stated above, we can sum up that, the design variables considered are the base circle radius of the cam, the eccentricity and the radius of the ball follower. The objective function includes three different components. The first one influences the mass of cam via the size of the base circle radius. The other two terms are related to the performance of the system, they are associated with the pressure angles for the rise and the fall follower motion. In this study, all of the three components of the objective function have the same weight, they are equally penalized. Besides, other possibilities can easily be incorporated, but of course, they will depend on the specific problem to be solved.

Hence, to optimize the cam size, the cam designer must choose the values of parameters h, β_1,β_2, R_b^{lb}, R_b^{ub}, $\varepsilon^{\mathrm{lb}}$, ε^{ub}, R_r^{lb}, R_r^{ub} to satisfy all the designing conditions (B_1 to B_{10}) to obtain the minimization of (R_b, ε, R_r) of the groove cam design.

2.4 Application design

In order to confirm the design effect of the proposed solution method above. A constant-diameter cam was designed using the data shown in tables 2.1 and 2.2.

A groove cam rotates in constant speed, and two ball followers move to reciprocating displacement with double harmonic function [6]. The equations for double harmonic function are given followings:

for the rise

$$s=\frac{h}{2}\left\{\left[1-cos\left(\pi\frac{\theta}{\beta}\right)\right]-\frac{1}{4}\left[1-cos\left(2\pi\frac{\theta}{\beta}\right)\right]\right\}, \quad (2.61)$$

for the fall

$$s=\frac{h}{2}\left\{\left[1+cos\left(\pi\frac{\theta}{\beta}\right)\right]-\frac{1}{4}\left[1-cos\left(2\pi\frac{\theta}{\beta}\right)\right]\right\}. \tag{2.62}$$

Table 2.1: Displacement conditions for groove cam

Segment	Cam angle(^{o})	Total angle of segment β(^{o})	Motion type mm	Function
1	0-180	180	12 rise	Double harmonic
2	180-360	180	12 return	Double harmonic

Table 2.2: Design parameters for groove cam

Parameters	Value
Prime circle radius R_p (mm)	14
Eccentricity(ε)/mm	0
Ball radius (follower) R_r (mm)	3

By using DYNACAM of Robert L. Norton. The corresponding displacement, velocity, acceleration diagram of the groove cam is depicted in figure 2.6. From the curves plotted in figure 2.6, it can be observed the ball's response of velocity and acceleration are continuous and smooth across the entire interval. Also, by observing figure 2.7 it is visible that the value of the pressure angle at the contact point obtains the maximum value of 21.32°. Therefore, the results of calculating are satisfied with the cam law design.

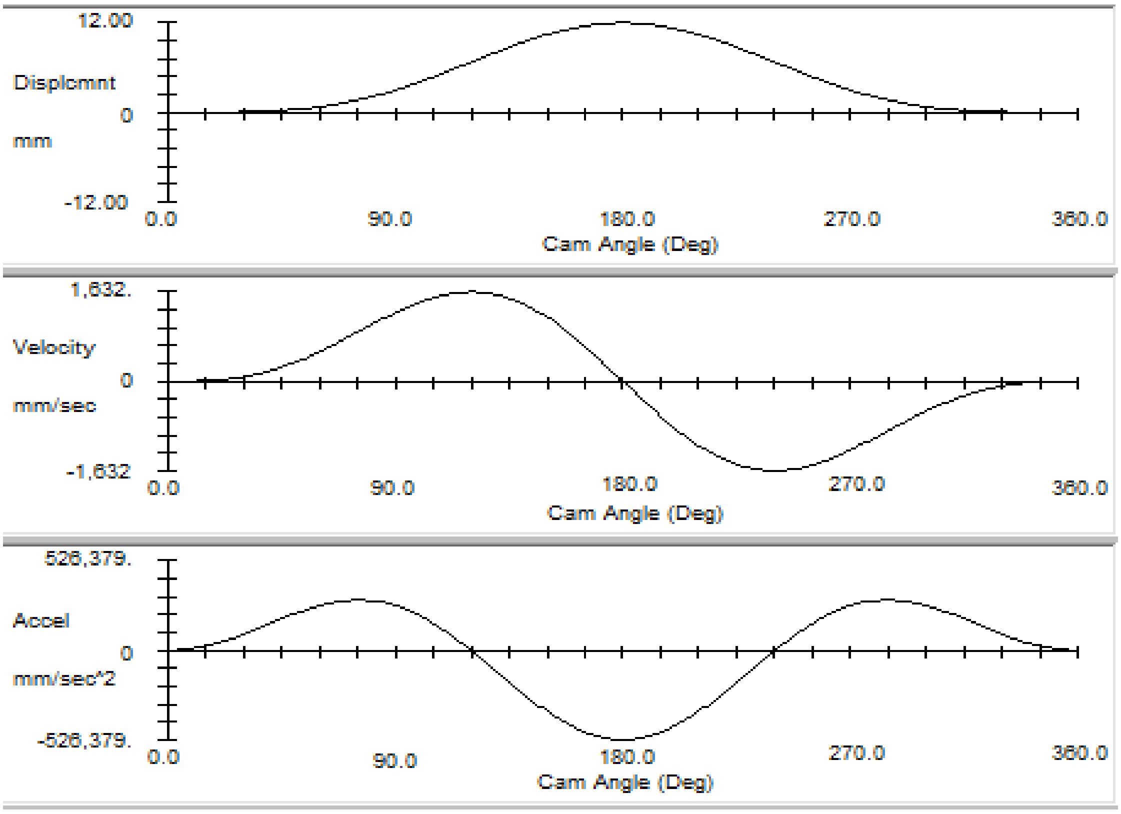

Figure 2.7: Displacement, velocity, acceleration of the groove cam

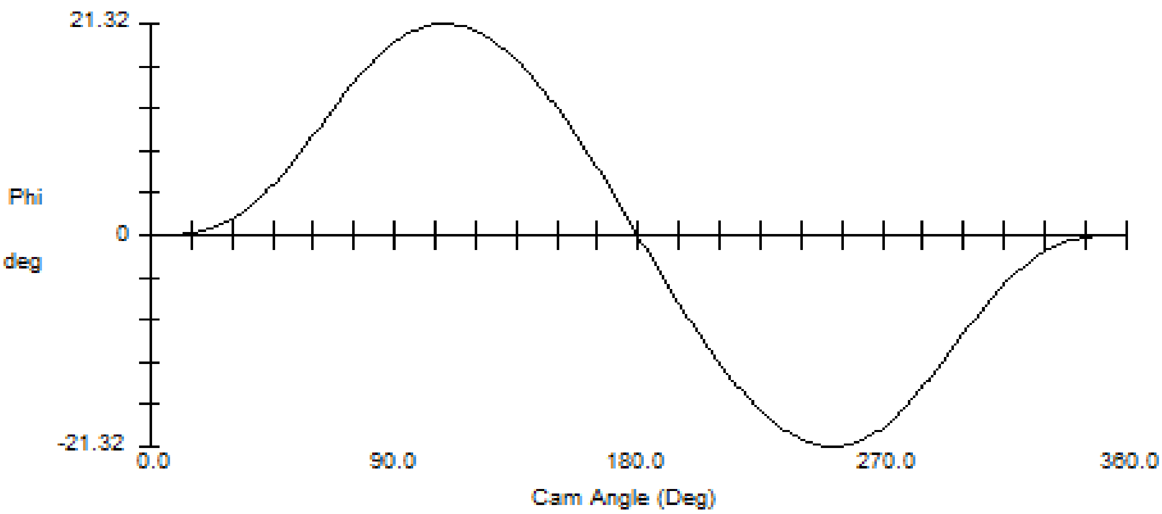

Figure 2.8: Pressure angle at the contact point of the groove cam

Chapter 3

CONTACT STRESSES

3.1 Contact stresses and failure

When two bodies with curved surfaces in contact, for example, ball and groove, sphere-one-sphere…in which the relative motions between the surfaces are essentially pure sliding, such as a groove cam runs against a spherical ball. When two surfaces are in pure rolling contact or are primarily rolling in combination with a small percentage of sliding, a different surface failure mechanism comes in play, called surface fatigue. Many applications of this condition exist such as cam with roller followers, ball and roller bearings, gear tooth contact.

The stresses introduced in two materials contacting at a rolling interface are highly dependent on the geometry of the surfaces in contact as well as on the loading and material properties. The general case allows any three-dimensional geometry on each contact member and as would be expected, its calculation is the most complex. Two special geometry cases are of practical interest and are also somewhat simpler to analyze. These are sphere-on-sphere and cylinder-on-cylinder. In all cases, the radii of curvature of one mating surface, these special cases can be extended to include the sub-cases of sphere-on-plane, sphere-in-cup, cylinder-on-plane, and cylinder-in-trough. It is only necessary to make the radii of curvature of one element infinite to obtain a plane, and negative radii of curvature define a concave cup or concave trough surface. For example, some ball bearings can be modeled as sphere-on-plane and some roller bearings and cylindrical cam followers as cylinder-in-trough.

As a ball passes over another surface, the theoretical contact patch is a point of zero dimensions. A roller against a cylindrical or flat surface theoretically contacts along a line of zero width. Since the area of each of these theoretical contact geometries is zero, any applied fore will then create infinite stress. We know that this cannot be true, as the materials would instantly fail. In fact, the materials must deflect to create sufficient contact area to support the load at some finite stress. This deflection creates a semi-ellipsoidal pressure distribution over the contact patch. In general case, the contact patch is elliptical as shown in figure 3.1 a**.** Spheres will have a circular contact patch, and cylinders create a rectangular contact patch as shown in figure 3.1 b.

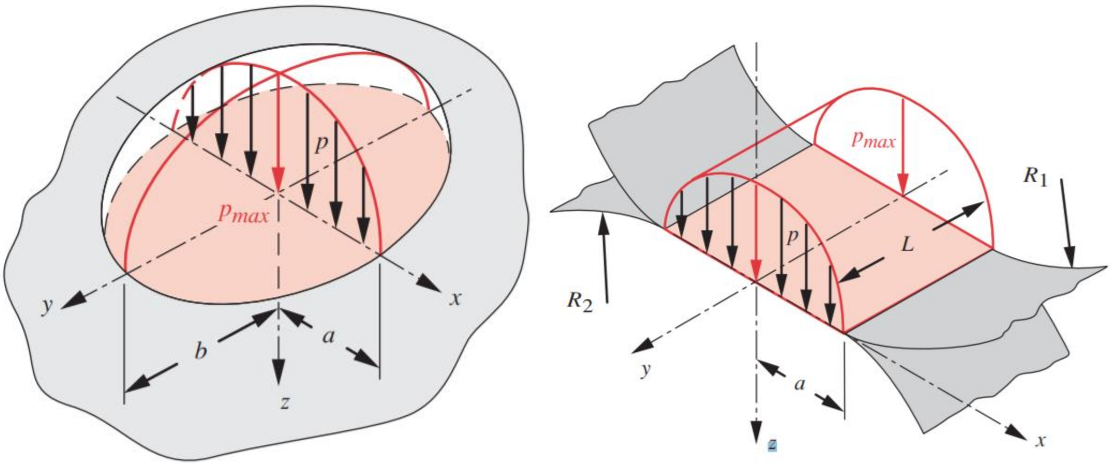

a) Ellipsoidal pressure distribution b) Rectangular pressure distribution

Figure 3.1: Pressure distributions and contact zones of spherical, cylindrical and general Hertz contact [6]

Consider the case of a spherical ball rolling in a straight line against a flat surface with no slip, and under a constant normal load is depicted in figure 3.2. If the load is such as to stress the material only below its yield point, the deflection in the contact patch will be elastic and the surface will return to its original curved geometry after passing through contact. The same spot on the ball will contact the surface against on each succeeding revolution. The resulting stresses in the contact patch are called contact stresses or Hertz stresses. The contact stresses in this small volume of the ball are repeated at the ball's rotation frequency. This creates a fatigue-loading situation that eventually leads to a surface fatigue failure.

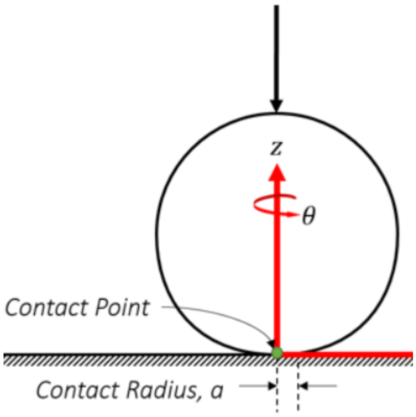

Figure 3.2: A spherical ball-on-flat surfaces [21]

This repeated loading is similar to a tensile fatigue-loading case. The significant difference, in this case, is that the principal contact stresses at the center of the contact patch are all compressive, not tensile. Fatigue failures are considered to be initiated by shear stress and continued to failure by tensile stress. There is also shear stress associated with these compressive contact stresses, and it is believed to be the cause of crack formation after many stress-cycles, which slowly spreads toward the surface. Example when the rolling elements move over such cracking figure 3.3**,** particles of the material breaks off. This is called pitting. Such pitting spreads progressively and possibly makes the bearing malfunction. This type of damage develops over rather a long time, and the damage is spread over and it rapidly proceeds to failure by spalling (*the loss of large pieces of the surface*) as shown in figure 3.4.

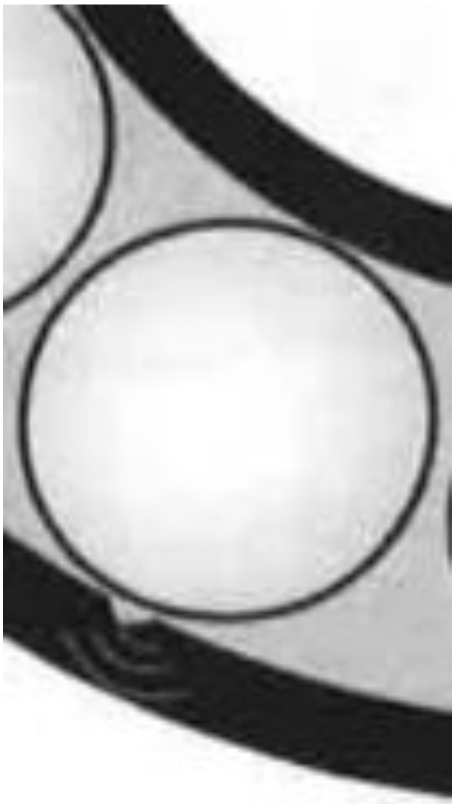

Figure 3.3: Cracking on the outer race of the ball bearing [22]

If the load is large enough to raise the contact stress above the material's compressive yield strength, then the contact-patch deflection will create a permanent flat on the ball. This condition is sometimes called false brinelling because it has a similar appearance to the indentation made to test a material's Brinell hardness. Such a flat on even one of its ball or rollers makes a ball or roller bearing useless.

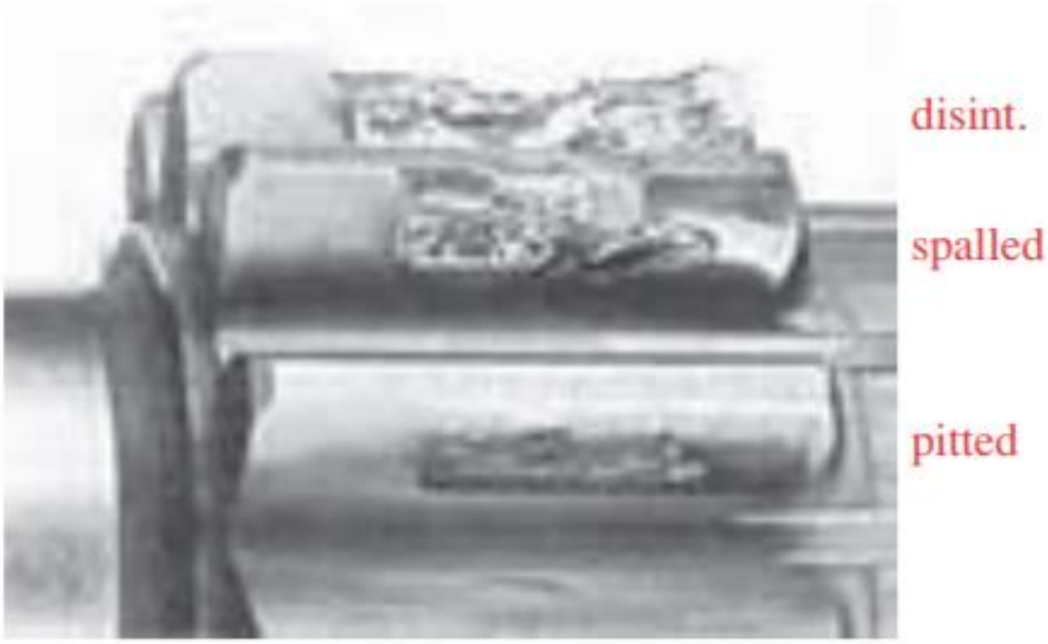

Figure 3.4: Spitting and spalling and disintegration of gear teeth [6]

Therefore, we will now investigate the contact-patch geometries, pressure distributions, stresses and deformations in rolling contacts starting with the relatively simple geometry of sphere-on-flat. General, it is evaluated by the Hertz theory of elastic contact [23] following section below.

3.2 Hertz theory of elastic contact

The first satisfactory analysis of the stresses at the contact of two elastic solids is due to Hertz. He was studying Newton's optical interference fringes in the gap between two glass lens and was concerned at the possible influence of elastic deformation of the surfaces of the lens due to the contact pressure between them. His theory established during in the year 1880, around considerable interest when it was first published and has stood the test of time. In addition to static loading, he also attempted the quasi-static impacts of spheres. Hertz also attempted to use his theory to give a precise definition of hardness of a solid in terms of the contact pressure to initiate plastic yield in the solid by pressing a harder body in contact with it. This definition has proved unsatisfactory because of the difficulty of detecting the point of the first yield under the action of contact stress. A satisfactory theory of hardness had to wait for the development of the theory of plasticity [23].

Hertz formulated the conditions expressed by equations which must be satisfied by the normal displacements on the surface of the solids. He first made the hypothesis that the contact area is, in general, elliptical, guided no doubt by his observations of interference fringes such as those shown in figure 3.5. He then introduced the simplification that, for the purpose of calculating the local deformations, each body can be regarded as an elastic half-space loaded over a small elliptical region of its plane surface. By this simplification, generally followed in contact stress theory, the highly concentrated contact stresses are treated separately from the general distribution of stress in the two bodies which arises from their shape and the way in which they are supported.

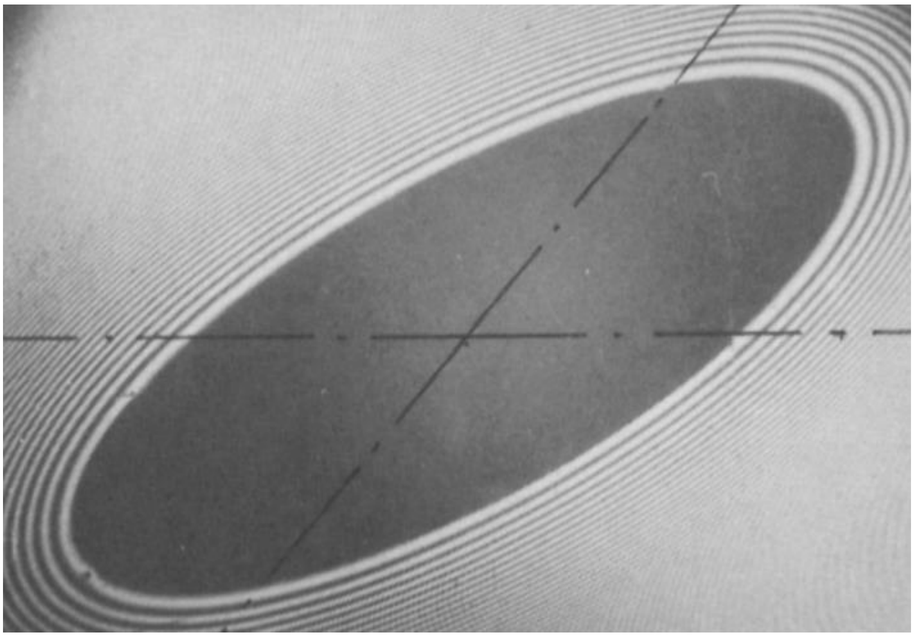

Figure 3.5: Geometry of surfaces in contact under loading [23]

In addition, the well-developed methods for solving boundary value problems for the elastic half-space are available for the solution of contact problems. In order for this simplification to be justifiable two conditions must be satisfied: 1) the significant dimensions of the contact area must be small compared with the dimensions of each body and 2) with the relative radii of curvature of the surfaces. The first condition is obviously necessary to ensure that the stress field calculated on the basis of a solid which is infinite in extent is not seriously influenced by the proximate roughly of its boundaries to the highly stressed region. The second condition is necessary to ensure firstly that the surface just outside the contact region approximate roughly to the plane surface of a half-space, and secondly that the strains in the contact region are sufficiently small to lie within the scope of the linear theory of elasticity. Metallic solids loaded within their elastic limit inevitably comply with this latter restriction. However, caution must be used in applying the results of the theory to low modulus materials like rubber where it is easy to produce deformations which exceed the restriction to small strains.

Finally, the surfaces are assumed to be frictionless so that only a normal pressure is transmitted between them. Although physically the contact pressure must act perpendicular to the interface which will not necessarily be planar, the linear theory of elasticity does not account for changes in the boundary forces arising from the deformation they produce. Hence, in view of the idealization of each body as a half-space with a plane surface, normal tractions at the interface are taken to act parallel to the z-axis and tangential tractions to act in the x-y plane.

Designating the significant dimension of the contact area by a_h, the relative radius of curvature by ρ_p, the significant radii of each body by R_1 and R_2 and the significant dimensions of the bodies both laterally and in depth by L we may summarize the assumptions made in the Hertz theory as follows:

i) Surfaces are continuous and non-conforming, which means that initial contact is a point or a line $a_h \ll \rho_p$;

ii) The strains are small $a_h \ll \rho_p$;

iii) Each solid can be considered as an elastic half-space: $a_h \ll R_{1,2}$, $a_h \ll L$;

iv) Surfaces are frictionless and cannot penetrate into each other.

3.3 Applied for studying case

For conducting to the thesis, the idea of altering the roller follower by using the balls is designed for a groove cam mechanism. By applying this technology one, the cam model constitutes one circular groove (cam) is the diving component, the other one is the driven component (the output). The moments and velocities are transferred by the balls between. The transmission is done with a variation of the radius of the circular groove cam, where balls roll along the grooves and perform the pure motion.

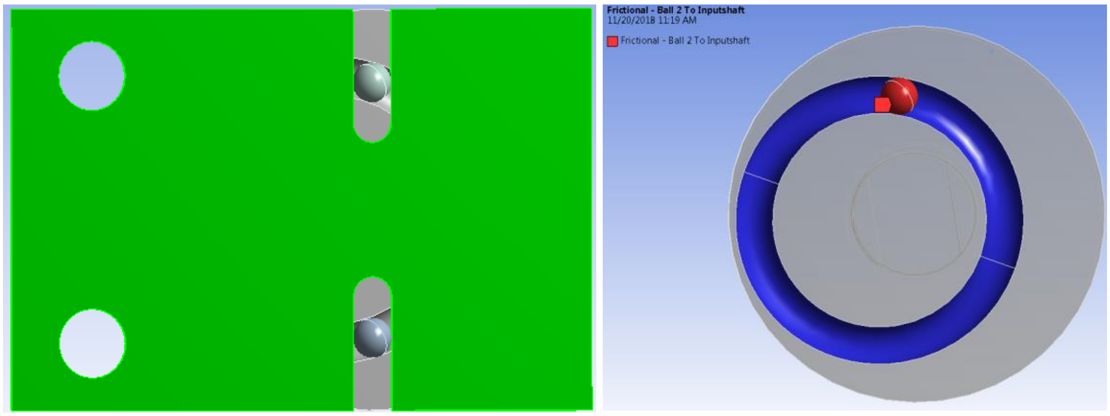

Figure 3.6: The ball on a circular groove surface contact

Thus, the stress analysis of the ball and groove surfaces must be interesting in this design and should take into account in this research. This topic will be discussed in detail in the following sections.

Consider the case of a spherical ball rolling in a circular groove cam with no slip, under a constant normal load. Which can be treated like as the case of ball bearings, it means can be modeled as sphere-on-plane contact type as shown in figure 3.6.

Now we will investigate the contact-patch geometries, pressure distributions, stresses, and deformations in rolling contacts with the relative geometry of the balls and their grooves cam following.

3.3.1 Analysis and calculate the forces acting on the steel ball

For this case of study, a rotary motion from an electric motor is transmitted to the input camshaft has a torque value of 1 Nm, made the input camshaft to rotate at the same constant angular velocity. In fact of the design principles, we just need to design a straight groove on the output shaft and middle part. But to reduce the forces acting on the steel balls as well as to forces evenly distributed across the cam mechanism while working. We should design on the output shaft which has more one groove. Therefore, make the cam mechanism works smoothly and stable. In this study, the cam mechanism was designed has two straight grooves.

Because all forces acting on each steel ball has equal value. Therefore no loss of generality we can calculate the forces acting on the steel ball in a straight groove as following:

$$F = \frac{1}{n}\frac{M}{D}, \tag{3.1}$$

where F is the force acting on the steel ball, M is the moment acting on the input cam shaft, D is the distance from the center of rotation to the point of force and n is the number of the straight grooves on the output camshaft.

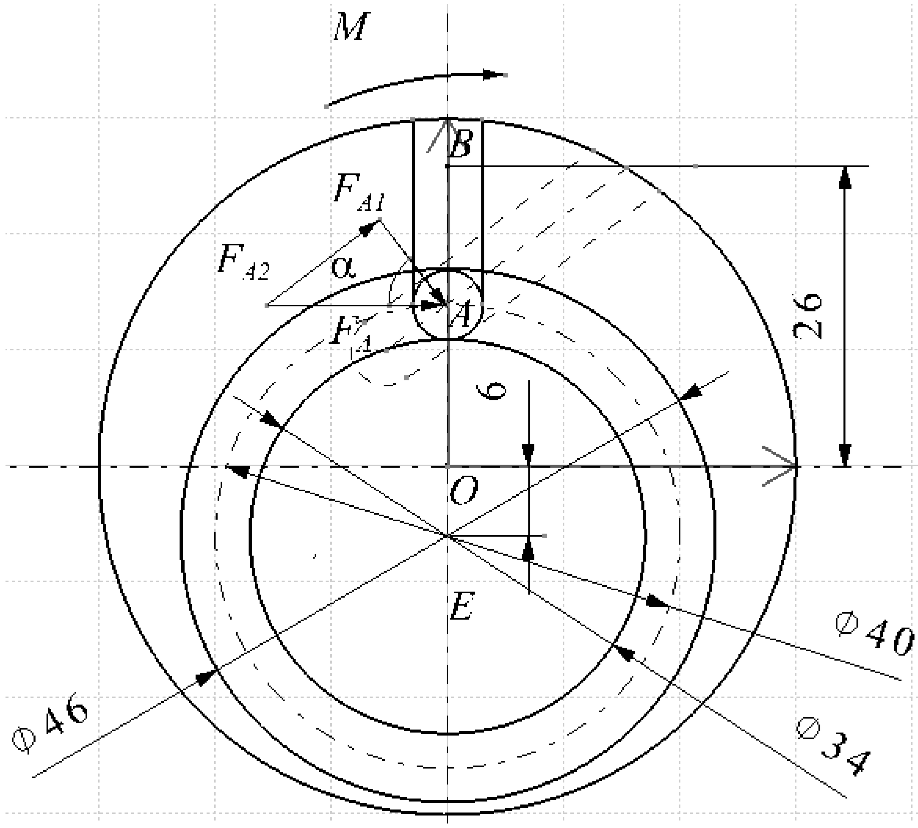

Figure 3.7: Diagram placed forces on the ball

When the cam mechanism works, the steel ball always moves along in the straight groove on the middle part from point A (the nearest point to the axis's rotation of the input camshaft) to point B (the farthest point) correspond to about the smallest eccentric and the greatest of the input cam shaft. Therefore, the forces acting on the ball in the groove achieve the greatest value when it is the nearest to the axis's rotation center. From the diagram in figure 3.7 we calculated the maximum force acting on the ball follows:

$$F = \frac{1}{n}\frac{M}{OA}. \tag{3.2}$$

In this design, given n=2, M=1 Nm, $OA = 14 \cdot 10^{-3}$ m.

By substituting the magnitude of parameters in equation (3.2) we got the magnitude of

$$F_A = \frac{1}{2}\frac{1}{14 \cdot 10^{-3}} = 35.714(N)$$

where OA is the distance from *O* center of input cam shaft to *A* point, F_A is the force perpendicular to the OB at *A*. F_A is divided into F_{A1} (the normal force, which is the force always perpendicular to the side wall of the straight groove) and F_{A2} (the sliding force, which is force always parallel with the center line of the straight groove).

$$F_{A1} = F_A \cos\alpha, \qquad (3.3)$$

$$F_{A2} = F_A \sin\alpha, \qquad (3.4)$$

where α is the angle between the direction of the force F_A and the force $\boldsymbol{F_{A1}}$. Which also is the angle by the straight groove axis on the output shaft and the vertical direction, in this design $\alpha = 30$ degrees. The F_{A1} makes the output camshaft rotating, the force F_{A2} made the steel ball to slide along the straight grooves of the output shaft.

Substituting the magnitude of F_A into equation 3.3 and 3.4 obtained:

$F_{A1} = 35.714cos30 = 30.929$(N),

$F_{A2} = 35.714sin30 = 17.875$(N).

3.3.2 Calculation of the contact pressure and contact stress for the steel balls and the groove

The contact between the ball with right and left of the side wall of the straight groove of the output camshaft was assumed like as contact of a sphere-on-plane. The calculation was done in Hertz contact stress.

A geometry constant can be defined that depends only on the radius R_f and R_r of two contact surfaces

$$B = \frac{1}{2}\left(\frac{1}{R_f} + \frac{1}{R_r}\right), \qquad (3.5)$$

where R_f, R_r are the radius of the plane and the steel ball respectively. To account for this case of sphere-on-plane, R_f becomes infinite, making $1/R_f$ gets zero. We got the magnitude of

$$B = \frac{1}{2}\left(\frac{1}{\infty} + \frac{1}{3\cdot 10^{-3}}\right) = 166.67 \text{ (m}^{-1}\text{)}.$$

The balls and all parts of the cam mechanism were made of steel so the material constant was determined as follows:

$$m_1 = \frac{1-v_1^2}{E_1}, \quad m_{12} = \frac{1-v_2^2}{E_2}. \tag{3.6}$$

Where v_1, v_2 are the Poisson's ratios of the steel materials of the ball and the groove cam and E_1, E_2 are the corresponding Young moduli. In this case $v_1 = v_2 = 0.3$ *and* $E_1 = E_2 = 2\cdot 10^{11}$(N/m).

Hence the magnitude of

$$m_1 = m_2 = \frac{1-0.3^2}{3\cdot 10^{11}} = 4.55 \cdot 10^{-12} \text{ (m}^2\text{/N)}.$$

The radius of the contact-patch of the contact between the steel ball and the straight groove is the form:

$$a_h = \sqrt[3]{0.375\,\frac{(m_1 + m_2)}{B} F_{A1}}\,. \tag{3.7}$$

The magnitude of

$$a_h = \sqrt[3]{0.375\,\frac{2\cdot 4.55\cdot 10^{-12}}{166.667}\,30.929} = 8.587\cdot 10^{-5}\text{(m)}.$$

The area of the contact patch of the contact between the steel ball and the straight groove is found from the equation:

$$A = \pi a_h^2, \tag{3.8}$$

the magnitude of

$$A = \pi \cdot (8.587 \cdot 10^{-5})^2 = 2.317\cdot 10^{-8}\text{(m}^2\text{)}.$$

The average and maximum contact pressure can be found respectively

$$P_{aveg} = \frac{F_{A1}}{A}, \tag{3.9}$$

$$P_{max} = \frac{3}{2}\frac{F_{A1}}{A}. \tag{3.10}$$

Substituting the magnitude of F_{A1} and A into equation 3.9 and 3.10 obtained:

$$P_{aveg} = \frac{30.929}{2.317 \cdot 10^{-8}} = 1335(\text{MPa}),$$

and

$$P_{max} = \frac{3}{2}\frac{F_{A1}}{A} = \frac{3}{2}1335 = 2002.5\ (\text{MPa}).$$

The maximum normal stress in the center of the patch at the surface was found

$$\sigma_{zmax} = -P_{max} = 2002.5(\text{MPa}) \tag{3.11}$$

$$\sigma_{xmax} = \sigma_{ymax} = \frac{(1+2v)}{2}P_{max}\ . \tag{3.12}$$

Thus

$$\sigma_{xmax} = \sigma_{ymax} = \frac{(1+2 \cdot 0.3)}{2}2002.5 = 1602\ (\text{MPa}).$$

There is also principal shear stress induced from these principal normal stresses

$$\tau_{yzmax} = \frac{P_{max}}{2}(\frac{1-2v}{2} + \frac{2}{9}(1+v)\sqrt{2(1+v)}\ , \tag{3.13}$$

the magnitude of shear stress obtains

$$\tau_{yzmax} = \frac{2002.5}{2}(\frac{1-2 \cdot 0.3}{2} + \frac{2}{9}(1+0.3)\sqrt{2(1+0.3)} = 666.65\ (\text{MPa}).$$

Actually, the value is not maximum at the surface, but rather at a small distance $Z_{@\tau max}$ below the surface. Its location under the surface is expressed by the following relationship

$$Z_{@\tau max} = a_h\sqrt{\left(\frac{2+2v}{7-2v}\right)}, \tag{3.14}$$

the magnitude is obtained

$$Z_{@\tau max} = 8.587 \cdot 10^{-5}\sqrt{\left(\frac{2+2 \cdot 0.3}{7-2 \cdot 0.3}\right)} = 5.473 \cdot 10^{-5}\ (\text{m}).$$

All the stresses found so far exist on the centerline of the patch. At the edge of the patch, at the surface, there is a condition of pure shear stress with the magnitude

$$\tau_{xy} = P_{max}\left(\frac{1-2\cdot v}{3}\right) = 2002.5\left(\frac{1-2\cdot 0.3}{3}\right), \tag{3.15}$$

final value

$$\tau_{xy} = 267 \text{ (MPa)}.$$

Chapter 4

NUMERICAL METHOD

4.1 Finite element method approach

In this section, we analyze the general methods that ANSYS uses in solving for the desired results. As the name suggests, the finite element method (FEM) first requires meshing the system that is to be analyzed into a finite number of elements. In ANSYS, one can manually create the mesh configuration, or can alternatively let the software use a special algorithm to generate the mesh profile. Depending on the level of accuracy of the results that is desirable, one can choose to refine the mesh, so that there will be more elements near any region in the model. Having a greater number of elements in the system can allow the results to converge within appropriate bounds. It should also be noted that an element is generally comprised of multiple nodes. A configuration of the nodes in each element can vary for different element types. For example, an element, PLANE 183, has the configuration, as shown below.

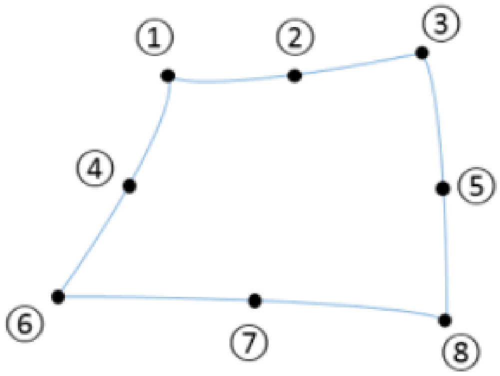

Figure 4.1: The configuration of PLANE 183 [24]

Each of the eight nodes shown above can be described by displacement vectors (translational and rotational components, depending on the element type) and by fore vectors. Finite element method first solves for the nodal displacement field with the specified boundary conditions. The underlying system of equations that ANSYS solves for is shown below.

$$[K]\{u\} = \{f\}. \tag{4.1}$$

Thus,

$$\{u\}=[K]^{-1}\{f\}, \tag{4.2}$$

Where $[K]$ is referred to as the global stiffness matrix, and contains n by n components, where n is equal to the total degrees of freedom of the system. On the other hand, $\{u\}$ and $\{f\}$ are column matrices with n components, which represent nodal displacement fields and nodal force fields, respectively. After specifying the appropriate boundary condition in ANSYS, it then solves for these displacement and force fields simultaneously.

However, in the case of our Hertz contact problem, we note that the system is a highly nonlinear problem, due to the mechanical interactions between multiple components of the system. The fact that the boundary condition at the contact interface between the sphere and the rigid plate changes throughout the loading process indicates that an iterative approach is necessary to converge the solutions. More specifically, we observe that the state of traction and the stiffness of the system depend on the displacement near the contact interface.

$$[K(u)]\{u\} = \{f(u)\} \tag{4.3}$$

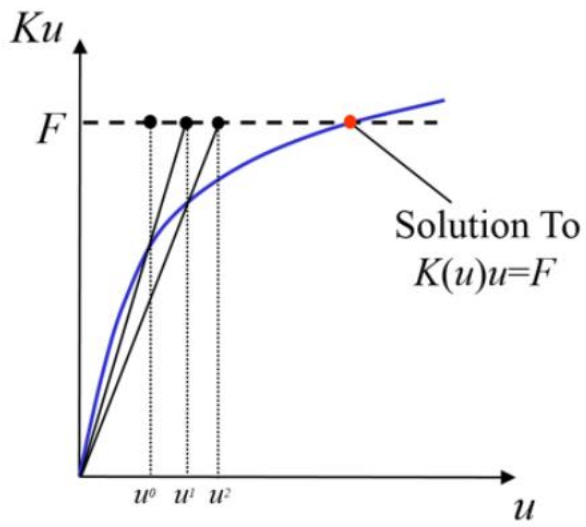

Figure 4.2: Schematic of the successive approximation method

By default, ANSYS requires that force reaction balance is satisfied within a given tolerance level.

If the method of linear analysis is selected, the solution would most likely fail to converge for a system that contains a variable contact interface since only a single iteration would be performed. To overcome this issue, we introduce the Newton-Raphson (*NR*) method in solving for the solution. Given an initial guess, *NR* method generates a sequence of guesses that converges to a root of the equation. This method is based on making successive approximations to a solution using the previous value of u to determine $K(u)$.

$$\{u^{r+1}\}=[K(u)^{r}]^{-1}\{f\}, \tag{4.4}$$

In addition to the Newton-Raphson method, other techniques can be applied, in order to help convergence issues that might arise. This method, known as incremental loading technique, makes subdivisions of the load into smaller steps. While increasing the number of sub-steps may require more computation, it helps to linearize the solution by making smaller loads, such that the residuals between iterative solution and true solution also become smaller. It must be noted that these two techniques can be applied to our finite element analysis individually or can be used simultaneously. Using both of these, however, is most recommended, since incremental loading technique can help decrease the number of iterations required to obtain a converged solution.

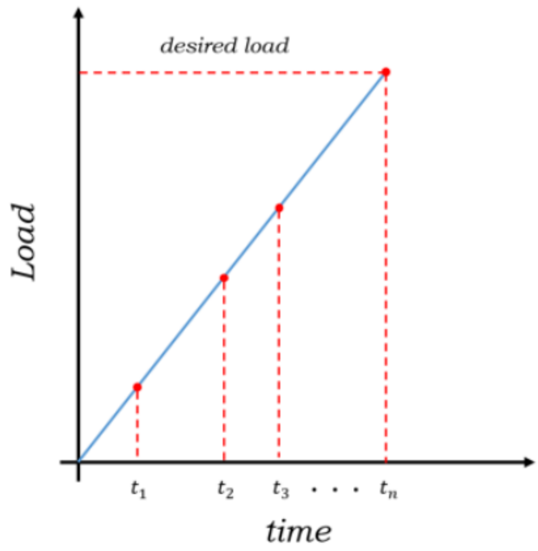

Figure 4.3: Schematic of incremental loading technique

Once the solution has converged, the nodal displacement fields obtained from the final equilibrium iteration can be further used to generate the strain and stress distribution at each node. In FEM, analyses, similar to the ones found under Mathematical Model section, are adapted to compute these nodal fields. However, we have to modify our approach slightly to take into account the fact that we now have a finite number of elements. This calls for a linear, first-order approximation method among the neighboring elements in computing strain distribution.

4.2 Application for the design case

The mechanism was drawn in CATIA V5-R16, as mentioned above. Which are solid bodies have the following specifications: All components were assumed to be solid for the following simulations in the FEM programmes used [23].

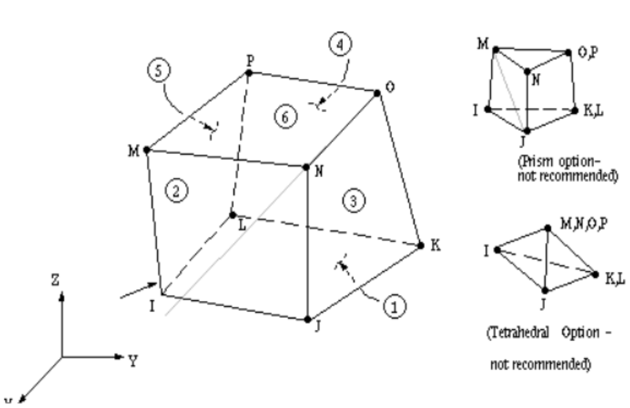

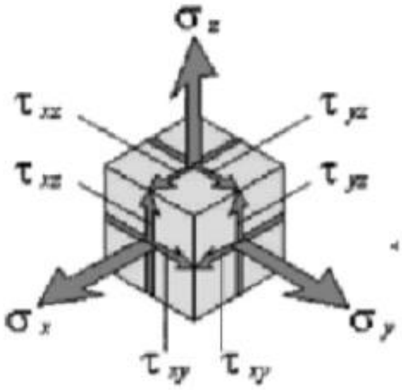

Figure 4.4: Degrees of freedom of a solid body [23]   Figure 4.5: Von Mises stress [23]

Von Mises stress:

σ= normal stress in x, y, z-direction

τ= shear stress in xy, yz, zx plane

The mathematical definition in general state of tress is defined as followed:

$$\sigma_v=\sqrt{\sigma_x{}^2+\sigma_y{}^2+\sigma_z{}^2-\sigma_x\sigma_y-\sigma_y\sigma_z-\sigma_z\sigma_x+3\left(\tau_{xy}^2+\tau_{yz}^2+\tau_{zx}^2\right)} \tag{4.5}$$

Von Mises plastic distortion hypothesis is shown in figure 4.5 the value, which gives a result when a material gets from elastic area to plastic area. After certain stress intensity, the material deformation cannot back in its original state after the load is relieved. One the plastic state reached, irreparable harm is done to the material's structure. The Von Mises stress is a common analysis for not too brittle materials like steel or aluminum.

By using ANSYS for investigating contact problems in groove cam design, the contact finite element analysis (FEA) can show information under contact [25], such as contact stress, strain, penetration and so on, which play a significant role in the optimum design of cam mechanism. The analysis of the contact problem is a major concern in many engineering applications. The numerical modeling of practical contact problems requires special attention because the actual contact area between the contacting bodies is usually not known in advance. With the change of load, material, boundary condition or other factors, touch or separation will take place between surfaces, most frictional effects on contact problems need to be considered. They may be disordered as well as nonlinear. ANSYS gives a good blueprint for contact analysis which can take friction heat and electrical contact into account. It also has a special contact guide which is conveniently for creating contact pairs. The internal expert system of contact analysis does not require any set of related contact parameter in a general contact analysis. So it can easily establish contact analysis [26-28].

The study takes the contact between the balls and their grooves in the groove cam mechanism as an example, discussed and built finite element three-dimensional model by using Finite Element Analysis ANSYS workbench software. Based on the results show that solving the ball contact problems with ANSYS workbench software is feasible and it has a good agreement with the stress and deformation of the actual situation. The FEM results provide a reference for the design, optimization and failure analysis of cam mechanism and have practical engineering value.

4.3 Finite Element Calculations

Assume that contact between the ball and its circular groove likes as contact of a sphere on a sphere and contact between the ball and its straight groove likes as contact of sphere-on-flat plate. Hertz elastic contact theory has solved the calculation problems of contact stress and deformation of the balls and their grooves of the groove cam mechanism successfully. It uses the following assumptions to solve the contact shape and dimension and surface pressure distribution of elastic solids.

i) The first, the objects contact with each other which only produce elastic deformation obey Hook's law.

ii) The second, the contact surface is smooth, which only have the effect of the normal force.

iii) The third, contact size is much smaller than the size of the curvature radius of the contact bodies' surface. Contact problem of ball and groove basically corresponds with the Hertz assumption.

In contact problem involved two boundaries, it is natural that take on the boundary as target surface and take the other on a contact surface. Surface - surface contact is very suitable for those problems just as: interference fitting installation, or embedded contact, forging and deep - drawing. Typical of surface-surface contact's analysis steps include:

(1) Build a 3D geometry model and mesh;

(2) Identify contact pairs;

(3) Name target surface and contact surface;

(4) Define the target surface;

(5) Define contact surface;

(6) Set up element key options and real constants;

(7) Define and control rigid goal's movement (only applicable in rigid-flexible contact);

(8) Apply the necessary boundary condition;

(9) Define solution options and load steps;

(10) Solve contact problems;

(11) Look over and analyze results.

Model foundation

3D analytic model of the groove cam is established by using CATIA software. Chamfer and edges have little effect on contact stress and deformation of the groove cam, so it is ignored when modeling. However under the condition that the model should be simplified as far as possible so that the computational time could be reduced, simply and accurately reflects the mechanical property of the solid model. By use of CATIA the groove cam mechanism model is built as figure 4.6 and imported into ANSYS figure 4.7.

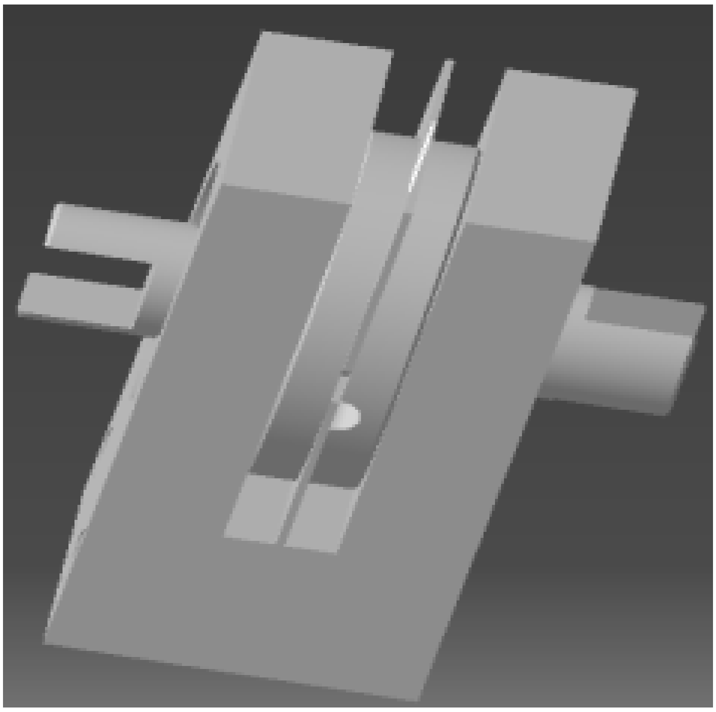

Figure 4.6: The first groove cam design model

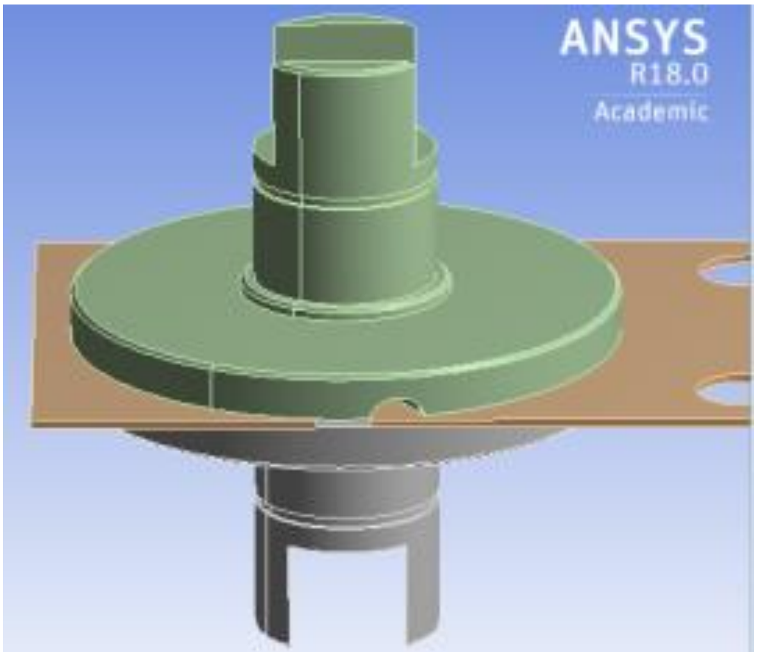

Figure.4.7: The imported model in ANSYS

In theory, it is feasible that a model can be changed such as material property, retrained displacement and applied load, and so on. Therefore, in this case, the groove cam mechanism model which is created and imported into ANSYS without its frame and the bearings part. Hence, the groove cam mechanism in ANSYS workbench is composed of the input cam shaft, output shaft, middle part, and the balls as shown in figure 4.7. The material of all parts is steel, the elasticity model is 2 *E*5 MPa, Poisson's ratio is 0.3

Meshing

Meshing is the most key link in the process of finite element analysis. And its quality has a direct influence on the precision and speed of the calculation. There are several kinds of the meshing methods in ANSYS following:

Free meshing methods: by using the free meshing method the hexahedron unit cannot be applied, but the refined mesh is convenient. And it has not any special requirement for the model. It is advised to use the quadratic tetrahedrons unit along with smart sizing for intelligent control over the grid size.

Mapped meshing method: by using the mapped meshing method the hexahedron unit can be applied. It is more precise than the free meshing method and also reduces the calculating time, but there is a special geometrical shape requirement of the model. The model can be obtained by gluing areas. Specifically, it is suggested to use Boolean operations to divide a complicated model by means of tetrahedrons or hexahedrons. Then the mapped meshing method can be used.

Sweeped meshing method: by using this sweeped meshing method a boundary face is meshed and sweeped through a given path to obtain the final result. The rotational parts as the input camshaft and out shaft, as well as the ball of the groove cam mechanism, are to this method.

The meshing result of the groove cam based on ANSYS is shown in figure 4.8. The element size is set 0.2 mm for each contact pairs. The other parts mesh in free meshing, but its smart size is set up in 1 to avoid the differences in the grid size. And it is useful to improve the precision of the FEA.

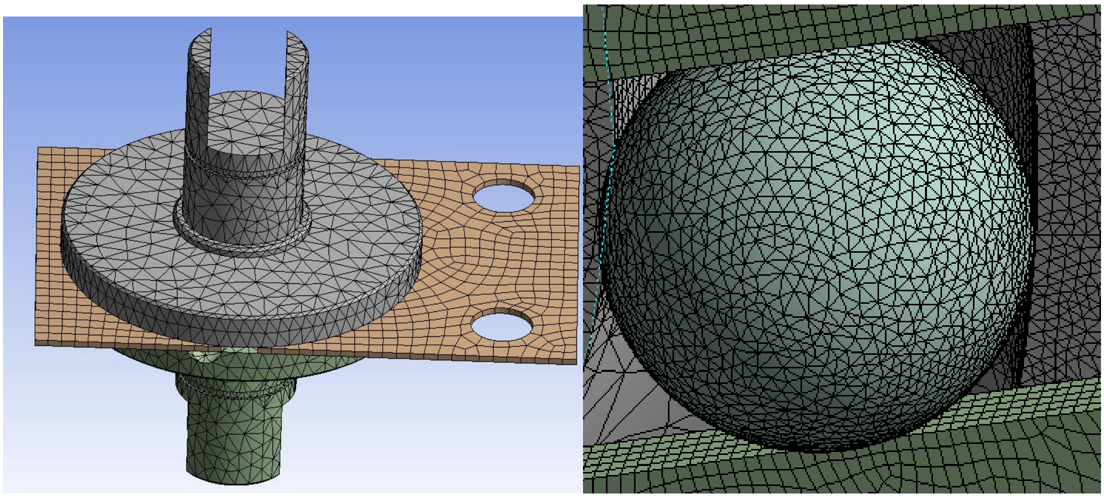

a) b)

Figure 4.8 a) the meshed model, b) the mesh of contact pairs between the ball and their grooves

Contact setting

Multi-body which has area-area contact needs to establish contact pairs. There are several principles in appointed interface and target surface of contact pairs as followings. First, if the thickness of two surface meshes is different, the thin surface is appointed contact surface and the thick one is target surface. Second, when the concave and convex surface contact with each other concave is appointed contact surface and convex is target surface. Third, if the area size of two surfaces is obviously different, the little one is appointed contact surface and the big one is the target surface. Last, when the stiffness of the two surfaces is different, the soft surface is the contact surface and the hard one is the target surface.

Define the contact pairs is frictional. Taking separately the groove surface of the input cam shaft, output shaft, and middle part as the contact surface and taking correspondingly sphere surface of the ball as the target surface, each two contact pairs can be built as shown in figure 4.9 to 4.11. It is necessary that to make sure the contact is a flexible body to the flexible body between the ball and the groove of each part. In every contact pair, the friction coefficient is set 0.15 and normal contact stiffness factor is set at 0.1(if the value is excessive, it will cause some problems which contact analysis do not convergent) and contact formula uses the pure Penalty function.

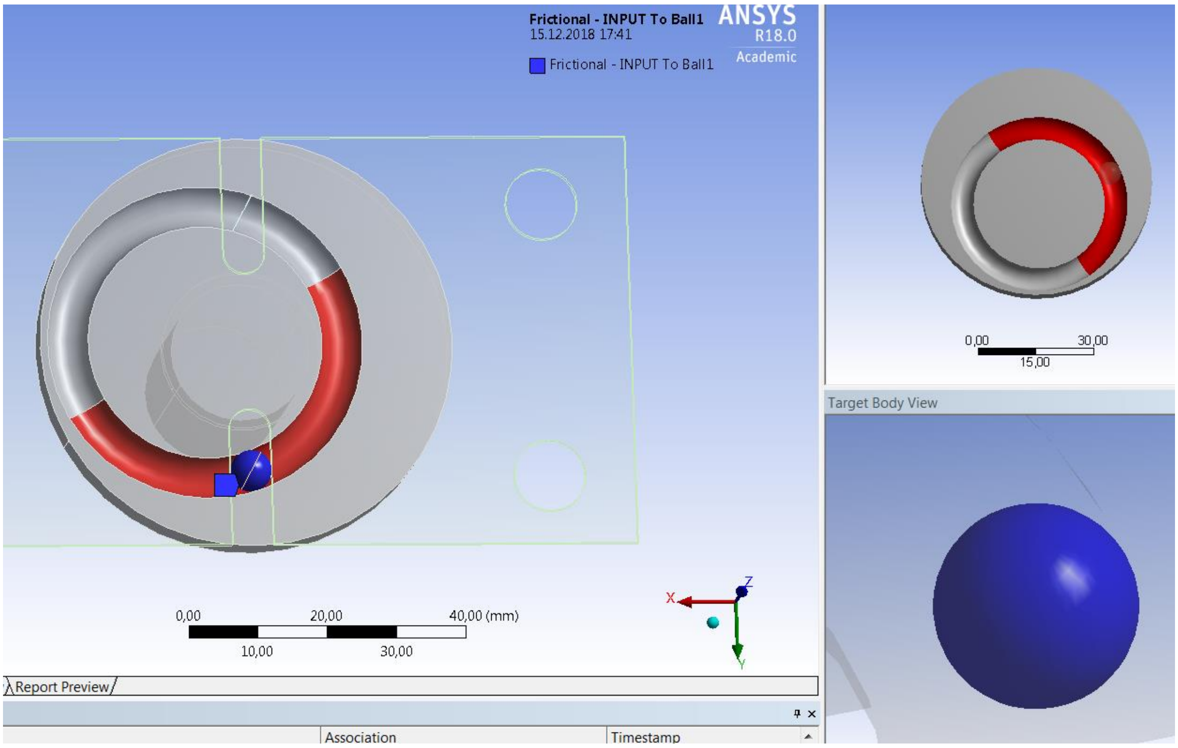

Figure 4.9: The frictional contact between the ball1 and its circular groove of the input camshaft

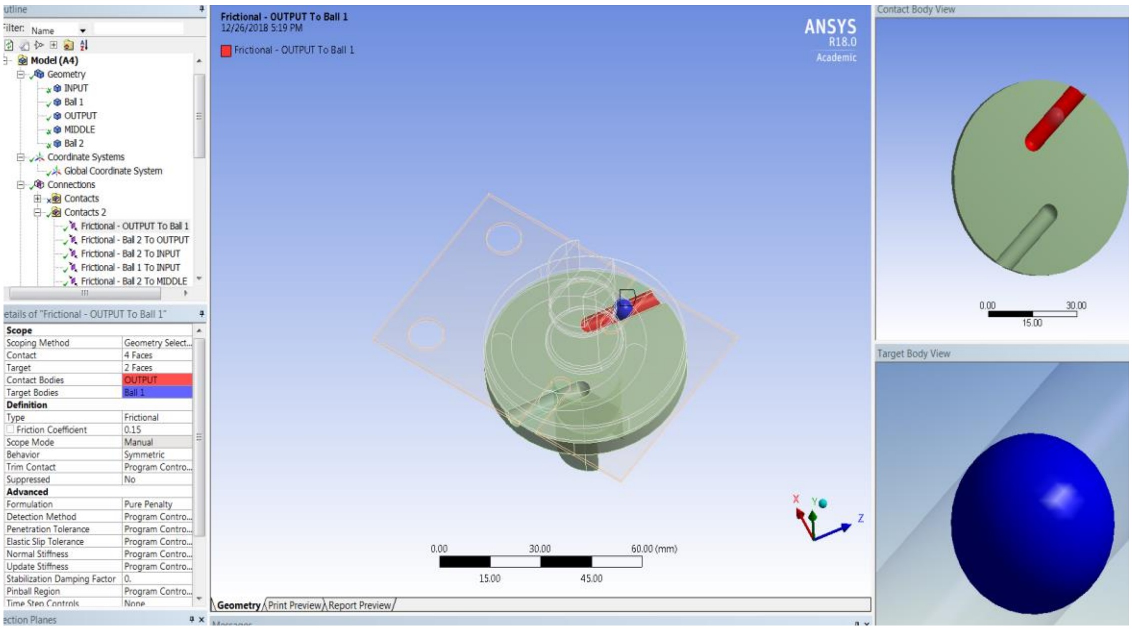

Figure 4.10: The frictional contact between the ball 1 and its straight groove of the output shaft

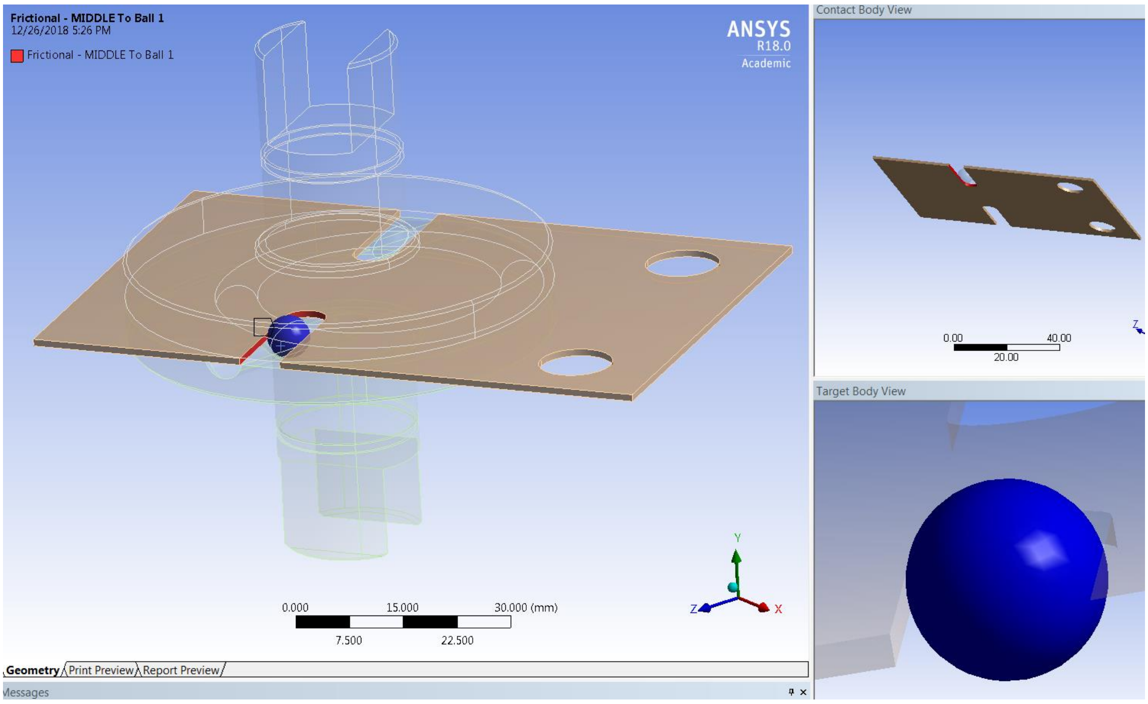

Figure 4.11: The frictional contact between the ball1 and its straight groove of the middle part

Similarly, the contact pairs between the ball 2 and the last groove of each part in contact also established.

Apply loads

According to the actual working status and the design model of the groove cam, constraints are applied. Boundary condition restrained all degrees of freedoms (DOF) of the middle part (fixed support). Both the input and the output shaft is supported by the ball bearing to assist the rotation motion. Hence, added frictionless support constraint to the input and output shaft. Load on the mechanism including the inertial load and non-inertial load. The inertial load consists of gravity and rotation speed, non inertial load is a radial load. So in this case, applied moment load to the input cam shaft is given 1Nm. The constraints and load are shown in figure 4.12.

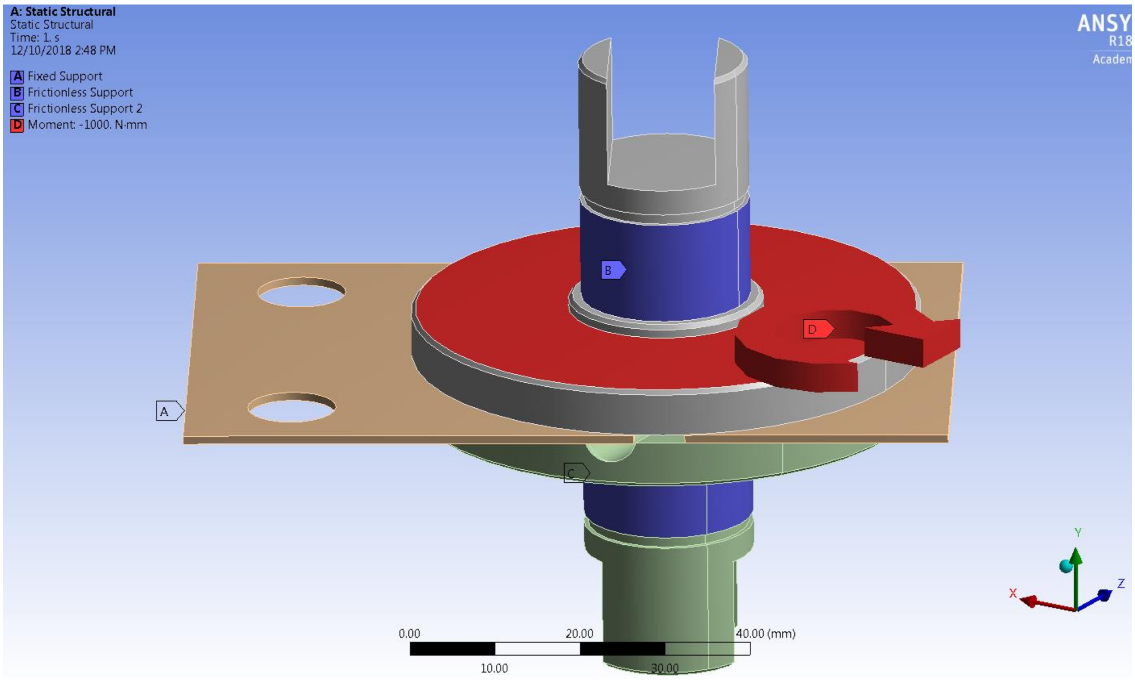

Figure 4.12: The constraints and load of the first model for analysis

Result analysis

Through the finite element simulation was made by ANSYS, contact stress and deformation distributions of the balls and the grooves, as well as the size and shape of the contact areas, were investigated in the following.

It can be seen in figure 4.13 and figure 4.14 show Von Mises total strain. The biggest total displacement and strain of the groove cam mechanism respectively is 0.03mm, 0.002mm. Specifically, the bigger contact displacement mainly concentrated on the ball and straight groove of the output shaft.

From figure 4.14 and figure 4.15 we can also know that the contact areas had an approximate ellipse or rectangular shape in the contact area of the ball and the groove, which was consistent with the Hertz contact theory.

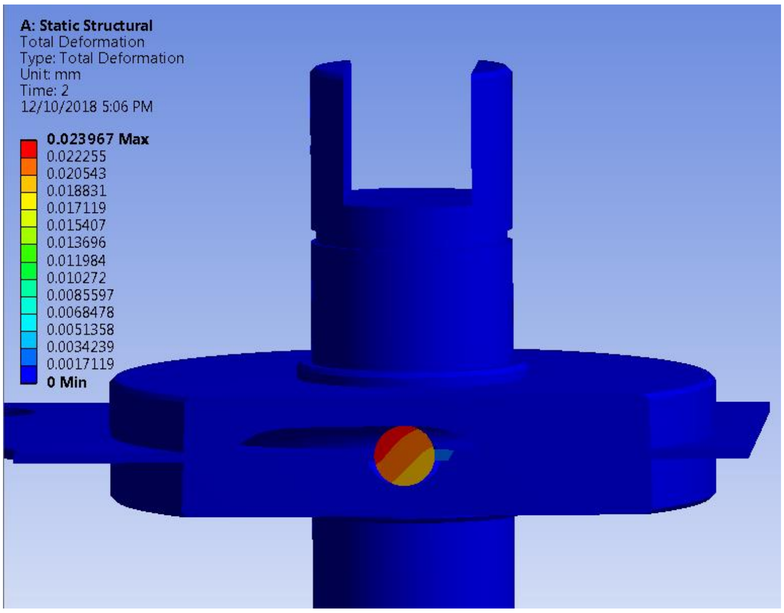

Figure 4.13: View section of distribution of deformation on the groove cam mechanism

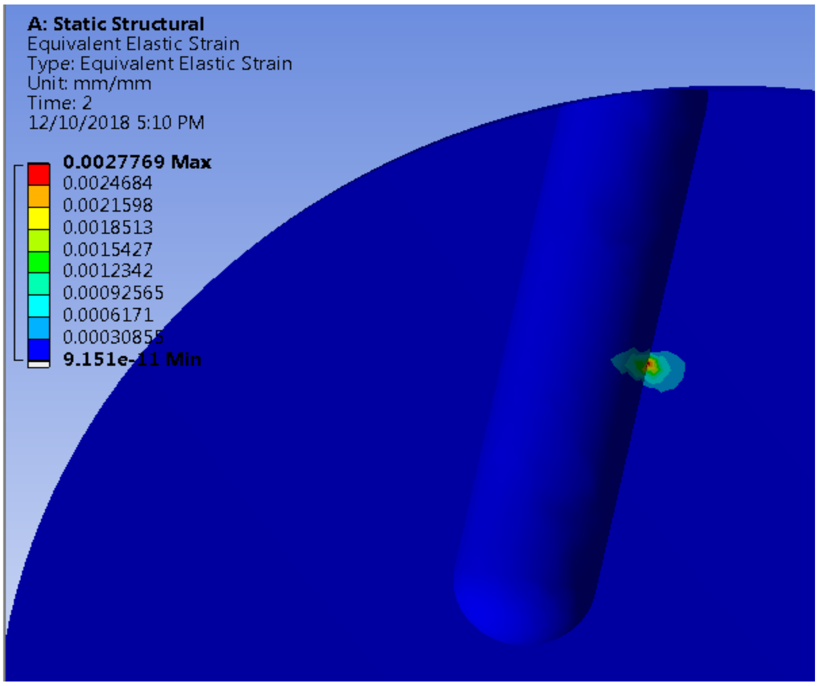

Figure 4.14: The equivalent strain distribution on the straight groove of the output shaft

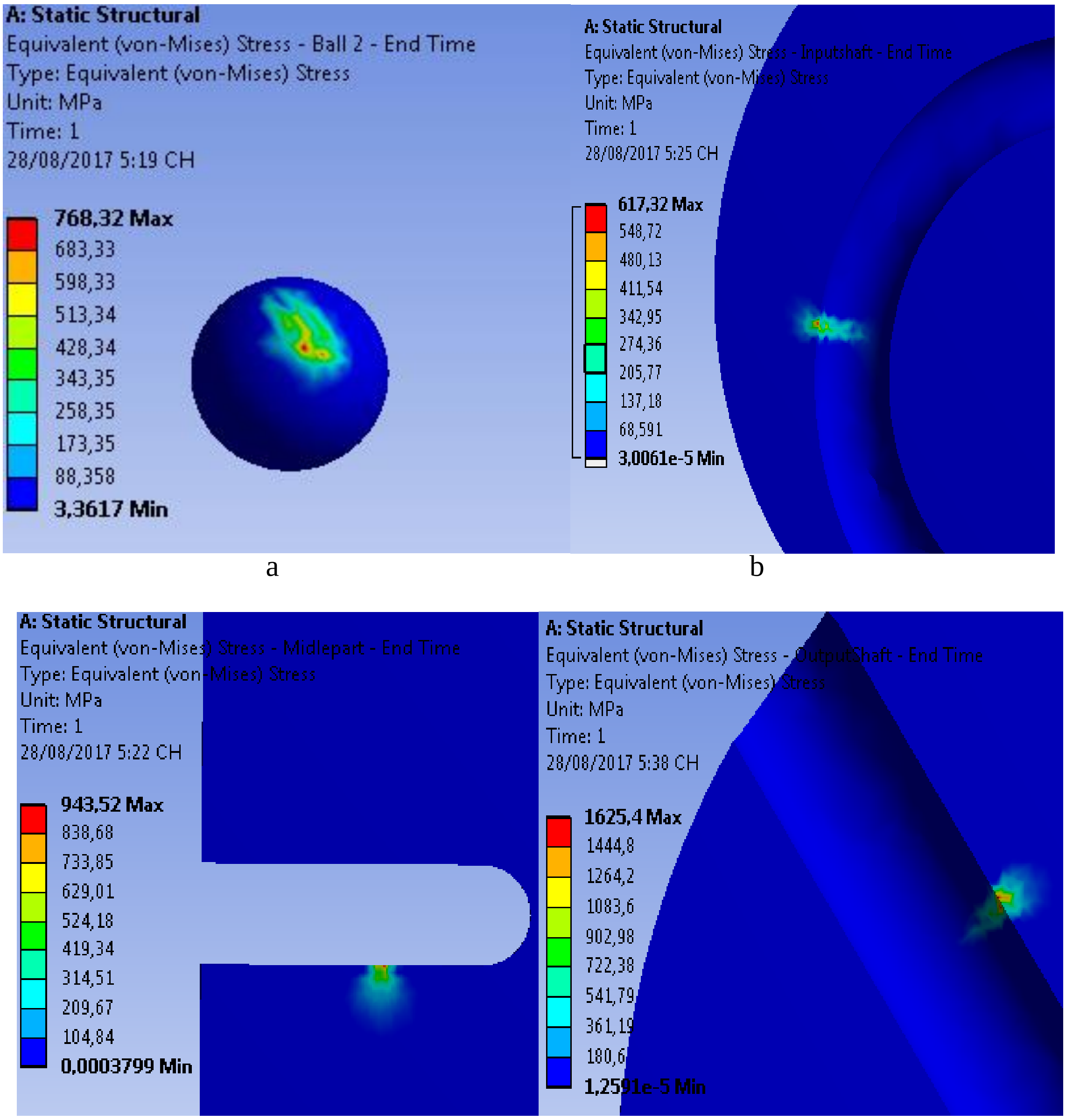

c d

Figure 4.15: The equivalent stress of cam mechanism, (a) view on the ball, (b) view on the circular groove of the middle part, (c) view on the circular groove of the input shaft, (d) view on the straight groove of the output shaft

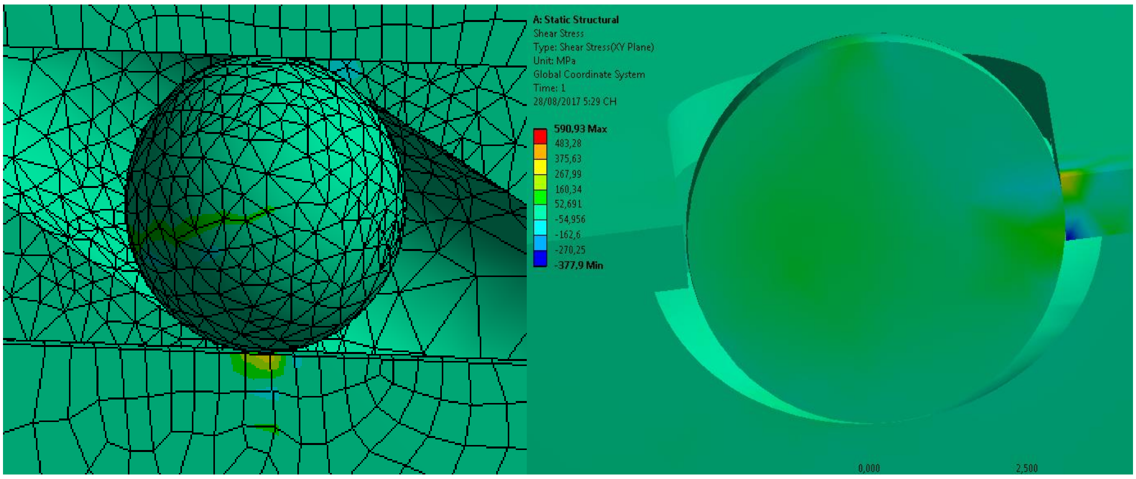

Figure 4.16: Shear stress cam mechanism

The maximum shear stress between the ball and the groove was reached to 590 MPa is shown in figure 4.16. The maximum value is located at the contact surfaces between the ball and its straight groove of the middle part.

The contact stress from the Hertz theory is actually the biggest contact pressures. As can be seen from figure 4.17 the maximum contact stress, which takes the value 2093 MPa, occurs at the contact point where the steel ball is in contact with the straight groove surface of the output shaft. Also, each of the contact areas between the ball body and the groove of the input camshaft, output shaft, and the middle part is shown in a shape of elliptical distribution (three elliptical areas), contact stress values become smaller from the center to outward gradually, which is consistency with Hertz theory.

Local contact stress of the steel ball is very large. This is due to the contact load between the ball elements and the straight groove of the middle part only act in a very small area (the thickness of the middle part is 1mm). Although the contact loads are not great, the maximum value of contact stress is allowable. Contact stress exists only in a small local area, even if the contact stress may exceed the yield limit of structural steel, microscopic plastic deformation occurs only within the local area. The contact area becomes large after plastic deformation, and contact stress decreases to less than the yield strength of the material, so it would not cause structural damage in short term. But attention still should be paid sufficiently results from the ball body and the straight groove of the middle part enters the loading zone periodically, contact stress and deformation are changing unstable. Hence, for long-term operation in the above condition susceptibly may cause fatigue failure, and even pitting corrosion.

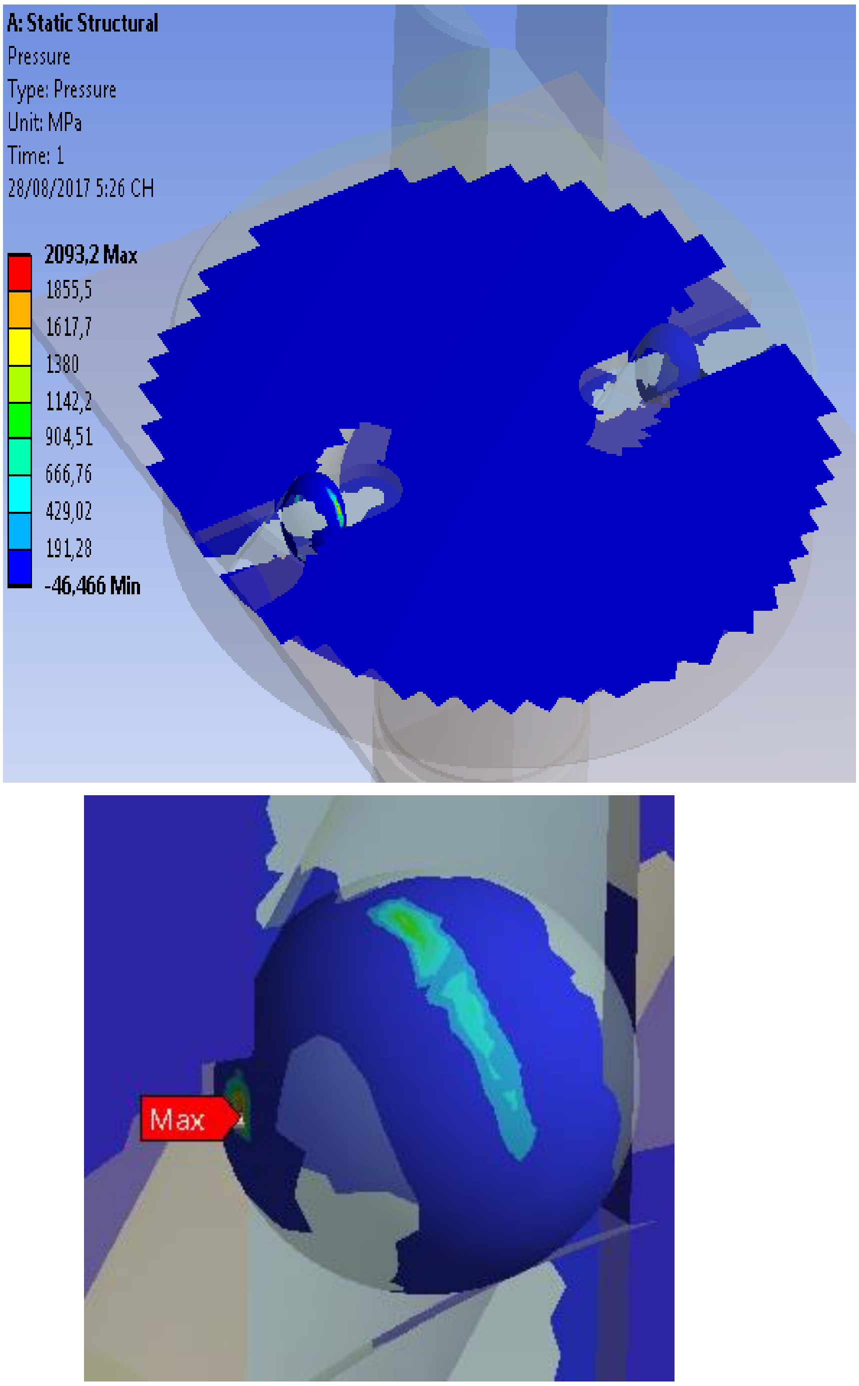

Figure 4.17: Pressure stress distribution of the groove cam mechanism

Through simulations refer to figure 4.14 and 4.17 the calculation results of the maximal contact shear stress and contact pressure was 590 MPa, 2093 MPa respectively, while the Hertz theory value was 666.65 MPa, 2002.5 MPa respectively which were referred to the chapter 3. The comparison revealed that there was good consistency between the Hertz theory solution and the finite element solution.

For more information about the difference between the finite element solution and Hertz theory, which were clearly expressed in table 4.1.

Table 4.1 the difference between finite element solution and Hertz theory solution

Parameter	Hertz theory solution	Finite element solution	Difference
Maximum contact stress	2002.5 MPa	2093 MPa	4.52%
Maximum shear stress	666.65 MPa	590 MPa	11.50%

Table 4.2 presents the maximum Hertz pressure allowed for some common materials. The values are given in MPa, with P_a, the allowable pressure for a static load. It is not advised to apply more than 40% of P_a to reach an infinite fatigue life.

Table 4.2 allowable pressure of some common materials [MPa] [4]

Material	P_a maximum	The recommended value of P_{max}
Stainless	650	260
Improved steel	1600 to 2000	640 to 800
Grey cast iron	400 to 700	60 to 280
Aluminum	62.5	25 to 150
Polyamide	25	10

Obviously, referring to table 4.2 we can strongly confirm that both values of maximum pressure obtained from the Hertz theory and finite element method are able to apply in design. Although indeed the calculating values are slightly bigger than the allowable pressure of steel material, the difference is not too much. Therefore, the result can be acceptable in practice.

Chapter 5

OPTIMIZATION OF THE GROOVE CAM MECHANISM

In the design of cam mechanism, the two main factors that must be considered first are the selection of a proper motion curve and the requirement for the radius of curvature of the cam profile to be greater than a minimum limit to avoid undercut phenomenon. Therefore, to optimize the groove cam mechanism, the design must meet the above requirements.

Based on the previous results of the chapters, we assumed that all the factors of design for the groove cam are satisfactory. The mechanism can be workable in practice. So in this chapter, we focus on how to reduce the contact stress between the ball and the groove in design to reach the maximum recommended value contact pressure for steel material, which is a significant key for optimum design of the groove cam.

In our case, when the mechanism works each steel ball body in contact with three grooves, which are the groove of the input camshaft, middle part, and the output shaft. The ball is spherical, the groove of the input camshaft is circular and the groove of the middle part and the output shaft are straight. Therefore, in the previous design when calculated we assumed that the contact between the ball and the straight groove is like contact between sphere-on-flat plate. It may cause of the high contact pressure in this case.

For a given groove cam profile, the maximum value of the Hertz pressure is obtained for the minimum radius of curvature of the groove cam. Obviously, from the equations 3.5, 3.7 and 3.10 it is easy to know that the Hertz pressure is a maximum when a_h is a minimum and the magnitude of the force is a maximum. Consequently, the higher a_h and the smaller force makes the Hertz pressure is lower.

The radius of the contact-patch of the contact a_h depends on several parameters, amongst them, the equivalent radius of the contact (geometry constant B) following equation 3.5

$$B = \frac{1}{2}\left(\frac{1}{R_f} + \frac{1}{R_r}\right),$$

R_r is the radius of the ball, which is constant and R_f is the radius of the groove in contact with the ball (in this case which is either of a radius of circular groove cam or the groove of the output shaft or the groove of the middle part). Therefore, B (a_h) depends only on R_f. Finally, for a given cam profile, a_h is a minimum when R_f is a minimum. Hence, to compute the maximum value of the Hertz pressure, we have to consider the lowest value of R_f.

Obviously, the maximum value of the pressure depends on several parameters, namely, the shape of the parts in contact, the number of the groove of the output shaft, the material of the parts in contact, the load applied. Therefore, we have different ways to minimize Hertz pressure in design.

i) Increase the number of the groove of the output shaft;
ii) Decrease the minimum value of the radius of the R_f by changing the shape of the groove cam as well as the groove shape of the output shaft and middle part;
iii) Decrease the load applied;
iv) Choose a material with a lower Young modulus, i.e., a more compliant material, thus increasing the surface of contact, hence, decreasing the pressure. However, when the material is more compliant, its plastic domain occurs for smaller stresses ;
v) Together with change the shape of the frame to make the mechanism is more stable.

Based on the result of the previous chapters combines with stated suggestions above, in this chapter, we can choose the way to optimize the groove cam mechanism following:

Firstly, in the previous design model, the groove of the output shaft which was design is a straight groove. Therefore, it could make the contact stress between the ball and the straight groove quite big. Hence, in this content, we should change the straight groove by a curved groove, also changing the shape of the frame.

Secondly, instead of the straight groove of the output shaft by the curved groove and changed the flat surface of the straight groove of the middle part by spherical surface. By this replacement, the shape of the ball and the groove of the middle part is the same size. Therefore, it may increase more elements in contact between the ball and the groove of the middle part. Hence, the maximum contact pressure may also reduce.

5.1 Optimization of the groove cam by changing the groove shape of the output shaft

Given the results of the previous calculation, it was decided to reduce the Hertz pressure while maintaining the circular groove of the input camshaft and the material as well as the load applied of the previous design. To carry out this design we must follow some procedures below.

5.1.1 Trajectory of the groove shape of the output shaft

The working profile of the groove cam is formed by the trajectory of the contact point *C* between the ball and the circular groove. Obviously, the direction of relative velocity V_c at the contact point is normal to the common normal line at the contact between the groove cam and the ball. This property of the groove cam and ball can be expressed by

$$V_c.n_c=0,$$

where V_c is a vector of relative velocity of the ball with respect to the cam; n_c is a unit vector of the common normal line. Using this equation, called meshing equation, the contact point on groove cam can be determined. If the contact point is found, the profile of the groove cam will become known.

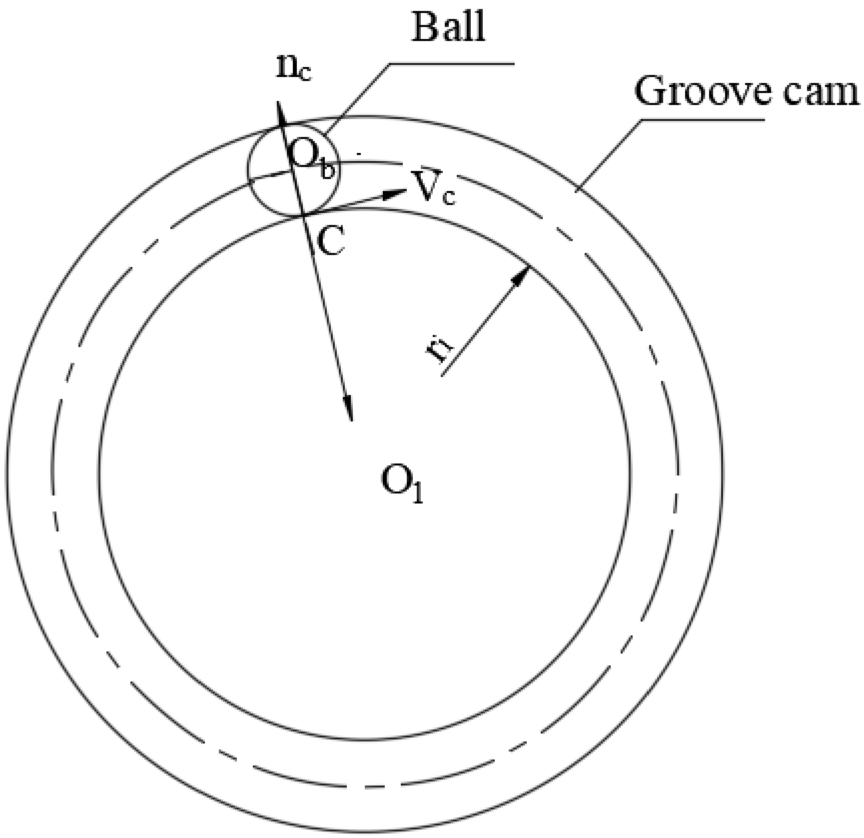

Figure 5.1 Relative motion of the ball versus the groove cam

From kinematics of a particle, we assumed the center of the ball is a particle. Therefore, when we know the space path of the contact point between the ball and the groove cam in motion simultaneously, from that the trajectory of the center of the ball (pitch curve of the groove cam) can be obtained by offsetting a distance equal to the radius of the ball.

Due to the ball in contact with three grooves, including the circular groove of the input camshaft, the straight groove of the middle part and the groove of the output shaft. Therefore, the position of the ball center relates to three trajectories including the trajectory of the pitch curve of the cam, the follower and the output's groove.

To find the trajectory of the groove of the output shaft we use inverse model and coordinate systems to analysis follow

The reverse model is used to translate the relative motion of followers with respect to cam into absolute motions, that is, let the cam stationary and the follower and the frame rotate at the same velocity as the cam but in the direction opposite to the cam at the same time, the follower reciprocate in the pre-defined motion with respect to the frame.

Figure 5.2 is a generalized model of the groove cam mechanism, the cam rotates counterclockwise at a constant angular velocity and drives the output shaft. To express the motion of each part in a groove cam, three coordinate systems are set. The first is called a Cam coordinate system (CCS) $X_1O_1Y_1$ with an origin fixed at the axis of the cam to describe the cam shape. The second is a frame coordinate system (FCS) XOY with an origin located on the cam axis and its Y-axis normal to the path of translating follower (the trajectory of the ball center in the straight groove of the middle part). This coordinate system coincides with the coordinate system of the middle part. This coordinate describes the position and motion of the ball with respect to the cam. In an initial position where the rotational angular θ is 0; the coordinate axis OX coincides with the axis O_1X_1. The third is an output coordinate system (OCS) $X_2O_2Y_2$ with an origin fixed at the axis of the output shaft used to describe the shape of the groove of the output shaft. In reality, the CCS and OCS are movable, and the FCS is stationary.

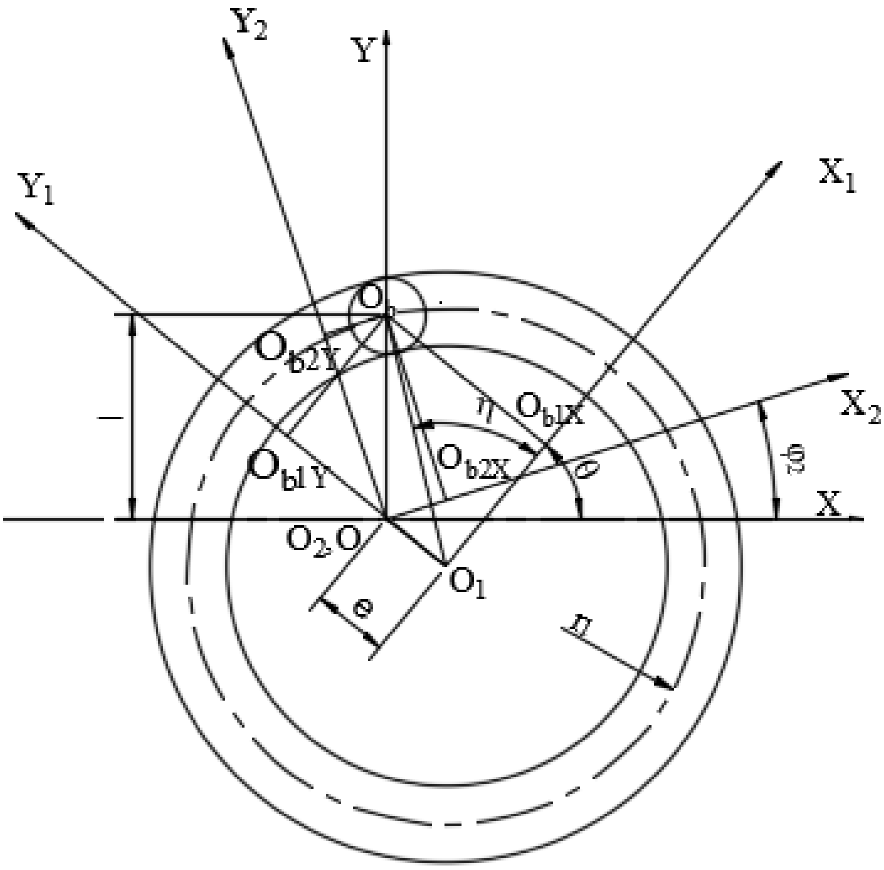

Figure 5.2 Generalized model of a groove cam

Vectors are used to represent kinematical quantities and expression such as position. From figure 5.2, the position of the ball's center O_b can be expressed in vector form as

$$\overrightarrow{OO_b} = \overrightarrow{OO_1} + \overrightarrow{O_1O_b} \ . \tag{5.1}$$

The vector OO_b in the frame coordinate system (FCS) as

$$OO_b{}^o = \begin{bmatrix} 0 \\ l \end{bmatrix}, \tag{5.2}$$

also, we have the vector $OO_1 \ and \ O_1O_b$ in the frame coordinate system (CCS) as

$$OO_1{}^1 = \begin{bmatrix} 0 \\ -e \end{bmatrix}, \tag{5.3}$$

$$O_1O_b{}^1 = \begin{bmatrix} r_1 cos\eta \\ r_1 sin\eta \end{bmatrix}, \tag{5.4}$$

with l is the distance between the center O and the ball's center at the initial position and e is the eccentric distance between the rotating center of the cam and the center of the circular groove.

Substituting equations (5.3) and (5.4) into (5.1) obtained

$$OO_b{}^1 = \begin{bmatrix} r_1 cos\eta \\ r_1 sin\eta - e \end{bmatrix}.$$

Hence, the vector OO_b in the frame coordinate system (FCS) obtained

$$OO_b{}^o = R_{z,\theta} OO_b{}^1 = R_{z,\varphi_2} OO_b{}^2, \tag{5.5}$$

with $R_{z,\theta}, R_{z,\varphi_2}$ are rotating matrices of the z-axis with respect to θ and φ_2 respectively, and can be expressed following

$$R_{z,\theta} = \begin{bmatrix} cos\theta - sin\theta \\ sin\theta \quad cos\theta \end{bmatrix}, \tag{5.6}$$

and
$$R_{z,\varphi_2} = \begin{bmatrix} cos\varphi_2 - sin\varphi_2 \\ sin\varphi_2 \quad cos\varphi_2 \end{bmatrix}. \tag{5.7}$$

Substituting equations 5.2 and 5.6 into 5.5 we got

$$\begin{bmatrix} 0 \\ l \end{bmatrix} = \begin{bmatrix} cos\theta - sin\theta \\ sin\theta \quad cos\theta \end{bmatrix} \begin{bmatrix} r_1 cos\eta \\ r_1 sin\eta - e \end{bmatrix} = \begin{bmatrix} r_1 \cos(\theta + \eta) + esin\theta \\ r_1 sin(\theta + \eta) - ecos\theta \end{bmatrix}. \tag{5.8}$$

Equation 5.8 can rewrite by as

$$r_1{}^2 = e^2 sin^2\theta + (l + ecos\theta)^2 = l^2 + 2lecos\theta + e^2 - r_1{}^2 = 0.$$

In this case the trajectory of the groove of output shaft undefined, therefore, at the initial position we assumed that the output coordinate system (OCS) situated like as figure 5.2.

If we want to design the trajectory of the groove is curved, for a simplification case we assumed that the curve may a circle and can be expressed by an equation in (OCS) as

$$(x - a)^2 + (y - b)^2 = R_2{}^2, \tag{5.9}$$

with a, b are coordinates of the circle center and R_2 is the radius of the circular groove of the output shaft.

We can express the position of A in the (OCS) following

$$OA^2 = \begin{bmatrix} lsin\varphi_2 \\ lcos\varphi_2 \end{bmatrix}, \tag{5.10}$$

with φ_2 is the rotational angle of the output coordinate system.

Substituting the values of x and y from equation 5.10 into 5.9 we obtained

$$(lsin\varphi_2 - a)^2 + (lcos\varphi_2 - b)^2 = {R_2}^2. \tag{5.11}$$

Rewrite equation 5.11 got

$$2l(asin\varphi_2 + bcos\varphi_2) = {R_2}^2 - l^2 - a^2 - b^2, \tag{5.12}$$

Denoted $sin\mu = \frac{a}{\sqrt{a^2+b^2}}$ and $cos\mu = \frac{b}{\sqrt{a^2+b^2}}$. (5.13)

Substituting equation 5.13 into 5.12 obtained

$$2l(sin\mu sin\varphi_2 + cos\mu cos\varphi_2) = \frac{{R_2}^2 - l^2 - a^2 - b^2}{\sqrt{a^2+b^2}}, \tag{5.14}$$

Finally, the obtained equation following as

$$2l(cos\varphi_2 - \mu) = \frac{{R_2}^2 - l^2}{\sqrt{a^2+b^2}} - \sqrt{a^2+b^2}. \tag{5.15}$$

For a simplification case of design, we given a value of parameters then solve the equation 5.15 to find R_2 or a.

An example is given l=14mm, $\varphi_2=0^0$, assumed the center of the circular groove of the output leans on the x-axis, hence, b=0.

From equation 5.15 we can choose one of two values and the last parameter can be taken.

5.1.2 Drawing the second design model

The input camshaft and the straight grooves of the middle part were remained like in the previous case (see figure 2.2a). In this case just instead of the straight groove by the curved groove on the output shaft.

The design model was designed by CATIA software

Figure 5.3 shows the shape of the groove of the output shaft of the first design and after the redesign.

Figure 5.4 depicts the shape of the middle before and after modification. For the first design model is clearly less stable than the new design because the first one has just one side was fixed while the last one both sides were fixed hence, the structural model is strengthened.

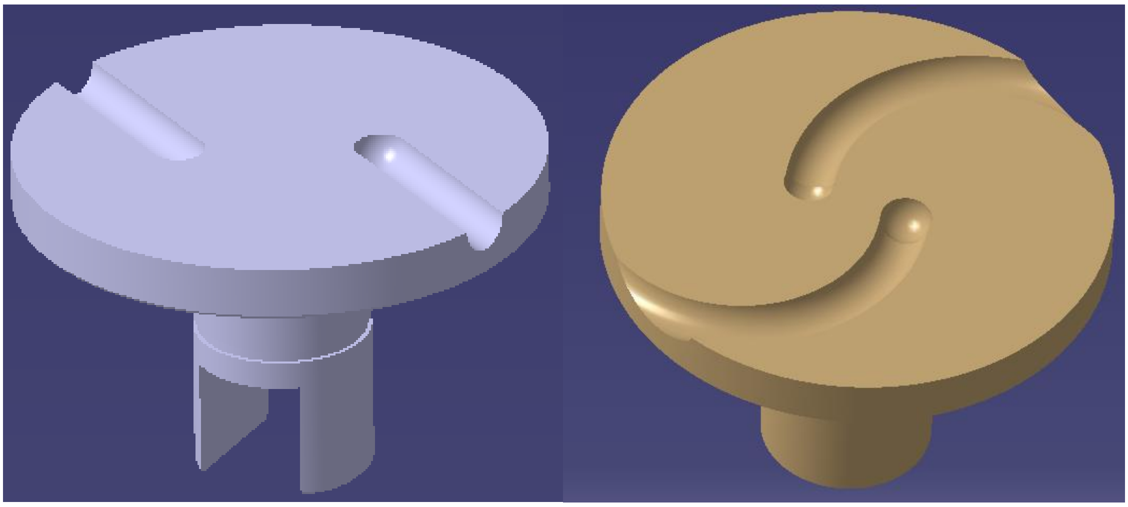

a) b)

Figure 5.3 3D model of the output shaft for a) the first design, b) the second design

Figure 5.5 shows the shape of the frame of the groove cam. As the middle part, the new frame design after modifying became more stability.

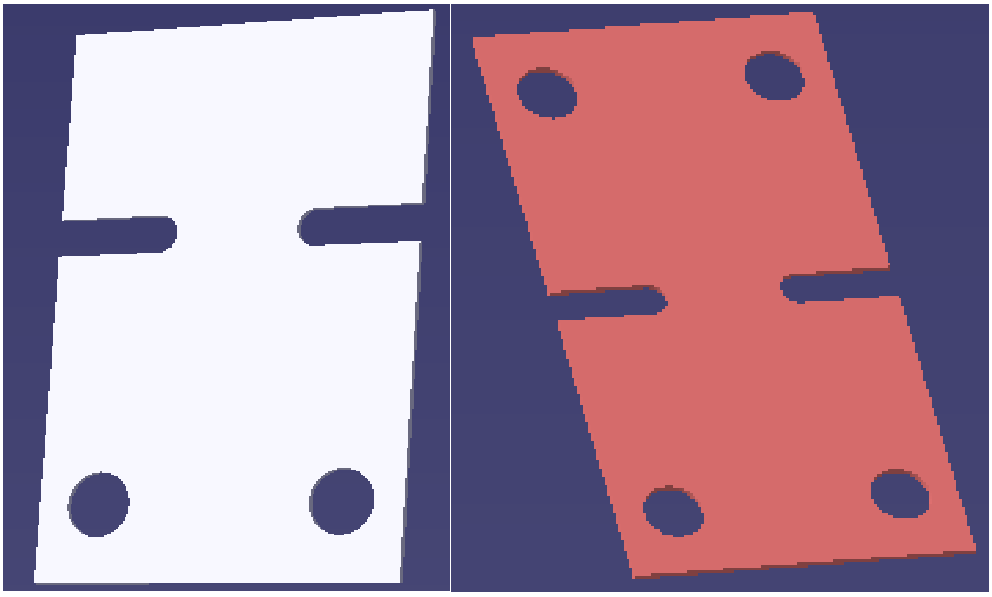

a) b)

Figure 5.4: a) the first design model of the middle part, b) the second design model of the middle part

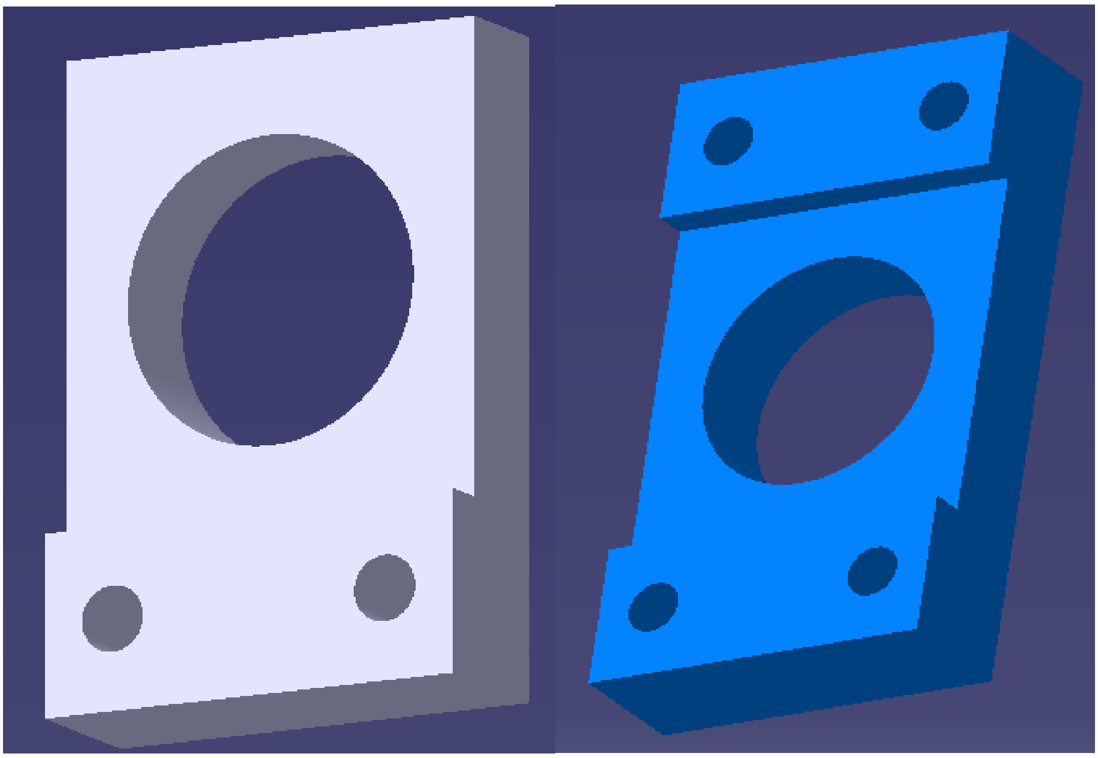

a) b)

Figure 5.5 a) the first model, b) the second design model of the frame

5.1.3 Calculation of contact pressure of the steel ball and the curved groove by Hertz theory

In this case, the groove of the output shaft is a curve. Therefore, the contact between the ball and the curved groove can be modeled as contact of sphere-on-cup. With the sphere is the ball and the cup is the curved groove. By applying the Hertz theory the calculation can be done following.

Rewrite equation 3.5 to obtain the geometry constant

$$B = \frac{1}{2}\left(\frac{1}{R_r} + \frac{1}{R_f}\right), \tag{5.16}$$

where R_f and R_r are the radius of the curved groove and the steel ball, respectively. With R_f has minus value because which is a concave surface.

Substituting the value of R_f, R_r into the equation 5.16 to obtain

$$B = \frac{1}{2}\left(\frac{1}{3\cdot 10^{-3}} + \frac{1}{-20\cdot 10^{-3}}\right) = 83.333(\mathrm{m}^{-1}).$$

Due to the steel ball and the curved groove are made of steel material, therefore, all the magnitude of the Poisson's ratios, Young moduli, and material constants are kept as the previous case.

The radius of the contact-patch of the contact between the steel ball and the curved groove is obtained

$$a_h = \sqrt[3]{0.375\frac{(m_1 + m_2)}{B}F_{A1}}.$$

The magnitude of

$$a_h = \sqrt[3]{0.375\frac{2\cdot 4.55\cdot 10^{-12}}{83.333}30.929} = 1.082\cdot 10^{-4}(\mathrm{m}).$$

The area of the contact patch of the contact between the steel ball and the curved groove is found from the equation:

$$A = \pi a_h^2,$$

the magnitude of

$$A = \pi\cdot(1.082\cdot 10^{-4})^2 = 3.678\cdot 10^{-8}(\mathrm{m}^2).$$

The average and maximum contact pressure can be found respectively

$$P_{aveg} = \frac{F_{A1}}{A} = \frac{30.929}{3.678 \cdot 10^{-8}} = 841(\text{MPa}),$$

$$P_{max} = \frac{3}{2}\frac{F_{A1}}{A} = \frac{3}{2}841 = 1262(\text{MPa}).$$

5.1.4 Applied finite element analysis for the second design model

To solve the contact pressure between the ball and their grooves for the second proposal we assumed that all the steps and boundary conditions were set in the ANSYS Workbench environment is maintained in this example. We have just changed the fixed of the middle part due to the changing structural of the middle part and the frame as expressed above. Therefore, in the ANSYS Workbench environment, the fixed constraint of the groove cam was described as figure 5.6.

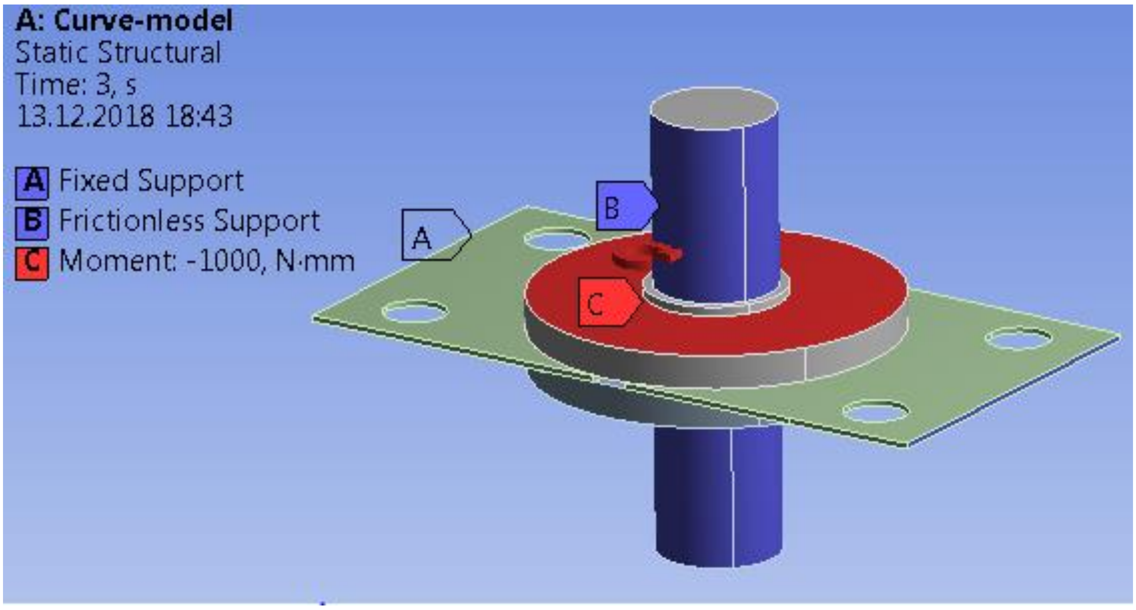

Figure 5.6 Setting boundary conditions of the second model for calculating in ANSYS

Figure 5.6 clearly shows that both sides of the middle part fixed.

The calculation was performed under the same boundary conditions as before. The result of calculation reveals that the maximum contact pressure reached the value of 1152 MPa, as shown figure 5.7 and 5.8.

From figure 5.7 and 5.8, we can know that the contact pressure change. The biggest pressure was at the contact point between the ball and the curved groove of the output shaft, and the lowest contact pressure existed at the contact between the ball and the groove of input camshaft, which was consistent with the fact. Moreover, the middle part is a thin part, therefore, the elements of the groove surface of the middle part participated in contact with the balls may not enough, cause increase the maximum contact pressure.

From the simulation result of the maximal contact pressure was 1152 MPa while the Hertz theory value was 1262 MPa. The comparison clearly showed that there was good consistency between the Hertz theory solution and the finite element solution. As can be seen in table 5.1

Also, the result obtained, it is easy to compare the maximum contact pressure with the first case, which is less than 45%. Therefore, the purpose of the optimal design with respect to reducing the Hertz pressure is obtained with the curved groove of the output shaft.

But if compared the maximum contact pressure of this case with the recommended value of the maximum pressure P_{max} for steel material (table 4.2), which is still larger. Therefore, we should improve the design to meet the goal of design. And this task will be expressed in the next section.

For getting more information can be seen in table 5.2.

In other hands, from figure 5.8, we can know that the contact area between the ball and the grooves of the input camshaft and output shaft had an approximate ellipse shape, which was consistent with the Hertz contact theory. But the contact area between the ball and the straight groove of the middle part is the unconventional case. Figure 5.8 is clearly shown that which looks like a circular shape, which may a question for the designer because according to the Hertz theory, the contact area common is ellipse or rectangle shape. Therefore, this problem can be solved in the next section.

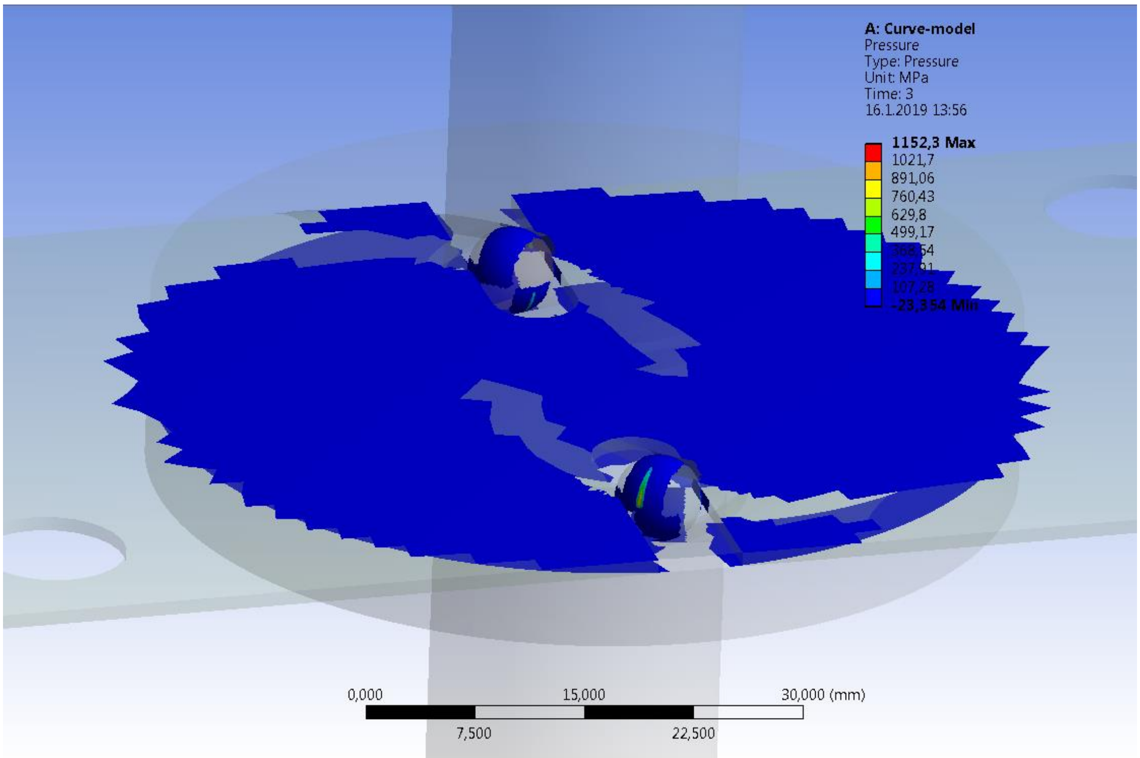

Figure 5.7: Distribution of contact pressure on the groove cam mechanism for the second design model

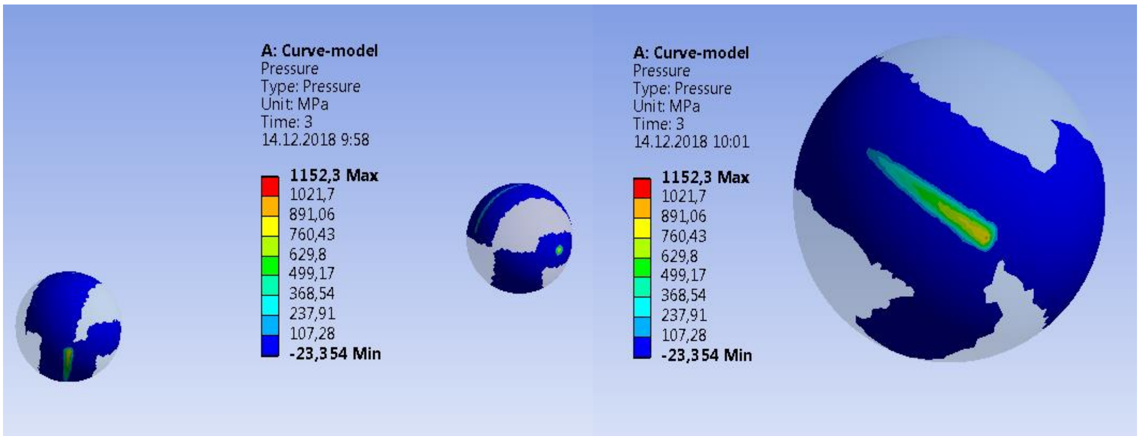

a) b)

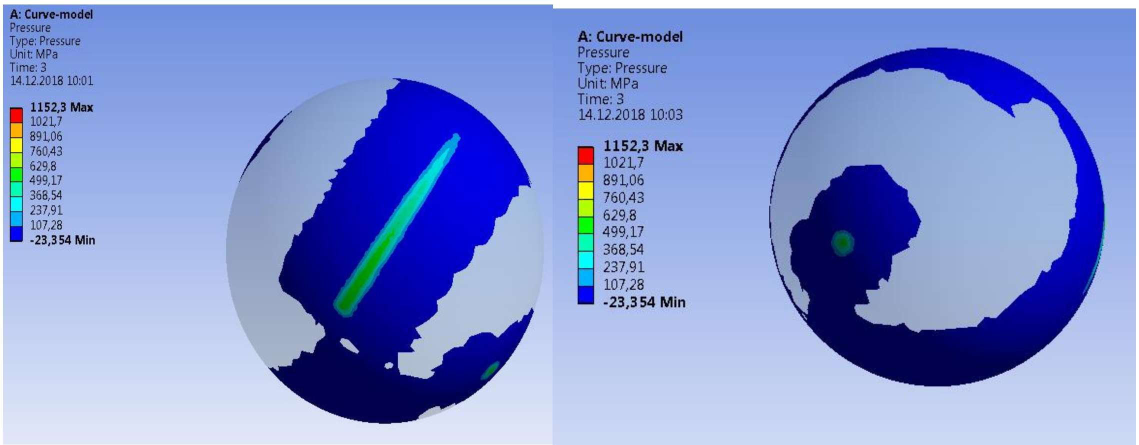

c) d)

Figure 5.8: Cloud chart about contact pressure on the ball in contact with their grooves for the second design model. A) on two balls, b) the contact area with groove curve of the output shaft, c) the contact area with the groove of input camshaft, d) the contact area with the straight groove of the middle part

In addition, ANSYS analysis can acquire other information under contacts, such as contact penetration and contact sliding distance, contact friction stress and so on as figures 5.9 and 5.10.

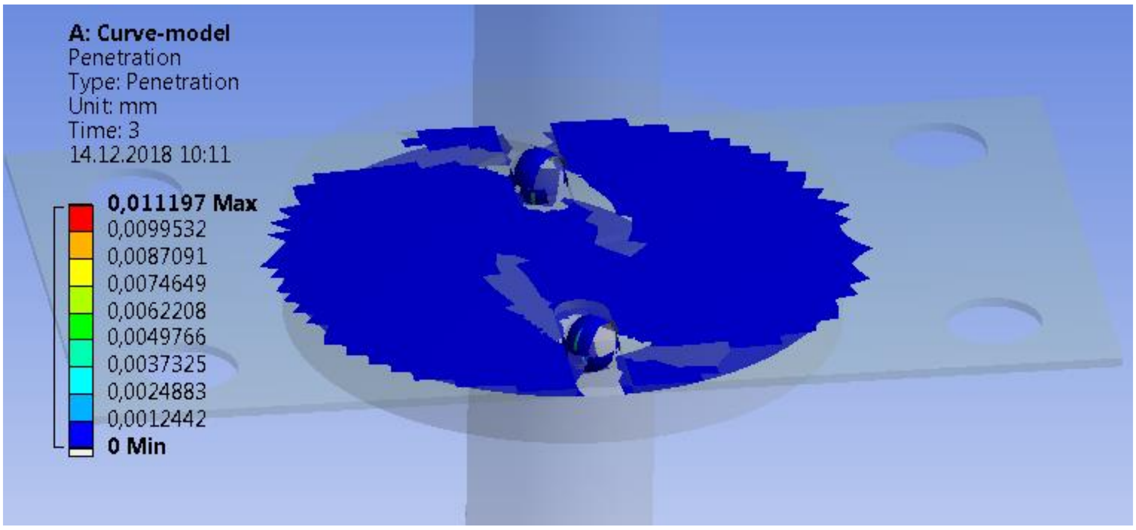

Figure 5.9: Contact penetration

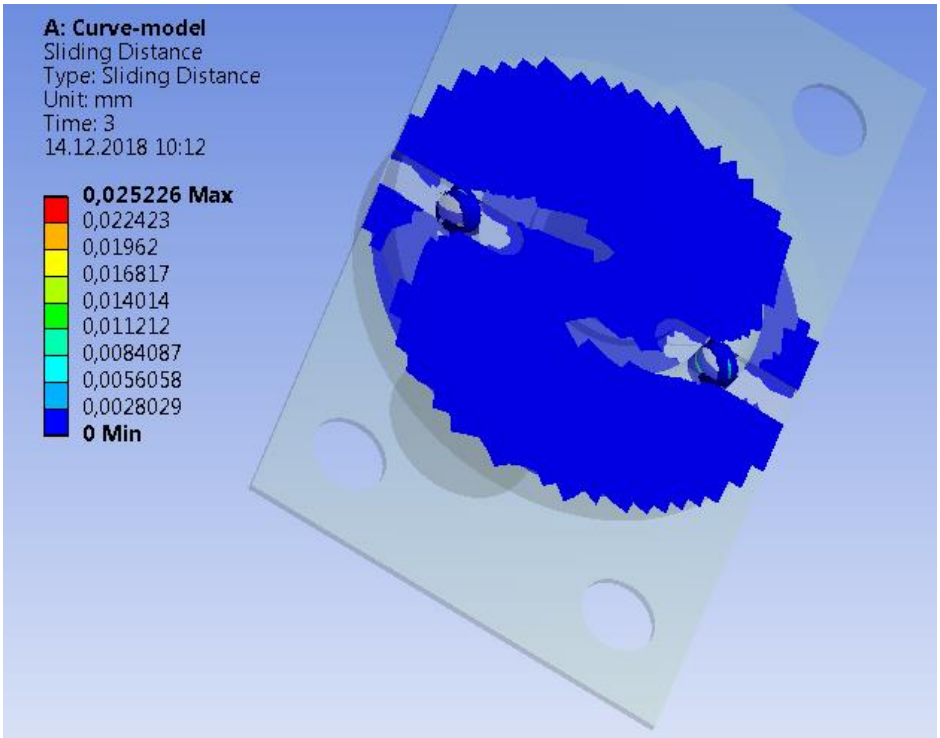

Figure 5.10: Contact sliding distance

Table 5.1 Comparison pressure [MPa] for the second design model

Parameter	Hertz theory solution	Finite element solution	Difference
Maximum contact pressure	1262	1152	8.7%

Table 5.2 Comparison contact pressure [MPa] between two design models

Solution	Fist design model	Second design model	Difference
Finite element	2093	1152	45%

5.2 Optimization of the groove cam by changing the groove surface of the middle part

5.2.1 Redesign the surface of the straight groove

The goal of the optimal design of the groove cam mechanism is to reduce the maximum contact pressure between the ball and their grooves to approach the recommended value *Pmax* (for steel material is 800 MPa). Based on the results obtained of two previous cases, by instead the straight groove of the output shaft by the curved groove, the maximum contact pressure of the mechanism reduced by 45%.

Therefore, in this section, we may think about changing the contact surface of the straight groove of the middle part, because the middle part is a thin part, and both the previous cases, the contact surface of the straight groove participated in contact with the ball is a flat plate. Hence, the contact area between the ball and the straight groove may not enough, which may cause increasing the maximum contact pressure.

If replacing the flat plate of the straight groove of the middle part by a spherical surface, hereby the contact surface between the ball and the groove surface is the same size. Therefore, it can increase elements in contact between the ball and the groove of the middle part. Hence, the maximum contact pressure may also reduce.

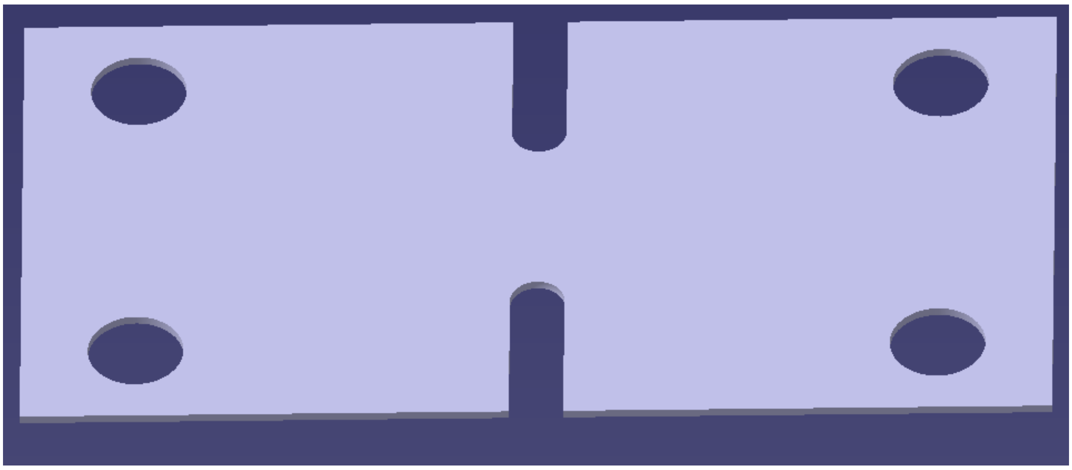

Figure 5.11: The middle part with the spherical surface of the straight groove

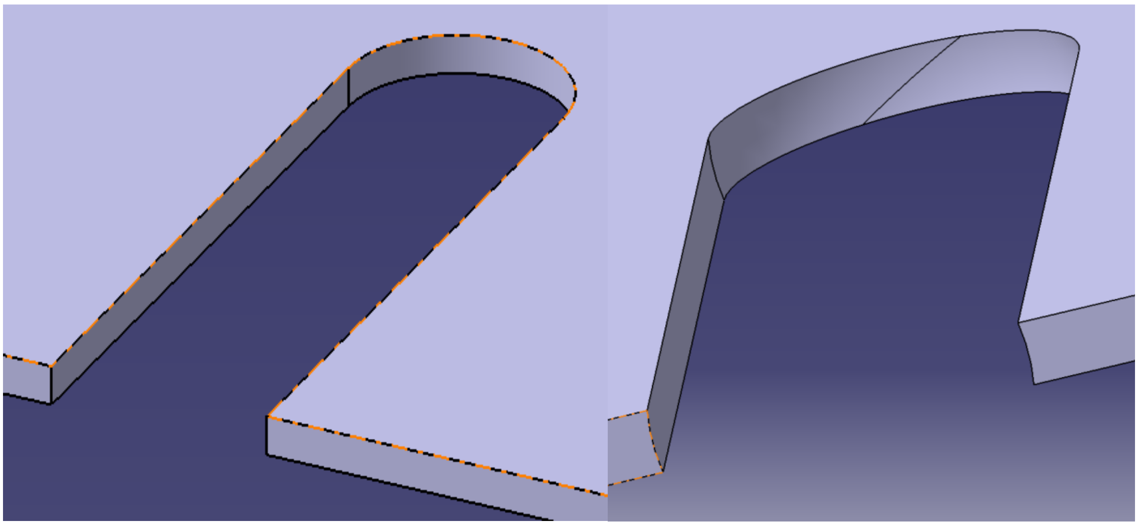

a) b)

Figure 5.12: a) view of the straight groove with the flat-plate surface, b) view of the straight groove with a spherical surface

5.2.2 Finite element solution

For the third design model, all parts of the groove cam in the second design model is maintained, including the material is still structural steel. We had a changing the surface of the straight groove as designed above.

The calculation was performed under the same boundary conditions as the previous cases.

By means of simulation, the contact change status can be got as figure 5.13

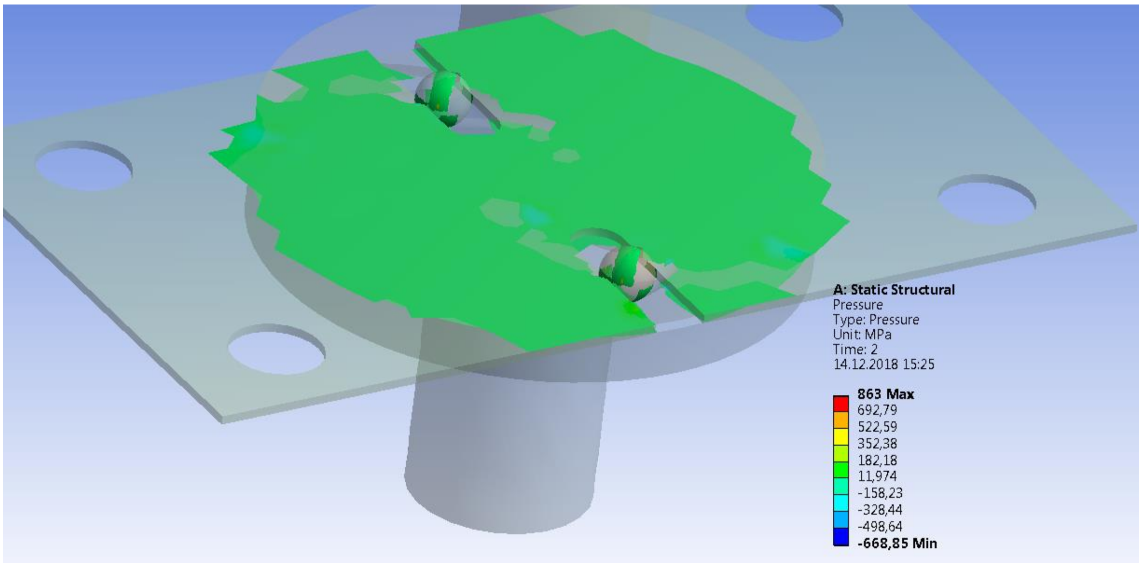

Figure 5.13: Distribution of contact pressure on the groove cam mechanism for the third model

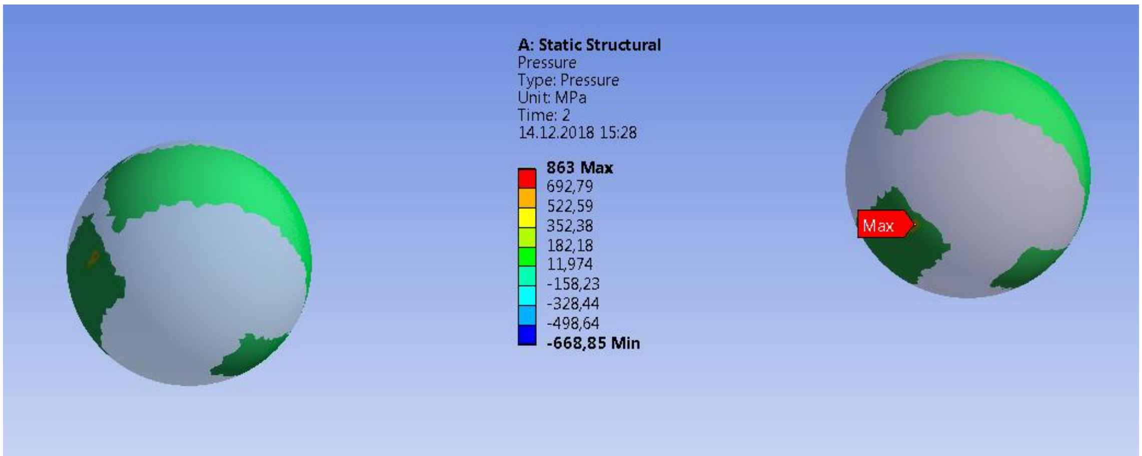

a)

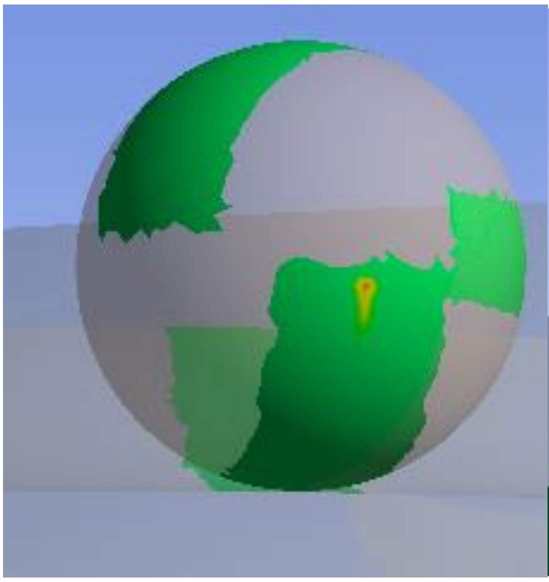

b)

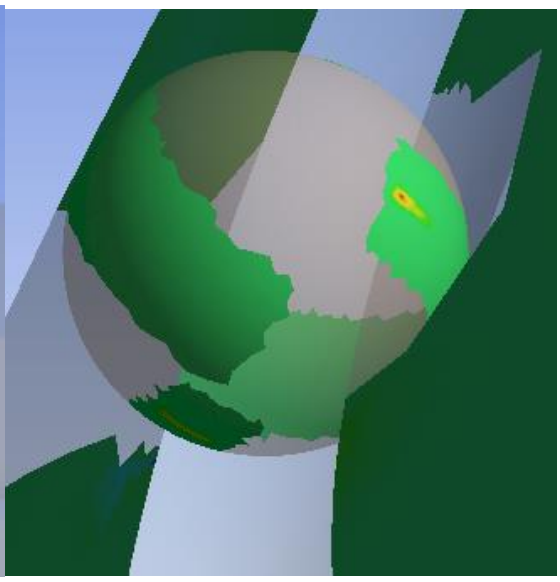

c)

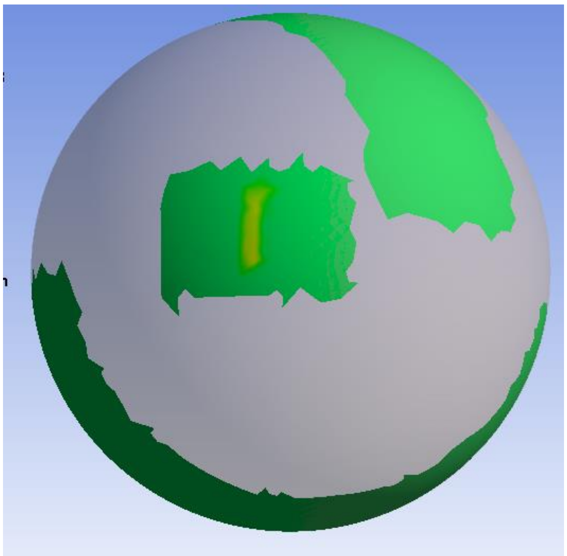

d)

Figure 5.14: Cloud charts about contact pressure on the ball in contact with their grooves of the third model design a) on two balls, b) the contact area with groove curve of output shaft, c) the contact area with the groove of input camshaft, d) the contact area with the straight groove of middle part

Figure 5.13 clearly shows that the maximum contact pressure, which takes the value 863 MPa, occurs at the contact point where the steel ball is in contact with the curved groove of the output shaft. The minimum contact pressure, which occurs at the contact point, where the steel ball is in contact with the circular groove of the input camshaft and which got the value 668 MPa.

Moreover, the maximum contact pressure, in this case, is approaching the recommended value *Pmax* (800 MPa). It is a very impressive number. Hence, in this case, it can be proved that the way to optimize the groove cam mechanism was successful in design.

Table 5.3 comparison contact pressure for the third design model and recommended value P_{max}

The third design model	Recommended value (P_{max})	Difference
863	640 to 800	7.9%

In addition, from figure 5.14, we can clearly know that all the contact areas had an approximate ellipse shape in the contact area of the ball and their grooves, which was consistency with the Hertz contact theory. It means that the question in the second design model was answered.

Based on the results of the numerical simulation, the shapes of the groove on each part for optimization of the groove cam are selected. The calculated result is matched nearly perfectly and the calculation can be used for the general design of the groove cam. So we can strongly confirm that the optimal design of the groove cam mechanism with respect to the Hertz pressure is obtained the goal of studying. Therefore, the mechanism can be applied in practice.

Chapter 6

FABRICATION OF THE GROOVE CAM MECHANISM

In order to confirm that the proposed design can be manufactured and the mechanism can be able to work in practice. The first design model was suggested to fabricate. The whole of machining experiments were performed on a DMU 50-5axis milling and a MASTURN 32 lathe machines as shown in figure 6.1. These machines are available at the laboratory of Department of the Design of Machine Elements and Mechanism of Technical University of Liberec, Czech Republic.

As the previous calculations, the material used for designing in the study is structural steel, but for the purpose to simple machining in this case assuming that the workpiece made from aluminum alloys, and carbide tools are used for machining.

Below are some pictures that illustrated the manufacturing and assembling process of the mechanism as:

Figure 6.3 depicts two steps of the machining process of the input cam shaft.

Figure 6.4 shows the machining process of the frame on the milling machine.

Figure 6.5 illustrated all parts of the mechanism were manufactured.

Figure 6.6 shows the cam mechanism after assembling successfully.

No loss of generality, and for the purpose of future research, in this case, the output shaft and the middle part were designed and manufactured with four straight grooves as shown in figure 6.5.

a)

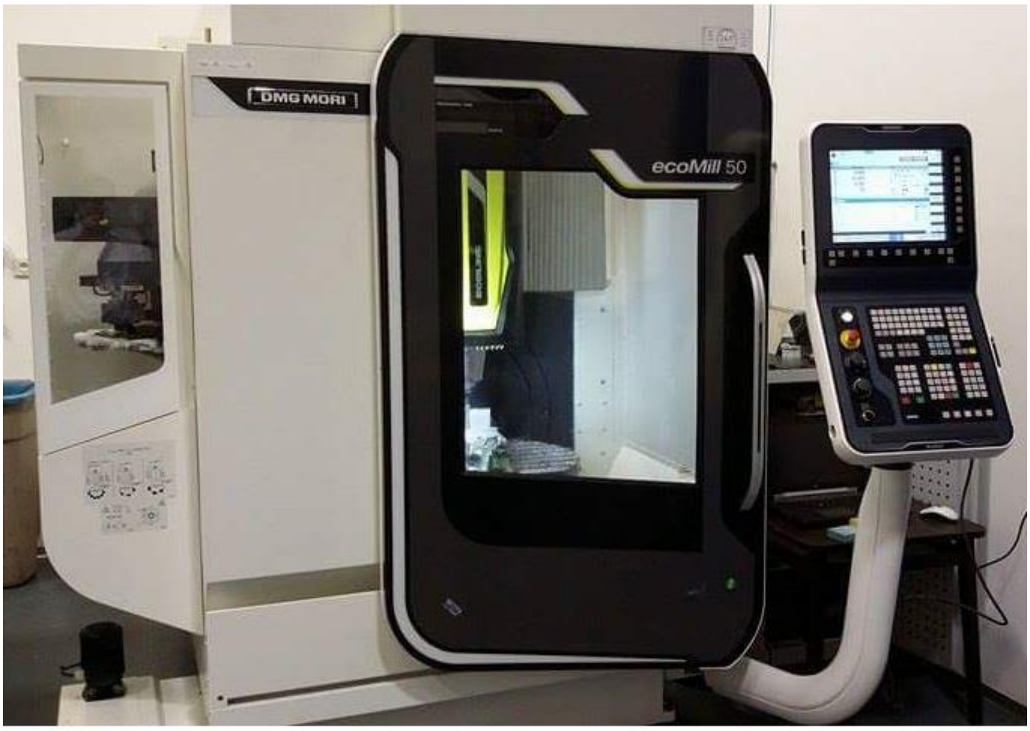

b)

Figure 6.1: A) DMU 50-5axis milling machine, b) MASTURN 32 lathe machine

Figure 6.2: Workpiece for machining

a) b)

Figure 6.3: The machining sequences of the input camshaft, a) on the lathe machine, b) on the milling machine

Figure 6.4: The frame is machining on milling machine

Figure 6.5: All the parts of the mechanism were fabricated successfully

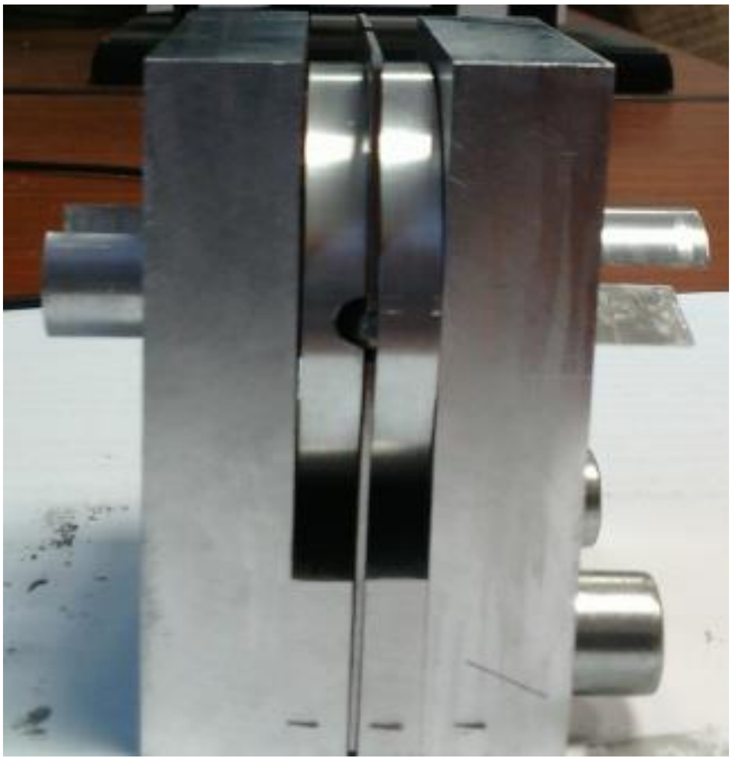

Figure 6.6: The first design model of the groove cam mechanism after assembling

Chapter 7

CONCLUSIONS

This chapter summarizes the research conducted in this dissertation. Some conclusions of the dissertation are also given. In addition, some synoptic contributions achieved from the research and some recommendations for future work are expressed, too.

7.1 Summary and conclusions

The target of the dissertation is to design a novel groove cam mechanism for converting the cam rotation to a desired rotary motion of the output shaft and proposes the ways to design optimization of the groove cam.

Initially, the first model of groove cam is suggested to design. The mechanism is composed mainly of a rotary input camshaft, a rotary output shaft, a middle part, and two balls and a frame to mount all these parts. According to this design on the top of the input camshaft has an eccentric circular groove and both grooves on the middle part and the output shaft are designed with the straight grooved shape. Also, its operating principle is explained in the thesis.

In the next step, due to the contact between the balls with their grooves on each part of the cam mechanism is very important can directly affect the lifespan and be ability working of the structure of the groove cam. Therefore, the determining of the contact stresses between the balls and their grooves on the output camshaft, the middle part as well as the circular groove of the input camshaft by using both theory and fine element analysis methods were done. Based on the results of both Hertz theory and finite element methods were shown that there was good consistency between the two methods. The stated was expressed in table 4.1.

From the results of the first design model, we recognized that the maximum contact pressure between the balls and their grooves are slightly quite bigger the allowable pressure of steel material. Therefore, to the expected of reducing the contact pressure of the balls and their grooves, the second design model is introduced. For this model, all the parts in the first design model are maintained we just changed the straight groove of the output shaft by the curved groove. Then, recalculated contact pressure for the second model under the same boundary conditions as the previous case. Based on the results obtained, it is obviously revealed that the maximum contact pressure of the second design model is less than the first one is 45% (refer to table 5.2). Therefore, the purpose of the optimal design with respect to reducing the Hertz pressure is obtained with the curved groove of the output shaft.

But if compared the result of the second design model with the recommended value of the maximum pressure P_{max} for steel material, which is still quite larger. Therefore, in the next step, the third design model of the groove cam is suggested to design. In this model, we just replaced the flat plate of the straight groove of the middle part by a spherical surface and other parts of the second design model remained, hereby the contact surface between the ball and the groove surface of the middle part is the same size. Therefore, it can increase elements in contact between the ball and the groove of the middle part. Hence, the maximum contact pressure reduced. And actually, from the result of the numerical simulation for the third design model proved that the maximum contact pressure, in this case, is approaching the recommended value P_{max} (800 MPa). It is a very impressive number. Thus the way to optimize the groove cam mechanism was successful in design.

Table 7.1 Contact pressure [MPa] of all design models

Solution	Fist design model	Second design model	Third design model
Finite element	2093	1152	863

Finally, the shapes of the groove on each part for optimization of the groove cam are selected. The calculated result is matched nearly perfectly and the calculation can be used for the general design of the groove cam. So we can strongly confirm that the optimal design of the groove cam mechanism with respect to the Hertz pressure is obtained the goal of studying.

Therefore, we can conclude that the objectives of the thesis have been fulfilled during the solution of this task.

Like other designs, the groove cam mechanism has advantages and disadvantages.

The main advantages of the proposed design are listed below:

1) The design mechanism is able to be practical and it is easy to design and manufacturing.
2) By applying the steel ball in the design, so that the ball just carry out pure rolling without sliding. Therefore, the contact between the ball and their grooves is the same as in all ball bearings in general.
3) The groove cam design, which is the form of a form-closed. Therefore, compared with a force-closed cam mechanism, the design withstands lower contact stress and no force is required to maintain the contact between the cam and the ball; compared with a conjugate cam mechanism, the groove cam mechanism is simpler in construction because only one cam is needed. So, it occupies small space and has lower cost; compared with a constant-breadth cam mechanism of which the cam profile should be convex everywhere, the cam mechanism possesses wider adaptability to the output motion because its groove cam profile could be concave
4) Another point in its favor of this design is the cam mechanism used the ball for followers, with the ball is commonly used in production machinery where their ease of replacement and availability from bearing manufacturers stock in any quantities are advantages.

Some main drawbacks of the dissertation can be enumerated as follows:

1) The major drawback of the grooved cam is the phenomenon of crossover shock. Every time the acceleration of the follower changes sign, the inertial force also does so. This causes the balls to abruptly shift from one side of the grooved cam to the other. Due to the clearance between the balls and the circular groove, even if the clearance is very small, there will still be an opportunity for the balls to develop some velocity in its short trip across the groove, and it will impact the other side. This causes significant balls to slip and high wear on the ball followers compared to an open.
2) The crossover shock can be reduced or eliminated by improving the cam surface to get high precision to control the clearance, but it makes the cam design tends to be more expensive.

7.2 The theoretical benefits of dissertation thesis

1) Developed kinematic analysis of the groove cam and a methodology to deal with optimization of the groove cam size based on the most suitable cam operating conditions, namely in what concerns to the maximum allowed pressure angle, the radius of curvature based circle radius, ball radius, and eccentricity.
2) An ANSYS software was developed to fulfill the calculating tasks in the research such as contact pressure, penetration, friction stress on the groove cam mechanism.
3) Both Hertz theory and finite element methods were applied to determine the contact pressure between the balls and their grooves of the groove cam. The results have shown that the computational values were consistent with theoretical values.

7.3 The practical benefits of dissertation thesis

1) This dissertation proposed and designed a new groove cam model that can be used in practical and very workable. Therefore, the design can have a lot of potential applications in industries. Especially, in high-power drivers due to the small size and great reliability of the mechanism. Also, all vehicles due especially to high efficiency and power density, becaue in the design used the ball for transmitting motion. Therefore, the mechanism performed pure rolling motion.
2) The dissertation brought out the newest idea design for designing cam mechanism by using the ball, where the ball plays the role of a follower in the cam mechanism. Until now there are very few references can be found in the literature that addresses the issue of the application of the ball for designing the cam field. So the research may help to open the new trend for designing cam mechanism in the years coming up.

7.4 Future work

Although this dissertation makes some useful contributions to the field of cam design, it is still necessary to carry out some more work to improve the dissertation. As listed above, the dissertation has some disadvantages that need to be overcome. The following are some recommendations for future work.

1) On the basis of the finding result presented in this thesis, work on the remaining issues is continuing and will be presented in future research. Future work will involve designing with more grooves of the output shaft, which depends on the requiring designs.
2) To optimize this mechanism considers many tasks need to research involving such as the machine processing, heat treatment, surface coating to improve the precision of all parts, especially, the surface of the ball and the grooves to avoid or eliminate the crossover shock phenomenon. With regards to that, either the experimental technique or the simulation model should be made to enable its practical application in further.
3) At present, the material used for calculation of this research is structural steel, which is a common material used in cam design. Nowadays with developing of the advanced material, it is necessary to expand to other material with a lower Young modulus, i.e., a more compliant material, thus increasing the surface of contact, hence, decreasing the maximum contact pressure. Moreover, when the material is more compliant, its plastic domain occurs for smaller stresses. Therefore, other material must be carried out in future to obtain the goal of optimal design for groove cam mechanism.

REFERENCES

[1] Robert, L.N. *Design of machinery, third edition*, Pearson 2006, ISBN 013-202012-2.

[2] Hanfried Kerle., Klaus Mauersberger. *A contribution to the history of cam mechanism-from Leonardo da Vinci till today*. International Symposiumon history of machines and mechanisms, http://doi 10.1007/978-1-4020-9485-9-10.

[3] Koster, M. P. *Vibration of cam mechanism*, SBN 333-17732-0.

[4] Chablat, D., Caro, S, and Bouyer, E. *The Optimization of a Novel Prismatic Drive, Problems of Mechanics*, 2007, No 1(26), pp. 32-42.

[5] Robert, L. N. *Cam design and manufacturing handbook*, New York Industrial Press Inc, ISBN 0-8311-3122-5.

[6] Robert, L. N. *Machine design an integrated approach*, third edition, Pearson 2006, ISBN 013-202012-2.

[7] http://www.sincroll.com/ws.php?page=index

[8] Marina Seidl. Bachelor of Engineering Thesis, *Continuously variable transmission*, Munich University of Applied Sciences, Germany and Cranfield University, England, 2011.

[9] Harold, A. R. *Cam Design Handbook*, McGraw-Hill, http://dx.doi.org/10.1036/0071433287.

[10] Angeles, J., Lopez-Cajun, C.S. *Optimization of Cam Mechanisms*, Kluwer Academic Publishers, Dordrencht,1991.

[11] Paulo Flores., et al. *Kinematics of the roller motion and cam size optimization of disc cam follower mechanism with translating roller followers*, Proceeding of IDET/CIE 2009, doi 10.1115/DETC2009-86039.

[12] Wilson, C. E. *Kinematics, and Dynamics of Machinery*, New York, Harper & Row Publishers, 1983, http://dx.doi.org/10.1036/0071433287.

[13] Waldron, K. J., Kinzel, G. L. *Kinematics, Dynamics, and Design of Machinery*, New York, John Wiley & Sons, In., 1999.

[14] Nguyen Van, H., Sevcik, L. *Design calculation of the cam mechanism for transmission between two concentric shafts*, 57th International conference of Machine Design Departments ICMD 2016, pp.137-140, ISBN 978-80-261-0609-8.

[15] Nguyen Van, H., Sevcik, L. *Apply steel balls for designing the cam mechanism*, Proceeding of 22ndInternational Conference Mechanika, pp. 118-121, ISSN 1822-2951.

[16] Nguyen Van, H., Sevcik, L. *The contact analysis of designing the cam mechanism by using ANSYS*, 58thInternational conference of Machine Design Departments ICMD 2017, pp.271-274, ISBN 978-80-213-2769-6.

[17] Nguyen Van, H., Sevcik, L. *Ball for cam mechanism design*, Proceeding of 12th International Conference for Young Researchers and Ph.D. Students in Slovakia 2018, pp 51-56, ISBN 978-80-8106-073-1.

[18] Shin, J. H., Li, L., Yang, H. D., Kwon, S. M. *Kinematical system of breadth cam profile design*, *J. Cent. South Univ. Technol*, 2011, 18:451-457, http://dx.doi.org/10.1007/s11771-011-0717-3.

[19] Michael, J., Rider. *Design and Analysis of Mechanism*, John Wiley & Sons, Ltd. 2015, ISBN 978-1-119-05433-7.

[20] Hua Q., Norikazu, I. *Profile design of constant-diameter cam with translating follower*, Vol 78 (2012) issue 791, pages 2563-2570, Doi.org/10.1299/kikaic.78.2563.

[21] https://confluence.cornell.edu/display/SIMULATION/ANSYS

[22] Elias Tomeh. *Diagnostic methodology of rolling element and journal bearings*, 2007, ISBN 987-80-7372-278-4.

[23] Johnson, K. L. *Contact Mechanics*, Cambridge University Press, 1985.

[24] https://confluence.cornell.edu/pages/viewpage.action?pageId=238913625

[25] Introduction to contact-ANSYS Mechanical structural nonlinearities

[26] Gopalakrishnan, T., Ruban, M. *Contact analysis of roller bearing using finite element method*, *Vels Journal of Mechanical Engineering*, 2015, Vol-2, 30-33.

[27] TANG Zhaoping., SUN Jianping. *The contact analysis for deep groove ball bearing based on ansys*, International Conference on Power Electronics and Engineering Application, 2011, pp. 423-428.

[28] Ju Hwan Shin., You Won Park. *ANSYS-Hertz Contact Mechanics*, https://confluence.conell.edu

[29] González-Palacios, M. A., Angeles, J. *Cam Synthesis*, Kluwer Academic Publishers B.V., Dordrecht, 1993.

LIST OF AUTHORS PUBLICATIONS

[1] Nguyen Van, Ha., Sevcik, L. *Design calculation of the cam mechanism for transmission between two concentric shafts*, 57th International conference of Machine Design Departments ICMD 2016, pp.137-140, ISBN 978-80-261-0609-8.

[2] Sevcik, L., M. Petru, and Nguyen Van, Ha. *Optimization and design modifications of the flange of the laminating machine*,57th International conference of Machine Design Departments ICMD 2016, pp.121-124, ISBN 978-80-261-0609-8.

[3] Nguyen Van, Ha., Sevcik, L. *Apply steel balls for designing the cam mechanism*, Proceeding of 22nd International Conference Mechanika, in Lithuania, 2017, pp. 118-121, ISSN 1822-2951.

[4] Sevcik, L., Nguyen Van, Ha. *Mechanical testing of stable flood defenses*, Proceeding of 22nd International Conference Mechanika, in Lithuania, 2017, pp. 343-347, ISSN 1822-2951.

[5] Nguyen Van, Ha., Sevcik, L. *The contact analysis of designing the cam mechanism by using ANSYS*, 58th International conference of Machine Design Departments ICMD 2017, pp.271-274, ISBN 978-80-213-2769-6, *Thomson Reuter, Indexed in ISI Wed of Knowledge.*

[6] Sevcik, L., Nguyen Van, Ha, and M. Petru. *Design of gas burner for the fire integrity testing of segmental doors*,58th International conference of Machine Design Departments, ICMD 2017, pp 326-329, ISBN 978-80-213-2769-6. *Thomson Reuter, Indexed in ISI Wed of Knowledge.*

[7] Nguyen Van, Ha., Sevcik, L. *Ball for cam mechanism design*, Proceeding of 12th International Conference for Young Researchers and Ph.D. Students in Slovakia, 2018, pp 51-56, ISBN 978-80-8106-073-1.

[8] Nguyen Van, Ha., Sevcik, L. *Profile design of groove cam with roller followers*, 59th International conference of Machine Design Departments ICMD 2018.

[9] Sevcik, L., Nguyen Van, Ha. *The loading of the crew protection structure of the ROPS according to different world standards*,59th International conference of Machine Design Departments ICMD 2018.